

The BBGKY hierarchy for ultracold bosonic systems

Sven Krönke^{1,2,*} and Peter Schmelcher^{1,2,†}

¹*Zentrum für Optische Quantentechnologien, Universität Hamburg,
Luruper Chaussee 149, 22761 Hamburg, Germany*

²*The Hamburg Centre for Ultrafast Imaging, Universität Hamburg,
Luruper Chaussee 149, 22761 Hamburg, Germany*

(Dated: March 23, 2022)

We establish a theoretical framework for exploring the quantum dynamics of finite ultracold bosonic ensembles based on the Born-Bogoliubov-Green-Kirkwood-Yvon (BBGKY) hierarchy of equations of motion for few-particle reduced density matrices (RDMs). The theory applies to zero as well as low temperatures and is formulated in a highly efficient way by utilizing dynamically optimized single-particle basis states and representing the RDMs in terms of permanents with respect to those. An energy, RDM compatibility and symmetry conserving closure approximation is developed on the basis of a recursively formulated cluster expansion for these finite systems. In order to enforce necessary representability conditions, two novel, minimal-invasive and energy-conserving correction algorithms are proposed, involving the dynamical purification of the solution of the truncated BBGKY hierarchy and the correction of the equations of motion themselves, respectively. For gaining conceptual insights, the impact of two-particle correlations on the dynamical quantum depletion is studied analytically. We apply this theoretical framework to both a tunneling and an interaction-quench scenario. Due to our efficient formulation of the theory, we can reach truncation orders as large as twelve and thereby systematically study the impact of the truncation order on the results. While the short-time dynamics is found to be excellently described with controllable accuracy, significant deviations occur on a longer time-scale in sufficiently far off-equilibrium situations. These deviations are accompanied by exponential-like instabilities leading to unphysical results. The phenomenology of these instabilities is investigated in detail and we show that the minimal-invasive correction algorithm of the equation of motion can indeed stabilize the BBGKY hierarchy truncated at the second order.

I. INTRODUCTION

Solving the full stationary or time-dependent Schrödinger equation for an interacting many-body system is an intriguing task, which is why various theoretical approaches rely on a description based on much fewer, effective degrees of freedom in order to avoid the exponential scaling of complexity with respect to the number of particles. These effective degrees of freedom involve a fictitious single-particle system in the density functional theory [1, 2], a subsystem consisting of few modes (Wannier functions in a lattice problem) in the large coordinate-number expansion [3–7] or a subsystem consisting of few particles in Green’s function [8, 9] as well as reduced density matrix approaches [10–14]. Having solved the problem for the effective degrees of freedom, predictions for certain classes of observables can be made without the knowledge of the full many-body wavefunction. Expectation values of arbitrary o -particle operators can be computed from the o -body reduced density operator for instance, implying that e.g. the energy expectation value of the full many-body system can be determined from the reduced two-body density operator alone if only binary interactions are involved [15]. Besides the computational advantage of

being potentially size-intensive, these subsystem-based methods constitute natural approaches for investigating e.g. whether and how certain subsystem properties of a closed many-body system thermalize when starting from a non-equilibrium initial state [16].

On the other hand, the lowest order reduced density matrices constitute a comprehensive analysis tool for characterizing many-body states [17–23]. This holds in particular for bosonic ultracold quantum gases where intriguing states of quantum matter such as a Bose-Einstein condensate or fragmented condensates [18, 19, 21, 22, 24–26] can be diagnosed by analyzing the one-body reduced density matrix. Due to the immense flexibility and the controllability of essentially all relevant parameters, these systems serve as an ideal platform for systematically studying the impact of correlations on the many-body quantum dynamics in an unprecedented manner [27–29]. For these systems, an efficient description of the quantum dynamics dealing only with a few effective degrees of freedom is highly desirable since experiments on ultracold ensembles can easily involve several hundred thousands or even millions of atoms. Because few-particle reduced density matrices are very handy for characterizing correlated many-body states, we aim here at a closed theory for the dynamics of these entities in the context of ultracold bosonic systems, i.e. the appropriately truncated quantum version of the Born-Bogoliubov-Green-Kirkwood-Yvon (BBGKY) hierarchy of equations of motion [10, 30–34].

While exactly solvable systems with analytically

* skroenke@physnet.uni-hamburg.de

† pschmelc@physnet.uni-hamburg.de

known reduced density operators are rare [35–41], truncating the BBGKY hierarchy usually involves a closure approximation (see [42] for an exception). For ultracold quantum gases being extremely dilute, a binary-collision closure approximation, neglecting three-particle correlations, is expected to be very suitable [43, 44]. The latter can be extended to higher-order correlations by means of a cluster expansion [45–54], and by using the particle-hole duality or a Green’s function method [55–58]. The Bogoliubov backaction method [59–64] as well as non-commuting cumulants [65, 66] constitute alternative but conceptually similar approaches. Recently, novel approaches using semi-classical correlations [67] or solving a time-dependent variational optimization problem [68] have been pursued.

At this point, it shall be noted that while there are numerous theoretical works on the BBGKY hierarchy and its truncation, the literature on the accuracy and numerical stability of this approach in dependence on the truncation order by explicit simulations is limited to the best of our knowledge [67–73]. The comprehensive study [69] unravels that instabilities as a consequence of the non-linear closure approximation can occur and lead to unphysical states, i.e. reduced density matrices that are not representable. In the context of electronic dynamics in atomic and molecular systems subjected to strong laser pulses, significant progress has been made by enforcing compatibility to lower-order reduced density matrices and stabilizing the truncated BBGKY equations of motion by a dynamical purification of their solution [72, 73].

Since most studies deal with fermions (for bosons, see [50–52] as well the BBGKY-related approaches [59–66]) and are based on the truncation of the BBGKY hierarchy after the second order, this work aims at a highly efficient formulation of the BBGKY such that it can be truncated at high orders by a closure approximation tailored to ultracold bosonic systems featuring a fixed number of atoms.

Our starting-point here is an efficient representation of the few-particle reduced density operators by tracing out particles from the variational ansatz for the full many-body wavefunction of the established Multi-Configuration Time-Dependent Hartree method for Bosons (MCTDHB) [74] (Section II). Similarly to the fermionic case [72, 73], we thereby employ an efficient, dynamically optimized single-particle basis. Representing the reduced density operators in terms of bosonic number states with respect to this time-dependent single-particle basis, we derive the truncated BBGKY hierarchy of equations of motion (EOM) from the MCTDHB EOM and provide a compact formulation of the result in the second-quantization picture (Section III). The properties of these equations are carefully discussed, their validity at also low but finite temperatures proven and a technically as well as conceptually useful spectral representation is provided. Thereafter, we discuss requirements on the truncation approximation for fulfilling certain conser-

vation laws and introduce a compatible cluster expansion for bosonic systems with a fixed number of atoms, where an appropriate normalization of the reduced density operators and symmetrization operators is essential (Section IV). This cluster expansion is formulated in a recursive way, which allows for going to truncation orders as large as twelve in our numerical simulations. In addition, we provide conceptual insights into the role of two-body correlations for dynamical quantum depletion and fragmentation. Since the truncation scheme does not ensure that important necessary representability conditions such as the positive semi-definiteness of the reduced density matrices are fulfilled in the course of the time-evolution, two novel, minimal invasive and energy-conserving correction schemes are developed, aiming at a dynamical purification of the solution of the truncated BBGKY EOM and at a correction of the EOM themselves, respectively (Section V).

Thereafter, we apply this methodological framework to two examples. The first scenario is concerned with the tunneling dynamics of bosonic atoms in a double-well potential. Treating the system in the tight-binding approximation allows us to go to large truncation orders without the need of dynamically optimizing the single-particle basis via the corresponding MCTDHB EOM. Thereby, we probe solely effects stemming from the truncation of the BBGKY hierarchy. Here, we find the short-time dynamics to be excellently described by the truncated BBGKY hierarchy and the accuracy to increase monotonously with increasing truncation order. For longer times, strong deviations are observed, which are linked to high-order correlations becoming dominant as well as exponential instabilities of the truncated BBGKY EOM resulting in unphysical solutions. The phenomenology of these instabilities is analyzed in detail and we show that the minimal-invasive correction scheme for the BBGKY EOM truncated at the second order can stabilize these EOM indeed.

In the second scenario, we consider a harmonically trapped bosonic ensemble subjected to an interaction quench. Here, we solve the full system of coupled EOM for the reduced density matrices and the dynamically optimized single-particle basis. For low excitation energies, we find the system to be highly accurately described by the truncated BBGKY approach. For higher excitation energies, however, exponential instabilities again occur. Also in this case, we can stabilize the BBGKY EOM truncated at the second order by our EOM correction scheme and obtain reasonably accurate results for longer times. Finally, we conclude and provide our perspectives in Section VII.

II. SETTING AND FORMAL FRAMEWORK

In the following, we first specify the general physical setting for which we aim to develop a theoretical description. Thereafter, we describe how the state of the whole

many-body system is efficiently represented by means of a dynamically adapted, truncated single-particle basis. Our ultimate goal, however, is not to theoretically describe the dynamics of the complete many-body system but to find an effective description for the dynamics of few-particle subsystems. Here, an efficient representation of such subsystem states is crucial, which we derive from the efficient representation of the total system state.

A. Physical setting

In this work, we are interested in effectively describing the non-equilibrium quantum dynamics of N identical bosons governed by the Hamiltonian $\hat{H} = \sum_{\kappa=1}^N \hat{h}_{\kappa} + \sum_{\kappa < \kappa'} \hat{v}_{\kappa\kappa'}$. Here, \hat{h}_{κ} denotes the one-body Hamiltonian acting on the particle κ , which typically consists of kinetic and external trapping potential contributions, and $\hat{v}_{\kappa\kappa'}$ refers to the binary interaction potential between the particle κ and κ' , an example of which is the contact potential $\hat{v}_{12} \propto \delta(\hat{x}^{(1)} - \hat{x}^{(2)})$ in the context of s -wave scattering ultracold atoms [27]. In what follows, all terms of the Hamiltonian may be explicitly time-dependent and for simplicity we mainly focus on the zero-temperature case while commenting on the validity of the resulting theory for low but finite temperatures in Section III B 1. Although we are in the end interested in effectively describing the dynamics of few-particle sub-systems, we nevertheless have to first describe how the total system state is represented, i.e. the many-body wavefunction in the mainly considered zero-temperature case.

B. Representation of the many-body wavefunction

Instead of relying on some fixed *a-priori* basis as commonly pursued, we employ the wavefunction representation of the Multi-Configuration Time-Dependent Hartree method for Bosons (MCTDHB) [74]. Here, the central idea is to use m time-dependent, dynamically optimized single-particle functions (SPFs), $|\varphi_i(t)\rangle$ with $i = 1, \dots, m$, as a truncated single-particle basis. By considering all bosonic number-states $|n_1, \dots, n_m\rangle_t$ with the SPFs as the underlying single-particle states and its occupation numbers summing up to the total number of particles, $\sum_{r=1}^m n_r = N$, a time-dependent many-body basis is constructed, with respect to which the many-body wavefunction is expanded

$$|\Psi_t\rangle = \sum_{\mathbf{n}|N} A_{\mathbf{n}}(t) |\mathbf{n}\rangle_t. \quad (1)$$

Here, $\mathbf{n} = (n_1, \dots, n_m)$ abbreviates a vector of occupation numbers and the summation is restricted to all \mathbf{n} with $\sum_{r=1}^m n_r = N$, which we indicate by the symbol $|N$. Using a variational principle, equations of motion (EOM) can be derived for both the expansion coefficients $A_{\mathbf{n}}(t)$ and the SPFs $|\varphi_i(t)\rangle$ [74]. These EOM, which we

explicate in Section III A, ensure that the SPFs move in an optimal manner such that the number of SPFs m , i.e. the numerical control parameter by increasing of which convergence can be achieved, can be drastically reduced compared to the case of a time-independent single-particle basis. In particular, m may often be chosen to be much smaller than the number of time-independent basis states (i.e. grid points) with respect to which the SPFs $|\varphi_i(t)\rangle$ are represented. Nevertheless, the number of terms in the full configuration-interaction expansion (1) equals $C_m^N \equiv \binom{N+m-1}{m-1}$, which increases drastically with an increasing number of bosons N . Even if convergence can be achieved with $m \ll N$, which is often the operating regime of MCTDHB, we have the scaling $C_m^N \sim N^{m-1}/(m-1)!$, which is not exponential in N but prevents going to huge systems of $N = \mathcal{O}(10^6)$ particles (unless $m = 2$). In the following, we omit the time-dependence of all entities in our notation and stress that all number states $|\mathbf{n}\rangle$ are always given with respect to the time-dependent SPF basis $|\varphi_i\rangle$ unless stated otherwise.

C. Representation of reduced density operators

Instead of describing the complete N -body system in terms of the wavefunction $|\Psi_t\rangle$ being expanded according to (1), we are concerned with the state of an o -particle subsystem, $o < N$, given by the o -body reduced density matrix¹ (o -RDM) of the wavefunction $|\Psi_t\rangle$

$$D_{(i_1, \dots, i_o), (j_1, \dots, j_o)}^o(t) = \langle \Psi_t | \hat{a}_{j_1}^\dagger \dots \hat{a}_{j_o}^\dagger \hat{a}_{i_o} \dots \hat{a}_{i_1} | \Psi_t \rangle. \quad (2)$$

Here \hat{a}_i (\hat{a}_i^\dagger) denotes the time-dependent bosonic annihilation (creation) operator corresponding to the i th time-dependent SPF, $|\varphi_i\rangle$, and obeying the canonical commutation relations $[\hat{a}_i, \hat{a}_j^\dagger] = \delta_{ij}$ and $[\hat{a}_i, \hat{a}_j] = 0$. Since we aim at a closed theory for the states of few-particle subsystems taking o -particle correlations systematically into account up to high orders o , an efficient representation of RDMs is vital. Starting with the abstract density operator of o -th order $\hat{D}_o = \sum_{i_1, \dots, j_o} D_{(i_1, \dots, i_o), (j_1, \dots, j_o)}^o |\varphi_{i_1} \dots \varphi_{i_o}\rangle \langle \varphi_{j_1} \dots \varphi_{j_o}|$ and using the bosonic symmetry, manifesting itself in an invariance of (2) under permutations of the first (last) o indices, we may expand the o -RDM with respect to SPF-based,

¹ For simplicity, we employ the same acronym ‘‘RDM’’ for referring to both the abstract reduced density operator and its representation as a matrix with respect to a given basis.

bosonic o -particle number-states

$$\hat{\rho}_o = \sum_{\mathbf{n}, \mathbf{m} | o} \rho_{\mathbf{n}, \mathbf{m}}^o |\mathbf{n}\rangle\langle\mathbf{m}| \quad \text{with} \quad (3)$$

$$\rho_{\mathbf{n}, \mathbf{m}}^o = \binom{N}{o}^{-1} \sum_{\mathbf{l} | N-o} A_{\mathbf{l}+\mathbf{m}}^* A_{\mathbf{l}+\mathbf{n}}$$

$$\prod_{r=1}^m \binom{l_r + m_r}{m_r}^{\frac{1}{2}} \binom{l_r + n_r}{n_r}^{\frac{1}{2}}.$$

We use the probabilistic normalization $\text{tr}(\hat{\rho}_o) = 1$ in this work, meaning $\hat{\rho}_o = \hat{D}_o(N-o)!/N!$, which turns out to be crucial for the definition of few-particle correlations for finite bosonic systems in Section IV.

As a matter of fact, the representation (3) of RDMs is beneficial in a three-fold manner: (i) Employing m dynamically adapted SPFs as the underlying single-particle basis can drastically reduce the necessary number of basis states for convergence [75]. (ii) Exploiting the bosonic symmetry strongly reduces the number of complex coefficients needed for representing an o -RDM, namely from m^{2o} for (2) to $(C_m^o)^2$ (if one does not make use of the hermiticity). In Fig. 1, we show the number of coefficients in dependence on o and m , showing clearly that we may effectively represent RDMs of relatively high order with Eq. (3) in contrast to Eq. (2). We note that the depicted range of m is highly relevant for practical applications since for not too strong correlations in the system, few (optimized) SPFs are often enough to properly capture the relevant physical processes due to the bosonic bunching-tendency [76–78]. (iii) Explicitly using bosonic number states as the many-body basis for expanding RDMs is very convenient for analytical manipulations and leads to equations of motion in a compact second-quantization representation, which is highly suitable for programming.

Having discussed an efficient representation of RDMs, we also have to consider how to efficiently perform operations on them. The super-operators that are crucial for this work cover the partial trace $\text{tr}_1(\cdot)$, which maps a bosonic o -body operator to an $(o-1)$ -body operator, a raising operation $\hat{R}_1(\cdot)$, which maps an o -body to an $(o+1)$ -body operator, and a joining operation $\hat{J}_{o_1}^{o_2}(\cdot, \cdot)$, which maps an o_1 - and o_2 -body operator to an (o_1+o_2) -body operator. In Appendices A and B, we introduce these operations and discuss their efficient application to e.g. RDMs being represented as (3). Using the formulas provided in these Appendices, one can easily see that the o -RDM (3) stems from integrating out $(N-o)$ degrees of freedom from the N -RDM, i.e. the total system state $\hat{\rho}_N = |\Psi_t\rangle\langle\Psi_t|$, meaning $\hat{\rho}_o = \text{tr}_{N-o}(\hat{\rho}_N)$, which implies the compatibility $\text{tr}_1(\hat{\rho}_{o+1}) = \hat{\rho}_o$ of the RDMs.

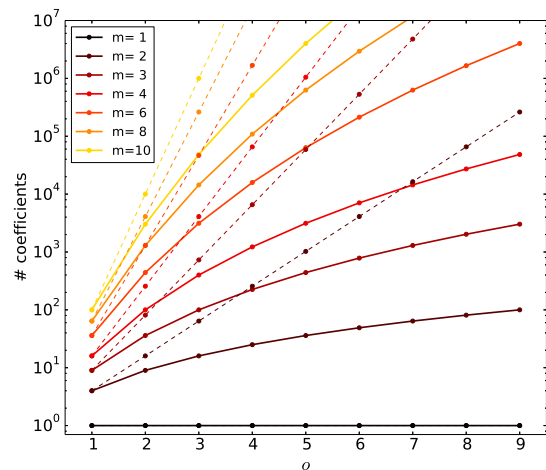


Figure 1. (color online) Complexity of representing the o -RDM, being measured by the number of complex-valued coefficients, in dependence on the order o for various numbers of SPFs m . Solid lines refer to bosonic number states as underlying basis functions, see Eq. (3), dashed ones to Hartree products, see Eq. (2). For $m = 1$, the solid and dashed line lie on top of each other. The hermiticity of RDMs is not taken into account. Making use of it would roughly reduce the number of coefficients by a factor of two.

III. EQUATIONS OF MOTION

Instead of starting with the time-dependent Schrödinger equation for deriving the EOM for the RDMs, we take the MCTDHB EOM of [74] for the wavefunction ansatz (1) as our starting point (see also [72] for the fermionic case). Thereby, we tacitly assume that the considered number m of dynamically optimized SPFs in the MCTDHB ansatz (1) is sufficient for obtaining converged results of desired accuracy up to some time t_f of interest. At the same time, our starting-point also covers the case of the Schrödinger equation in the limiting case $m \rightarrow \infty$. After briefly reviewing the MCTDHB EOM and their properties in Section III A, we present the corresponding hierarchy of EOM for the RDMs derived from the wavefunction ansatz (1) in Section III B and discuss equivalent representations in Section III C. By means of the latter, we draw important conclusions about the role of few-particle correlations for the dynamics in Section IV, where truncation approximations for the hierarchy of EOM are discussed.

A. MCTDHB equations of motion

The EOM of the MCTDHB theory [74] can be derived by applying the Lagrangian variational principle to the wavefunction ansatz (1), which ensures that the SPFs are dynamically adapted in a variationally optimal manner. As a result, one obtains a family of equivalent EOM, whose members are specified by fixing the

gauge $\langle \varphi_j(t) | i\partial_t | \varphi_k(t) \rangle = g_{jk}(t)$ with an arbitrary, possibly time-dependent hermitian $m \times m$ matrix g_{jk} , the so-called constraint operator [75]. For a given gauge g_{jk} , the expansion coefficients obey a Schrödinger equation with a time-dependent Hamiltonian matrix because of the employed time-dependent many-body basis (setting $\hbar = 1$)

$$i\partial_t A_{\mathbf{n}} = \sum_{\mathbf{m}|N} \langle \mathbf{n} | [\hat{H} - \sum_{j,k=1}^m g_{jk} \hat{a}_j^\dagger \hat{a}_k] | \mathbf{m} \rangle A_{\mathbf{m}}. \quad (4)$$

We stress here again that all time dependencies are suppressed in the notation. Correspondingly, the dynamics of the SPFs is governed by the following non-linear integro-differential equations

$$i\partial_t |\varphi_l\rangle = \hat{g}|\varphi_l\rangle + [1 - \hat{\mathbb{P}}] \left(\hat{h}|\varphi_l\rangle + (N-1) \sum_{q,p,r,s=1}^m f_{qp} f_{rs} [\hat{\rho}_1^{-1}]_{rl} \rho_{\mathbf{e}_q + \mathbf{e}_p, \mathbf{e}_r + \mathbf{e}_s}^2 [\hat{v}]_{sp} |\varphi_q\rangle \right), \quad (5)$$

where $\hat{g} \equiv \sum_{i,j=1}^m g_{ij} |\varphi_i\rangle\langle\varphi_j|$ and $\hat{\mathbb{P}} = \sum_{i=1}^m |\varphi_i\rangle\langle\varphi_i|$ projects onto the subspace spanned by the instantaneous SPFs. Besides the constraint operator, both the single-particle Hamiltonian $\hat{h} \equiv \hat{h}_1$ and the coupling to the ‘‘other’’ $(N-1)$ bosons via the mean-field operator matrix $[\hat{v}]_{sp} \equiv {}^{(2)}\langle \varphi_s | \hat{v}_{12} | \hat{\varphi}_p \rangle^{(2)}$ (the super-script (2) denotes a particle label) drive the time-evolution of the SPFs. We remark that despite of the naming ‘‘mean-field operator matrix’’ no mean-field approximation is involved (except for the limiting case $m = 1$). The matrix $[\hat{\rho}_1^{-1}]_{rl}$ refers to the inverse of the regularized² 1-RDM in SPF representation. As we expand also the 2-RDM with respect to two-particle number states, we attain the additional factors $f_{ij} \equiv \sqrt{(1 + \delta_{ij})/2}$ as compared to [74]. Moreover, the occupation-number vectors like \mathbf{e}_q , which occur in the indices of the 2-RDM, describe a state where one boson resides in the q th SPFs and all other SPFs are unoccupied. Thereby, $\mathbf{e}_q + \mathbf{e}_p$ refers to a two-particle state with one boson residing in the q th and one boson residing in the p th SPF. We note that the density matrices entering the MCTDH(B) EOM in the literature [74, 75] are the transposed of the RDM definition in this work, for which we have decided since it allows for evaluating expectation values of few-body operators in the usual manner, namely as the trace over the observable times the corresponding RDM, e.g. $\langle \sum_{\kappa=1}^N \hat{h}_{\kappa} \rangle = N \text{tr}(\hat{h}\hat{\rho}_1)$.

The solutions to Eq. (4), (5) for different gauges actually correspond to the same solution for the total wavefunction (1) since \hat{g} in Eq. (5) only induces a unitary transformation within the subspace spanned by the instantaneous SPFs, which is compensated by a correspond unitary transformation of the coefficients $A_{\mathbf{n}}$ induced by

the g_{jk} term in Eq. (4) [74, 75]. For any number of SPFs m , the MCTDHB EOM were shown to obey norm as well as energy³ conservation [74, 75] and to respect single-particle symmetries such as a parity symmetry if existent [81]. Finally, we remark that MCTDHB covers both Gross-Pitaevskii mean-field theory for fully Bose-Einstein condensed systems (given contact interaction) in the case of $m = 1$ and the exact Schrödinger equation⁴ in the formal limit $m \rightarrow \infty$ where $\hat{\mathbb{P}}$ becomes the identity.

B. BBGKY equations of motion

There are at least three ways how the EOM of the RDMs can be derived from the MCTDHB theory. (i) Since the elements of the o -RDM $\hat{\rho}_{\mathbf{n},\mathbf{m}}^o$ only depend explicitly on the expansion coefficients $A_{\mathbf{n}}$ (and not on the SPFs), one may differentiate Eq. (3) with respect to time and use the EOM (4). (ii) One could also take the time-derivative of $|\Psi_t\rangle\langle\Psi_t|$ using both Eq. (4) and (5), then trace out $(N-o)$ particles via Eq. (B5) and finally project onto o -particle number-states from the left and right. (iii) Instead of MCTDHB, one can equivalently start with the corresponding MCTDH EOM [75] such that individual particles are addressable via artificial labels. Thereby, one can directly apply the standard derivation of the BBGKY EOM (see e.g. [10]) and successively trace out particles in the von-Neumann like EOM for the N -RDM elements. After translating this first-quantization result to the second-quantization picture, one obtains the following EOM for the o -RDM

$$i\partial_t \rho_{\mathbf{m},\mathbf{n}}^o - \langle \mathbf{m} | [\hat{H}, \hat{\rho}_o] | \mathbf{n} \rangle = \langle \mathbf{m} | \hat{I}_o(\hat{\rho}_{o+1}) | \mathbf{n} \rangle. \quad (6)$$

Here, the von-Neumann like term $[\hat{H}, \hat{\rho}_o]$ with the Hamiltonian

$$\hat{H} = \sum_{i,j=1}^m (h_{ij} - g_{ij}) \hat{a}_i^\dagger \hat{a}_j + \frac{1}{2} \sum_{i,j,q,p=1}^m v_{ijqp} \hat{a}_i^\dagger \hat{a}_j^\dagger \hat{a}_q \hat{a}_p, \quad (7)$$

and $h_{ij} \equiv \langle \varphi_i | \hat{h} | \varphi_j \rangle$, $v_{ijqp} \equiv \langle \varphi_i \varphi_j | \hat{v}_{12} | \varphi_q \varphi_p \rangle$, describes the unitary evolution of the o -particle subsystem in the state $\hat{\rho}_o$ and accounts for all interactions within this subsystem. Interactions with the sub-system’s environment consisting of $(N-o)$ particles, however, render the overall dynamics non-unitary in general, which becomes manifest in the inhomogeneity of the EOM (6), the so-called collision integral

$$\hat{I}_o(\hat{\rho}_{o+1}) = \frac{N-o}{o+1} \sum_{i,j,q,p=1}^m v_{qjpi} [\hat{a}_q^\dagger \hat{a}_p, \hat{a}_i \hat{\rho}_{o+1} \hat{a}_j^\dagger], \quad (8)$$

² See [75] for a regularization recipe and [79, 80] for two recent alternatives to this regularization.

³ Higher order moments of a time-independent Hamiltonian are, however, not conserved in general [75].

⁴ Setting furthermore $g_{jk} = 0$ leads to the Schrödinger equation in a time-independent many-body basis.

coupling the dynamics of $\hat{\rho}_o$ to $\hat{\rho}_{o+1}$. Since this second-quantization formulation of the collision integral might appear less familiar compared to e.g. [10], let us reformulate the above expression. Using the mixed first and second quantization representation of Appendix B [see formula (B2)] and the representation (3), one easily verifies $\hat{a}_i \hat{\rho}_{o+1} \hat{a}_j^\dagger / (o+1) = {}^{(o+1)}\langle \varphi_i | \hat{\rho}_{o+1} | \varphi_j \rangle^{(o+1)}$, which may loosely be interpreted as the “state” of the o -particle subsystem conditioned on the $|\varphi_i\rangle \leftrightarrow |\varphi_j\rangle$ transition of a further particle. By employing the mean-field operator matrix $[\hat{v}]_{ji}^{(\kappa)} \equiv {}^{(o+1)}\langle \varphi_j | \hat{v}_{\kappa,o+1} | \varphi_i \rangle^{(o+1)}$ with $\kappa = 1, \dots, o$, we can translate $\sum_{q,p=1}^m v_{qjpi} \hat{a}_q^\dagger \hat{a}_p$ into the first-quantization picture in the o -particle sector, namely to $\sum_{\kappa=1}^o \hat{\mathbb{P}}^{(\kappa)} [\hat{v}]_{ji}^{(\kappa)} \hat{\mathbb{P}}^{(\kappa)}$ where the mean-field operator matrix and the projector act on the particle κ as indicated by the superscript index. Putting both ingredients together, we obtain a more familiar representation

$$\begin{aligned} \frac{\hat{I}_o(\hat{\rho}_{o+1})}{(N-o)} &= \sum_{\kappa=1}^o \sum_{i,j=1}^m [\hat{\mathbb{P}}^{(\kappa)} [\hat{v}]_{ji}^{(\kappa)} \hat{\mathbb{P}}^{(\kappa)}, {}^{(o+1)}\langle \varphi_i | \hat{\rho}_{o+1} | \varphi_j \rangle^{(o+1)}], \\ &= \sum_{\kappa=1}^o \hat{\mathbb{P}}^{(\kappa)} \text{tr}_1([\hat{v}_{\kappa,o+1}, \hat{\rho}_{o+1}]) \hat{\mathbb{P}}^{(\kappa)}, \end{aligned} \quad (9)$$

where the partial trace effectively runs over the SPFs only. The latter representation directly shows that the collision integral describes the interaction of any particle of the considered o -particle subsystem with one particle of its environment. Next, we briefly comment on some properties of the EOM.

1. Properties

Solved together with the EOM for the SPFs (5), the complete hierarchy of RDM EOM (6) (with $o = 1, \dots, N$) is equivalent to MCTDHB, of course, and thereby inherits all properties such as gauge invariance, norm, energy and, if existent, single-particle symmetry conservation. In particular, the solution of the complete hierarchy corresponds to an exact solution of the many-body Schrödinger equation for $m \rightarrow \infty$. Trivially, the RDM EOM respect the compatibility of the RDMs by construction, meaning $\partial_t \rho_{\mathbf{n},\mathbf{m}}^o = \langle \mathbf{n} | \text{tr}_1(\partial_t \hat{\rho}_{o+1}) | \mathbf{m} \rangle$. Although the above EOM are derived from MCTDHB and the RDMs are represented with respect to a dynamically optimized basis, the EOM for the matrix elements $\rho_{\mathbf{n},\mathbf{m}}^o$ are formally identical to the BBGKY EOM derived from the time-dependent Schrödinger equation [10], which one can see by using the representation (9) for the collision integral and translating the Hamiltonian (7) into the first-quantization picture for the o -particle sector. This is due to the fact that the elements $\rho_{\mathbf{n},\mathbf{m}}^o$ depend only on the expansion coefficients $A_{\mathbf{n}}$ (see Eq. (3)), which obey a linear Schrödinger-like equation (4). Moreover, in the limit $m \rightarrow \infty$ and the gauge $g_{ij} = 0$, the above equations exactly coincide with the BBGKY hierarchy of EOM represented in some time-independent basis (see e.g. [10]). In

the opposite limit $m = 1$, where all bosons are forced to reside in the same SPF, the time-derivative of the RDM elements vanishes and the dynamics is solely governed by Eq. (5), which becomes equivalent to the Gross-Pitaevskii mean-field equation for the case of contact interaction [74].

Since the BBGKY EOM derived from MCTDHB are formally identical to the BBGKY EOM stemming from the von-Neumann equation, the question of their validity at finite temperatures boils down to the question of whether Eq. (5) results in an optimal dynamics for the SPFs in this case. By purifying the N -RDM (see also [82]), we show in Appendix C in which sense Eq. (5) ensures optimality of the SPFs also for arbitrary mixed initial states $\hat{\rho}_N(0)$ of the total N -particle system, given that the N -particle dynamics is unitary. Thereby, the above equations can safely be applied also to the case of low temperatures as long as one can computationally account for sufficiently many SPFs to resolve all significantly populated single-particle states. Otherwise, one would have to combine the BBGKY approach with some suitable Monte-Carlo sampling technique, which, however, goes far beyond the scope and aims of this work.

In order to use the above BBGKY EOM for simulating the quantum dynamics of systems which are too large for a MCTDHB calculation, one needs to truncate the hierarchy of EOM at a certain order \bar{o} and approximate the unknown collision integral $\hat{I}_{\bar{o}}[\hat{\rho}_{\bar{o}+1}]$. This closure approximation may therefore be regarded as an additional approximation to the MCTDHB theory in the case of a finite number of SPFs m . If successful, the total particle-number N would directly⁵ enter the resulting theory only as a prefactor of the collision integral (8). While truncation schemes are discussed in Section IV, we provide in the following comments on (i) how to find an appropriate initial state for the o -RDM with $o = 1, \dots, \bar{o}$ (Section III B 2) and (ii) different representations of the BBGKY hierarchy (Section III C).

2. Initial-state calculation

In the following, let us assume that we have already truncated the BBGKY at the order \bar{o} by means of an appropriate closure approximation (see Section IV) and discuss different approaches for determining the initial RDMs $[\hat{\rho}_1(t=0), \dots, \hat{\rho}_{\bar{o}}(t=0)]$.

First, if the system is initially fully condensed or in a non-interacting thermal state, the initial o -RDM can be stated (semi-)analytically for arbitrary orders, given that the occupied single particle state(s) are known.

⁵ In some situations, however, the number of particles does affect the minimal number of SPFs required for convergence, cf. the Mott insulating state of ultracold bosons in an optical lattice at unit filling where one needs $m = N$.

Second, if, however, correlations do play a role initially, e.g. if the system is initially in the correlated ground-state of some reference Hamiltonian \hat{H}_0 , numerical methods such as MCTDHB with imaginary time propagation or improved relaxation [83] can be employed. Due to the closure approximation, however, the resulting o -RDM cease to be an exact stationary point of the EOM (6) (with \hat{H} replaced by the reference Hamiltonian \hat{H}_0). In such a situation, the initial RDMs can be improved by propagating the RDM EOM (6) with fixed SPFs and \hat{H} still replaced by the reference Hamiltonian \hat{H}_0 for some time and performing a time-average over the solution as done in [73].

Third, one may alternatively take some initial guess for $\hat{\rho}_o(t=0)$ with $o = 1, \dots, \bar{o}$, obtained e.g. from an accurate MCTDHB calculation or, if infeasible, a rough one taking too few SPFs into account⁶, and aim at finding a fixed point of the EOM (5), (6), where \hat{H} is again replaced by the reference Hamiltonian \hat{H}_0 . The MCTDHB EOM (4) in negative imaginary time leads to the following trace-conserving EOM for the N -RDM $\partial_\tau \rho_{\mathbf{n}, \mathbf{m}}^N = \langle \mathbf{n} | \{ \text{tr}(\hat{H}_0 \hat{\rho}_N) - \hat{H}_0, \hat{\rho}_N \} | \mathbf{m} \rangle$ with $\{ \cdot, \cdot \}$ denoting the anti-commutator. Given a gapped reference Hamiltonian \hat{H}_0 , the latter EOM exponentially contracts all initial states with $\langle E_0 | \hat{\rho}_N(0) | E_0 \rangle \neq 0$ to a state proportional to the projector onto the (approximate) ground state⁷ $|E_0\rangle$.

Taking partial traces of the above equation for the N -particle density operator, however, appears cumbersome to us. Instead, we find it technically more convenient to directly differentiate the RDMs with respect to (negative imaginary) time and perform manipulations similarly to the derivation of contracted Schrödinger equations [12, 13, 56, 58]. In Appendix D, we explicate this derivation for the 1-RDM. As in the case of contracted Schrödinger equations, one finds that the EOM for the o -RDM couples to both the order $o+1$ and $o+2$, which can be traced back to the N -RDM EOM featuring an anti-commutator instead of the commutator occurring for real-time dynamics. With the help of an appropriate truncation approximation (see Section IV), one can then relax an initial guess for the o -RDM to the (approximate) ground-state o -RDM. It would be very interesting to compare the performance of these EOM, which includes also an adaptive single-particle basis, to the conventional contracted Schrödinger equation approach [12, 13, 56, 58] and its anti-hermitian variant [84] (which could also be used for calculating the initial o -RDM, of course). Since we, however, focus on the properties of the

(truncated) BBGKY equations (5), (6) for many-body dynamics here, only situations with analytically known initial states are considered in the applications of Section VI.

C. Special representations of the BBGKY equations of motion

Before discussing truncation approximations in Section IV, we briefly inspect selected equivalent representations of the BBGKY EOM (5), (6) here, which turns out to be useful for both computational purposes and conceptual insights.

1. Single-particle Hamiltonian gauge

While any chosen gauge g_{ij} leads to the same solution for the o -RDM $\hat{\rho}_o$ as argued before, we empirically found that the single-particle Hamiltonian gauge $g_{ij} = h_{ij}$ is numerically more favorable for integrating the EOM (see also [75] for a similar observation for MCTDH). We suspect the following mechanism being responsible for this effect. The commutator $[\hat{H}, \hat{\rho}_o]$, expressed in the eigenbasis of \hat{H} , results in terms being proportional to the difference of two eigenenergies in the EOM (6), which might lead to stiff equations and small integrator time-steps. In the above gauge, however, the single-particle terms are removed from the Hamiltonian (7) such that the impact of these energy differences is reduced. Possibly, one might boost the integration further by incorporating also a fraction of the interaction energy into the constraint operator in an appropriate mean-field sense.

2. Natural-orbital gauge

Conceptual insights into the role of correlations can be gained by spectrally decomposing the o -RDM

$$\hat{\rho}_o = \sum_{r=1}^{C_m^o} \lambda_r^{(o)} |\phi_r^o\rangle\langle\phi_r^o| \quad (10)$$

and reformulating the BBGKY EOM as EOM for the so-called natural populations (NPs)⁸ $\lambda_r^{(o)}$ and natural orbitals (NOs) $|\phi_r^o\rangle$ [17]. For ultracold bosonic systems, the dynamics of the 1-RDM NPs is of particular interest for diagnosing quantum depletion and fragmentation into several Bose-Einstein condensates [18, 22, 25]. In the context of the MCTDH theory, it is well-known that

⁶ In order to perform the subsequent calculations accurately, one has to add further, e.g. randomly chosen SPFs and embed the given o -RDM with smaller m into an o -RDM with larger m such that those additional SPFs are unoccupied.

⁷ For a degenerate ground state, the asymptotic solution is proportional to $\hat{\rho}_N(0)$ projected from the left and right onto the ground-state manifold.

⁸ The terms 'natural population' and 'natural orbital' have originally been introduced for the 1-RDM only [17] but are employed for all orders in this work.

one can enforce the SPFs to coincide with the 1-RDM NO given that this coincidence is also ensured initially [75, 85, 86] by an appropriate choice of the constraint operator, which reads⁹ for indistinguishable particles and two-body interactions

$$g_{ij} = h_{ij} - (1 - \delta_{ij}) \frac{\langle \phi_i^1 | \hat{I}_1(\hat{\rho}_2) | \phi_j^1 \rangle}{\lambda_i^{(1)} - \lambda_j^{(1)}}. \quad (11)$$

Thereby, one finds that the 1-RDM NP dynamics is driven by the collision integral

$$i\partial_t \lambda_r^{(1)} = \langle \phi_r^1 | \hat{I}_1(\hat{\rho}_2) | \phi_r^1 \rangle, \quad (12)$$

and the corresponding NOs obey

$$i\partial_t |\phi_r^1\rangle = \hat{h} |\phi_r^1\rangle - \sum_{\substack{l=1 \\ l \neq r}}^m \frac{\langle \phi_l^1 | \hat{I}_1(\hat{\rho}_2) | \phi_r^1 \rangle}{\lambda_l^{(1)} - \lambda_r^{(1)}} |\phi_l^1\rangle \quad (13)$$

$$+ \frac{(N-1)}{\lambda_r^{(1)}} [\mathbb{1} - \hat{\mathbb{P}}] \sum_{q,p,s=1}^m f_{qp} f_{rs} \rho_{\mathbf{e}_q + \mathbf{e}_p, \mathbf{e}_r + \mathbf{e}_s}^2 [\hat{v}]_{sp} |\phi_q^1\rangle,$$

where the mean-field operator matrix $[\hat{v}]_{sp}$ has to be evaluated with respect to the NO basis. Before we proceed, some comments are in order here. (i) The EOM (12), (13) turn into the exact EOM for the 1-RDM NPs and NOs [42, 87–91] in the limit $m \rightarrow \infty$ where the last term in (13) vanishes. For a truncation of the single-particle basis to some finite m , the above EOM describe the variationally optimal dynamics of the NOs (see also [92]). (ii) The reciprocal eigenvalue $1/\lambda_r^{(1)}$ in (13) has to be regularized as usual (see footnote 2). (iii) In the case of NP degeneracies, both the constraint operator (11) and the NO EOM (13) can become undefined due to the ambiguity of the NOs within the degenerate subspace(s). One can cope with this issue by setting the g_{ij} to zero if $\lambda_i^{(1)} = \lambda_j^{(1)}$ [92] or regularize the difference $\lambda_i^{(1)} - \lambda_j^{(1)}$ in the equations [75]. Alternatively, a Taylor expansion of $\hat{\rho}_1(t + \Delta t)$ up to second order in Δt as performed in [79] should lift the ambiguity in many cases. In any case, initially non-degenerate NPs typically repel each other during the dynamics according to the Wigner-von-Neumann non-crossing rule [93] with the time t as the only “external” parameter, unless symmetries lead to non-incidental crossings [94]. Due to these technical subtleties, we do not employ the natural-orbital gauge for simulations but only for analytical insights into the essential features of the 2-RDM which actually drive the NP dynamics according to Eq. (12) (see Section IV C).

3. Spectral representation on all orders

While the constraint operator can only be used for deriving the spectral representation at the order $o = 1$, one

⁹ We note that the real-valued diagonal elements g_{ii} may be chosen arbitrarily.

may proceed for orders $o > 1$ by inserting the representation (10) into the EOM (6) and projecting the result onto NOs (see [42, 88–91] for the application of this strategy to the order $o = 1$). The result of this calculation is similar to Eq. (12) and the first line of Eq. (13), and reads

$$i\partial_t \lambda_r^{(o)} = \langle \phi_r^o | \hat{I}_o(\hat{\rho}_{o+1}) | \phi_r^o \rangle, \quad (14)$$

$$i\partial_t \phi_{r;\mathbf{n}}^o = \langle \mathbf{n} | \hat{H} | \phi_r^o \rangle - \sum_{\substack{l=1 \\ l \neq r}}^m \frac{\langle \phi_l^o | \hat{I}_o(\hat{\rho}_{o+1}) | \phi_r^o \rangle}{\lambda_l^{(o)} - \lambda_r^{(o)}} \phi_{l;\mathbf{n}}^o \quad (15)$$

where $\phi_{r;\mathbf{n}}^o \equiv \langle \mathbf{n} | \phi_r^o \rangle$. So again, only the collision integral drives the non-unitary dynamics of the o -RDM NPs, as expected. We note that the EOM (14) will be the starting-point for our construction of a novel correction algorithm for the truncated BBGKY EOM, which non-perturbatively enforces necessary representability conditions such as the positive semi-definiteness (see Section V B 2).

IV. TRUNCATION APPROXIMATION AND THE ROLE OF CORRELATIONS

Having discussed the BBGKY hierarchy of EOM stemming from the MCTDHB theory without further approximations, we investigate closure approximations for truncating the hierarchy at order \bar{o} here. This is to impose further approximations to the MCTDHB theory. While one effectively has to find an approximation for the unknown collision integral $\hat{I}_{\bar{o}}$ only, we pursue here the standard path of approximating the unknown $(\bar{o}+1)$ RDM by $\hat{\rho}_{\bar{o}+1}^{\text{appr}}$ such that we obtain for the approximate collision integral $\hat{I}_{\bar{o}}^{\text{appr}} = \hat{I}_{\bar{o}}(\hat{\rho}_{\bar{o}+1}^{\text{appr}})$. The general strategy in the following is to appropriately decompose the o -RDM into a part which can be constructed from lower order RDMs and a rest, which defines o -particle correlations. Then, the truncation approximation consists in neglecting the thereby defined $(\bar{o} + 1)$ correlations. Such an approach is expected to be appropriate for weak and intermediate interaction strengths, e.g. for studying the emergence of correlations on top of a Bose-Einstein condensate or fragmented condensates.

In the following, we first discuss requirements on such a closure approximation, which have to be fulfilled for respecting important conservation laws (Section IV A). Then, different cluster-expansion schemes and thereby different definitions of few-particle correlations are critically discussed in Section IV B. After these rather technical considerations, we conceptually analyze the role of two-particle correlations for the dynamics of 1-RDM natural populations, i.e. for dynamical quantum depletion or fragmentation of a bosonic ensemble (Section IV C).

A. Truncation approximation and conservation laws

While the bosonic symmetry is explicitly incorporated in our formal framework and thus trivially conserved, other symmetries and conservation laws are only obeyed by the truncated BBGKY EOM (5), (6) if the closure approximation $\hat{\rho}_{\bar{o}+1}^{\text{appr}}$ fulfills certain conditions. For analyzing these requirements, we partly follow the lines of [10] and [69] while taking the time-dependence of the SPFs into account, whenever necessary.

First of all, the traces of the RDMs are conserved for any truncation approximation $\hat{\rho}_{\bar{o}+1}^{\text{appr}}$ due to the commutator structure of the EOM (6). Second, any hermitian closure approximation $\hat{\rho}_{\bar{o}+1}^{\text{appr}}$ results in the conservation of hermiticity of the o -RDMs, again by virtue of the commutator structure of their EOM. Third, the conservation of compatibility can be studied by inspecting

$$i\partial_t \langle \mathbf{n} | [\text{tr}_1(\hat{\rho}_{o+1}) - \hat{\rho}_o] | \mathbf{m} \rangle = \langle \mathbf{n} | [\hat{H}, \text{tr}_1(\hat{\rho}_{o+1}) - \hat{\rho}_o] | \mathbf{m} \rangle + \kappa \langle \mathbf{n} | \hat{J}_o (\text{tr}_1(\hat{\rho}_{o+2}) - \hat{\rho}_{o+1}) | \mathbf{m} \rangle \quad (16)$$

with $\kappa = (N - o - 1)/(N - o)$. As in the case of the BBGKY hierarchy represented in some time-independent basis, the compatibility of the closure approximation, $\text{tr}_1(\hat{\rho}_{\bar{o}+1}^{\text{appr}}) = \hat{\rho}_o$ for all times, constitutes a sufficient condition for the conservation of compatibility of all lower order RDMs, given that these RDMs are compatible at the initial time of the propagation.

Fourth, we discuss energy conservation in the sense of $\frac{d}{dt} \langle \hat{H} \rangle_t = \langle (\frac{\partial}{\partial t} \hat{H}) \rangle_t$, where the partial derivative on the right hand side relates to a potential explicit time dependence of the Hamiltonian \hat{H} . Focusing on truncation orders $\bar{o} \geq 2$, one obtains the same results for the EOM (5), (6) as found for the BBGKY EOM being represented in a time-independent basis [69]. Namely, if the total energy expectation value of the system is calculated as

$$\langle \hat{H} \rangle_t = N \text{tr}(\hat{h}_1 \hat{\rho}_1) + \frac{N(N-1)}{2} \text{tr}(\hat{v}_{12} \hat{\rho}_2) \quad (17)$$

then energy conservation is ensured by the bosonic symmetry of the RDMs, independently of the chosen truncation approximation. If, however, one alternatively computes the energy expectation value as $\langle \hat{H} \rangle_t = N \text{tr}(\hat{k}_2 \hat{\rho}_2)$ with the auxiliary 2-particle Hamiltonian $\hat{k}_2 = [\hat{h}_1 + \hat{h}_2 + (N-1)\hat{v}_{12}]/2$ [15], then energy conservation requires the truncation approximation to respect the compatibility requirement.

Fifth, single-particle symmetries are conserved as long as the truncation approximation respects this symmetry, which means the following. Let $\hat{\pi}_\kappa$ denote a symmetry operation (e.g. parity transformation or translation) acting on the κ th particle and $\hat{\Pi}_n = \bigotimes_{\kappa=1}^n \hat{\pi}_\kappa$ the corresponding symmetry operation acting on n particles. Furthermore, we consider a Hamiltonian featuring this symmetry, i.e. $[\hat{\Pi}_N, \hat{H}] = 0$, and assume an initial state of definite symmetry. By transferring the line of arguments of [81] to the current situation, one can show

that the truncated EOM (5), (6) conserve this symmetry, i.e. $[\hat{\Pi}_o, \hat{\rho}_o(t)] = 0$ for $o = 1, \dots, \bar{o}$, if the following two conditions are met. (i) All initial SPFs, i.e. also initially unoccupied ones, are of definite symmetry, meaning $\hat{\pi}_1 |\phi_j(t=0)\rangle = e^{i\theta_j} |\phi_j(t=0)\rangle$ for some $\theta_j \in \mathbb{R}$. (ii) The reconstruction approximation $\hat{\rho}_{\bar{o}+1}^{\text{appr}}$ features this symmetry, $[\hat{\Pi}_{\bar{o}+1}, \hat{\rho}_{\bar{o}+1}^{\text{appr}}(t)] = 0$ at time t , given that the RDMs of lower order, from which $\hat{\rho}_{\bar{o}+1}^{\text{appr}}(t)$ is constructed, commute with the corresponding $\hat{\Pi}_o$ transformation.

Sixth, one can show that the g_{ij} gauge invariance of the EOM (5), (6) remains untouched under truncation if the truncation approximation $\hat{\rho}_{\bar{o}+1}^{\text{appr}}(t)$ transforms as a bosonic $(\bar{o}+1)$ -RDM under unitary transformation of the single-particle basis. When discussing the construction of compatible cluster expansions in Sections IV B 2 and IV B 3, this transformation behavior turns out to be a subtlety which has to be carefully analyzed.

Finally, we refer the reader to [95] for a comprehensive discussion of the impact of closure approximations on the time-reversal invariance of the BBGKY hierarchy.

B. Cluster expansions for finite bosonic systems

In the following, we first review the so-called cluster expansion for indistinguishable but spinless particles (Section IV B 1) and analyze its symmetrized variant for bosons (Section IV B 2). When critically inspecting the resulting definition of few-particle correlations, also in comparison to the corresponding cluster expansion for fermions, we pinpoint an issue concerning size-extensivity being related to a particularity of the bosonic symmetrization operator. For this reason, we briefly touch upon an alternative cluster expansion, being outlined in more detailed and critically discussed in Appendix E. Eventually, we arrive at a compatible, recursively formulated cluster expansion for bosons, which allows for going to large truncation orders (Section IV B 3). It is this cluster expansion which we employ in the applications of Section VI.

1. Cluster expansion for indistinguishable spinless particles

Following e.g. [10], the cluster expansion for a system of indistinguishable but spinless particles reads

$$\begin{aligned} \hat{\rho}_2^{(1,2)} &=: \hat{\rho}_1^{(1)} \hat{\rho}_1^{(2)} + \hat{c}_2^{(1,2)} & (18) \\ \hat{\rho}_3^{(1,2,3)} &=: \hat{\rho}_1^{(1)} \hat{\rho}_1^{(2)} \hat{\rho}_1^{(3)} + [\hat{c}_2^{(1,2)} \hat{\rho}_1^{(3)} + \hat{c}_2^{(1,3)} \hat{\rho}_1^{(2)} \\ &\quad + \hat{c}_2^{(2,3)} \hat{\rho}_1^{(1)}] + \hat{c}_3^{(1,2,3)} \\ \hat{\rho}_4^{(1,2,3,4)} &=: \hat{\rho}_1^{(1)} \hat{\rho}_1^{(2)} \hat{\rho}_1^{(3)} \hat{\rho}_1^{(4)} + [\hat{c}_2^{(1,2)} \hat{\rho}_1^{(3)} \hat{\rho}_1^{(4)} + \dots] \\ &\quad + [\hat{c}_3^{(1,2,3)} \hat{\rho}_1^{(4)} + \dots] + [\hat{c}_2^{(1,2)} \hat{c}_2^{(3,4)} + \dots] + \hat{c}_4^{(1,2,3,4)} \end{aligned}$$

etc. Here, the super-index in e.g. $\hat{\rho}_1^{(\kappa)}$ indicates onto which particle the respective operator shall act. The

occurring terms in this cluster expansion have an intuitive interpretation: e.g. $\hat{c}_2^{(1,2)}\hat{\rho}_1^{(3)}$ describes the situation in which the first two particles are correlated while the third one constitutes an independent “spectator”. Let us now briefly summarize the properties of this expansion and the resulting closure approximation: (i) Given a compatible family of RDMs $\hat{\rho}_o^{(1,\dots,o)}$, it is straightforward to see that all cluster operators are contraction-free, i.e. $\text{tr}_1(\hat{c}_o^{(1,\dots,o)}) = 0$. This implies that the truncation approximation of setting $\hat{c}_{\bar{o}+1}^{(1,\dots,\bar{o}+1)}$ to zero is compatible so that the truncated BBGKY EOM would conserve the compatibility of the RDMs. (ii) It is moreover easy to see that the above expansion is even termwise compatible, meaning that for each class of terms on the right hand side of order $(o+1)$ (indicated by square brackets), there exists a corresponding class of terms at order o that constitutes its partial trace, e.g. $\text{tr}_1([\hat{c}_2^{(1,2)}\hat{\rho}_1^{(3)} + \dots]) = \hat{c}_2^{(1,2)}$ if the partial trace is taken over the “third” particle. (iii) Given that the RDMs are invariant under the symmetry operation $\hat{\Pi}_o^{(1,\dots,o)} = \bigotimes_{\kappa=1}^o \hat{\pi}^{(\kappa)}$ where $\hat{\pi}$ denotes a single-particle symmetry operator, i.e. $[\hat{\Pi}_o^{(1,\dots,o)}, \hat{\rho}_o^{(1,\dots,o)}] = 0$, one can show by induction that also the clusters (and thus also the reconstruction functional at order $(\bar{o}+1)$) features this symmetry $[\hat{\Pi}_o^{(1,\dots,o)}, \hat{c}_o^{(1,\dots,o)}] = 0$. (iv) While the clusters and therefore the corresponding reconstruction functional do not single out any particle, meaning $\hat{P}_\pi \hat{c}_o^{(1,\dots,o)} \hat{P}_\pi = \hat{c}_o^{(1,\dots,o)}$ for any permutation $\pi \in S(o)$ and \hat{P}_π denoting the corresponding particle-permutation operator, they lack bosonic symmetry, i.e. $\hat{P}_\pi \hat{c}_o^{(1,\dots,o)} \neq \hat{c}_o^{(1,\dots,o)}$ in general. Thus, projecting onto the bosonic sector is in order here (see [10] and references therein for a more detailed line of argument), which is discussed in the following Section.

2. Symmetrization of the cluster expansion for indistinguishable bosons

Since the clusters as defined in Eq. (18) commute with the respective particle-transposition operators, it is sufficient to apply the respective symmetrization operator $\hat{S}_o = \sum_{\pi \in S(o)} \hat{P}_\pi / o!$ only from the right

$$\begin{aligned} \hat{\rho}_2 &=: \hat{\rho}_1^{(1)} \hat{\rho}_1^{(2)} \hat{S}_2 + \hat{c}_2 & (19) \\ \hat{\rho}_3 &=: (\hat{\rho}_1^{(1)} \hat{\rho}_1^{(2)} \hat{\rho}_1^{(3)} + [\hat{c}_2^{(1,2)} \hat{\rho}_1^{(3)} + \dots]) \hat{S}_3 + \hat{c}_3 \\ \hat{\rho}_4 &=: (\hat{\rho}_1^{(1)} \hat{\rho}_1^{(2)} \hat{\rho}_1^{(3)} \hat{\rho}_1^{(4)} + [\hat{c}_2^{(1,2)} \hat{\rho}_1^{(3)} \hat{\rho}_1^{(4)} + \dots] \\ &\quad + [\hat{c}_3^{(1,2,3)} \hat{\rho}_1^{(4)} + \dots] + [\hat{c}_2^{(1,2)} \hat{c}_2^{(3,4)} + \dots]) \hat{S}_4 + \hat{c}_4 \end{aligned}$$

etc. Apparently, the number of terms in this expansion increases rapidly with increasing order. While we provide a recursive scheme for efficiently evaluating clusters of high order in Section IV B 3, we address here the following more fundamental problems and the corresponding properties of the above cluster expansion: (i) ideal BECs of fixed particle number as correlation-free

reference states, (ii) compatibility, (iii) invariance under symmetries and (iv) size-extensivity. Finally, we briefly comment on differences to the corresponding cluster expansion for fermions.

First, it is natural to require that a correlation measure shall not testify correlations if the N -particle system is fully condensed, i.e. if the system is in a Gross-Pitaevskii mean-field state $|\Psi\rangle = \bigotimes_{j=1}^N |\phi\rangle$ with the condensate wavefunction $|\phi\rangle$. Here, we show that this is indeed the case for the clusters \hat{c}_o defined by (19). Obviously, the 1-RDM of such a BEC reads $\hat{\rho}_1 = |\phi\rangle\langle\phi|$. Evaluating the first class of terms on the right-hand-side of Eq. (19), we find at order o that $(\hat{\rho}_1^{(1)} \dots \hat{\rho}_1^{(o)}) \hat{S}_o = |\phi \dots \phi\rangle\langle\phi \dots \phi|$, i.e. the projector onto the o -fold Hartree product of the condensate wavefunction, which equals exactly $\hat{\rho}_o$. Thereby, all clusters vanish for this state.

We have explicated this illustrative calculation here only in order to demonstrate why we have decided to use the idempotent symmetrization operator $\hat{S}_o = \hat{S}_o^2$ and trace-one RDMs in the expansion (19). This is namely in contrast to most other works which typically use $D_{(i_1,\dots,i_o),(j_1,\dots,j_o)}^o$ (featuring trace $N!/(N-o)!$) as RDMs and $o! \hat{S}_o$ as the symmetrization operator for the cluster expansion, which is then also called cumulant expansion¹⁰ [10, 12, 13]. While the cumulant expansion is perfectly suitable for systems with vanishing chemical potential, e.g. photons [48], it testifies non-vanishing correlations on all orders for an ideal BEC with a fixed number N of atoms, even if N becomes large [50]. Thereby, this approach is not suitable for systematically taking correlations into account on top of a BEC. In numerical experiments, we have indeed observed that the truncated BBGKY EOM become almost immediately exponentially unstable and give wrong results if the cumulant expansion is used for the truncation (data not shown). To cure this flaw, we employ the trace-one RDM and the idempotent symmetrization operator for the cluster expansion in this work. In passing, we note that recently also an alternative solution to this problem based on a non-unitary transformation into the so-called excitation picture of a BEC has been developed [50–52].

Second, in order to conserve the compatibility of the initial RDMs, a cluster expansion should ideally respect compatibility, i.e. its clusters should be contraction-free. In contrast to the case of identical but spinless particles (Section IV B 1), however, neither is the expansion (19) termwise compatible nor are the thereby defined clusters contraction-free in general. This can be easily seen by inspecting the second order, for which a straightforward calculation gives $\text{tr}_1(\hat{c}_2) = (\hat{\rho}_1 - \hat{\rho}_1^2)/2$ (see also [46]). Thus, the partial trace of \hat{c}_2 vanishes only if $\hat{\rho}_1$ is idempotent, which is equivalent to the total system being in a

¹⁰ The cumulants can be calculated as derivatives of the generating function $\xi(\{\alpha_r\}, \{\alpha_r^*\}) = \ln(\langle \exp(\sum_r \alpha_r \hat{a}_r^\dagger) \exp(-\sum_r \alpha_r^* \hat{a}_r) \rangle)$ with respect to α_i and α_j^* and setting all α 's to zero (see e.g. [13]).

Gross-Pitaevskii mean-field state where all clusters vanish anyway (see also [34]). In Section IV B 3, we restore the compatibility of the cluster expansion (19) by means of a unitarily invariant decomposition of the cluster.

Third, as in the case of indistinguishable spinless particles, the clusters \hat{c}_o defined by Eq. (19) commute with the symmetry operator $\hat{\Pi}_o$ given that the state of the total system features such a symmetry. This is an immediate consequence of $[\hat{\Pi}_o, \hat{S}_o] = 0$.

Fourth, a cluster expansion should ideally be size-extensive in the sense that it does not testify correlations between two subsystems which feature no mode-entanglement between each other. Even in the absence of mode-entanglement, the bosonic particle-exchange symmetry does in general induce correlations between particles, which should be appropriately described by our methodological approach, of course. Such correlations should, however, be excluded from the correlation *definition*, on which a cluster expansion is based, so that higher order clusters can be neglected without impeding physical mechanisms that are induced by such bosonic-symmetry induced correlations. Here, we relax this requirement and only demand that a system consisting of two independent ideal BECs, i.e. the simplest case of a two-fold fragmented condensate, shall not feature \hat{c}_o correlations. While a single BEC is correlation-free as discussed above, the cluster expansion (19) unfortunately diagnoses correlations between these two independent BECs, which can be seen as follows. Suppose that $N_{A/B}$ atoms reside in the condensate wavefunction $|\phi_{A/B}\rangle$ such that the total system state reads $|\Psi\rangle = |N_A, N_B\rangle$. A straightforward calculation shows that two-particle correlations \hat{c}_2 are present in this case, even in the infinite particle limit $N = N_A + N_B \rightarrow \infty$ with $\lambda = N_A/N$ kept constant where one obtains the following expression

$$\hat{c}_2 = \lambda(1 - \lambda)|\phi_{AB}^+\rangle\langle\phi_{AB}^+| + \mathcal{O}(1/N) \quad (20)$$

with $|\phi_{AB}^+\rangle = (|\phi_A\phi_B\rangle + |\phi_B\phi_A\rangle)/\sqrt{2}$. So the correlation measure \hat{c}_2 testifies correlations between the two independent condensates, which stem solely from the bosonic particle-exchange symmetry.

In order to approximately cure this flaw of lacking size-extensivity, we have explored the construction of an alternative bosonic cluster expansion, which we, however, discard in the end due to a mathematical subtlety. Let us nevertheless briefly report on the concepts as well as pitfall here. Inspired by [96], the central idea is to modify the different classes of terms of the expansion (19) such that termwise compatibility is ensured and so-called multi-orbital mean-field states [97, 98] possess vanishingly small correlations. The latter means that there are an occupation-number vector \mathbf{k} and single-particle basis states such that the total wavefunction can be represented by a single permanent $|\Psi\rangle = |\mathbf{k}\rangle$. The second order of this alternative cluster expansion has been discussed in [99, 100] as well as applied for an in-depth analysis of quantum many-body dynamics far-off equilibrium

[100]. In Appendix E, we exemplarily outline the construction of this expansion. Unfortunately, however, it turns out that the thereby defined cluster operators may depend on the choice of the single-particle basis in the case of NP degeneracies, which hinders us to utilize this approach for truncating the BBGKY hierarchy. For this reason, we stick to the symmetrized cluster expansion (19) and make it compatible (see Section IV B 3).

Finally, we briefly compare the above properties to the fermionic case (with fixed particle number N). Here, the cumulant expansion is the appropriate approach since it ensures that Hartree-Fock states do not feature correlations [49] (whereas using the idempotent antisymmetrization operator and trace-one RDMs leads to correlations in this case). Analogously to the bosonic case, the cumulants turn out to be only contraction-free if the system is in a Hartree-Fock state. Yet surprisingly, the cumulants prove to be size-extensive [13, 101, 102].

3. Recursive formulation of the compatible symmetrized cluster expansion

We now come back to the symmetrized cluster expansion (19), make it compatible by means of a unitarily invariant decomposition [103–106] and finally give a recursive formulation allowing for an efficient evaluation at high orders.

Apparently, the cluster $\hat{c}_{\bar{o}+1}$ defined by (19) contains information about the RDMs of lower order such that neglecting it violates compatibility. These important pieces of information can be identified by the so-called unitarily invariant decomposition (UID) of hermitian bosonic operators [105, 106], which allows for uniquely decomposing any o -body operator $\hat{B}_o \in \mathcal{B}_o$ into $\hat{B}_o = \hat{B}_o^{\text{red}} \oplus \hat{B}_o^{\text{irr}}$ where \hat{B}_o^{red} contains all information about the partial traces of \hat{B}_o , i.e. $\text{tr}_1(\hat{B}_o^{\text{red}}) = \text{tr}_1(\hat{B}_o)$, and \hat{B}_o^{irr} covers what may be termed irreducible o -particle properties. This decomposition is unique in the sense of being invariant under unitary transformations of the single-particle basis. We further note that \hat{B}_o^{red} is a linear functional in all partial traces $\text{tr}_k(\hat{B}_o)$ of \hat{B}_o , which we explicate in Appendix F.

Analogously to [72, 73] dealing with fermions, we now define the $(\bar{o}+1)$ -particle correlations which are neglected in the truncation approximation to be the irreducible, i.e. contraction-free component of the cluster $\hat{c}_{\bar{o}+1}$ of the expansion (19) (see [46] for an alternative approach for ensuring compatibility). If we abbreviate the approximation for $\hat{\rho}_{\bar{o}+1}$ as induced by (19) by $\hat{\eta}_{\bar{o}+1} := \hat{\rho}_{\bar{o}+1} - \hat{c}_{\bar{o}+1}$, we obtain the following compatible closure approximation

$$\hat{\rho}_{\bar{o}+1}^{\text{appr}} := \hat{\eta}_{\bar{o}+1} + \hat{c}_{\bar{o}+1}^{\text{red}} = \hat{\rho}_{\bar{o}+1}^{\text{red}}[\hat{\rho}_1, \dots, \hat{\rho}_{\bar{o}}] \oplus \hat{\eta}_{\bar{o}+1}^{\text{irr}}. \quad (21)$$

Practically, this means that we have to calculate (i) $\hat{\eta}_{\bar{o}+1}$, which equals the right-hand-side of (19) when neglecting the unknown $\hat{c}_{\bar{o}+1}$, (ii) its contraction-free component $\hat{\eta}_{\bar{o}+1}^{\text{irr}}$ via the UID and (iii) the reducible component $\hat{\rho}_{\bar{o}+1}^{\text{red}}$

of the unknown $\hat{\rho}_{\bar{o}+1}$, which, however, depends only on its known partial traces, i.e. the RDMs which are propagated via the truncated BBGKY EOM.

In this way, the truncation approximation consists in replacing the exact $\hat{\rho}_{\bar{o}+1}^{\text{irr}}$ by $\hat{\eta}_{\bar{o}+1}^{\text{irr}}$. In passing, we note that the UID ensures only compatibility but not termwise compatibility as fulfilled by the alternative cluster expansion outlined in Appendix E. In contrast to this alternative cluster expansion however, the closure approximation (21) is invariant under unitary transformations of the SPFs as a consequence of the UID. Thus, the gauge

$$\hat{F}_{\sigma_1, \dots, \sigma_K}^{n_1, \dots, n_K} \equiv \left[\hat{c}_{\sigma_1}^{(1, \dots, \sigma_1)} \hat{c}_{\sigma_1}^{(\sigma_1+1, \dots, 2\sigma_1)} \dots \hat{c}_{\sigma_1}^{([n_1-1]\sigma_1+1, \dots, n_1\sigma_1)} \hat{c}_{\sigma_2}^{(n_1\sigma_1+1, \dots, n_1\sigma_1+\sigma_2)} \dots \hat{c}_{\sigma_K}^{(o-\sigma_{K-1}, \dots, o)} + \right. \\ \left. + \text{all distinguishable permutations of the particle labels} \right] \hat{S}_o, \quad (22)$$

where $o = \sum_{r=1}^K n_r \sigma_r$. Here, we assume the ordering $0 < \sigma_1 < \sigma_2 < \dots < \sigma_K$ as well as $n_r > 0$ for all $r = 1, \dots, K$. Now we may express the cluster \hat{c}_o of the expansion (19) as

$$\hat{c}_o = \hat{\rho}_o - \sum_{K=1}^{o-1} \sum_{\substack{n_1, \dots, n_K > 0 \\ 0 < \sigma_1 < \sigma_2 < \dots < \sigma_K}} \sum_{r=1}^K n_r \sigma_r = o \hat{F}_{\sigma_1, \dots, \sigma_K}^{n_1, \dots, n_K}. \quad (23)$$

As a matter of fact, this sum runs over as many symbols as there are integer partitions of the number o minus one, i.e. $P(o) - 1$ with $P(\cdot)$ denoting the partition function, such that we can use an algorithm which generates integer partitions for labeling the symbols of a given order. In appendix G, we prove the following two computation rules, which are sufficient for evaluating the symbol $\hat{F}_{\sigma_1, \dots, \sigma_K}^{n_1, \dots, n_K}$ in terms of the symbols of lower orders:

$$\hat{F}_{\sigma}^n = \frac{1}{n} \hat{J}_{(n-1)\sigma}^{\sigma} (\hat{F}_{\sigma}^{n-1}, \hat{c}_{\sigma}) \quad (24)$$

$$\hat{F}_{\sigma_1, \dots, \sigma_K}^{n_1, \dots, n_K} = \hat{J}_{o-n_K \sigma_K}^{n_K \sigma_K} (\hat{F}_{\sigma_1, \dots, \sigma_{K-1}}^{n_1, \dots, n_{K-1}}, \hat{F}_{\sigma_K}^{n_K}), \quad (25)$$

where again $o = \sum_{r=1}^K n_r \sigma_r$ and $\hat{J}_{o_1}^{o_2}(\cdot, \cdot)$ denotes the joining super-operator introduced in Appendix A. In our software implementation, we store for each symbol $\hat{F}_{\sigma_1, \dots, \sigma_K}^{n_1, \dots, n_K}$ at the order o the (integer-partition based) labels of the symbols of lower order that are needed for applying the respective computation rule. The required joining operations (A3) are implemented in a highly efficient manner by using the combinadic-number based labeling of bosonic number states [107] in combination with mapping tables [81] for easily addressing the label of the $(o_1 + o_2)$ -particle number state $|\mathbf{a}_1 + \mathbf{a}_2\rangle$ given the o_1 -particle number state $|\mathbf{a}_1\rangle$ and the o_2 -particle number state $|\mathbf{a}_2\rangle$.

Having recursively calculated all clusters \hat{c}_o up to the truncation order \bar{o} , the (incompatible) auxiliary closure

invariance of the truncated EOM (5), (6) with respect to the constraint operator g_{ij} is ensured by (21).

In order to construct the closure approximation (21) also at high truncation orders \bar{o} , we finally state an efficient recursive algorithm for evaluating the clusters \hat{c}_o of the expansion (19). The key idea here is to find computation rules for the different classes of expansion terms which are indicated in (19) by square brackets. If we define the one-body cluster by $\hat{c}_1 \equiv \hat{\rho}_1$, we can abbreviate the class of terms at order o which involves K different clusters, where the cluster \hat{c}_{σ_r} occurs n_r -times ($r = 1, \dots, K$), by the symbol

approximation $\hat{\eta}_{\bar{o}+1}$ can be constructed, from which we finally obtain the compatible closure approximation (21) via the UID (see Eq. (F2)). This is how we truncate the BBGKY hierarchy in the numerical simulations of Section VI.

C. On the role of two-particle correlations for dynamical quantum depletion

After the above technical considerations on how to properly define and evaluate few-particle correlations for constructing a cluster expansion, we investigate here the impact of two-particle correlations on the 1-RDM natural populations $\lambda_r^{(1)}$, which is highly relevant for understanding the mechanisms underlying dynamical quantum depletion and fragmentation of Bose-Einstein condensates [18]. We address this problem from two perspectives.

First, we analyze the role of the irreducible component $\hat{\rho}_2^{\text{irr}}$ on the 1-RDM dynamics. By inserting the decomposition $\hat{\rho}_2 = \hat{\rho}_2^{\text{red}} \oplus \hat{\rho}_2^{\text{irr}}$ together with the explicit expression (F2) for $\hat{\rho}_2^{\text{red}}$ into (6), we find the following

$$i\partial_t \langle \varphi_q | \hat{\rho}_1 | \varphi_p \rangle = \langle \varphi_q | ([\hat{h}_{\text{eff}}, \hat{\rho}_1] + \hat{I}_1(\hat{\rho}_2^{\text{irr}})) | \varphi_p \rangle, \quad (26)$$

where the effective single-particle Hamiltonian reads $\hat{h}_{\text{eff}} = \hat{h} - \hat{g} + \frac{N-1}{m+\frac{1}{2}} \text{tr}_1[\hat{v}_{12}(\mathbb{1} + \hat{P}_{12})]$ and \hat{P}_{12} permutes the particle labels 1 and 2. So the coupling of a single atom being in the state $\hat{\rho}_1$ to the remaining $(N-1)$ atoms via the collision integral $\hat{I}_1(\hat{\rho}_2)$ has a two-fold impact. While the reducible component $\hat{\rho}_2^{\text{red}}$ only leads to a renormalization of the single-particle Hamiltonian to \hat{h}_{eff} , an effect sometimes called Lamb shift in the context of open quantum-systems [108], non-unitary dynamics of the 1-RDM can only be induced by the irreducible component $\hat{\rho}_2^{\text{irr}}$. Thus, only these correlations can drive the

dynamics of the NPs $\lambda_r^{(1)}(t)$. We note that this result does not depend on whether the RDMs are represented in the dynamically adapted MCTDHB SPF basis or with respect to some time-independent basis. It is only important that the single-particle basis is finite, which is a technical requirement for the UID [103–106].

Second, we explicate the EOM (12) for the NPs $\lambda_r^{(1)}(t)$

$$\partial_t \lambda_r^{(1)} = 2(N-1) \sum_{i,j,k=1}^m f_{ik} f_{jr} \Im(v_{rjik} \rho_{\mathbf{e}_i+\mathbf{e}_k, \mathbf{e}_r+\mathbf{e}_j}^2), \quad (27)$$

where we remind the reader about the definition $f_{qp} = \sqrt{(\delta_{qp} + 1)/2}$. Employing the hermiticity of \hat{v}_{12} as well as $[\hat{P}_{12}, \hat{v}_{12}] = 0$, one easily verifies that the diagonal elements $\rho_{\mathbf{a}, \mathbf{a}}^2$ do not contribute to the right hand side of Eq. (27). As a result, the NP evolution can only be driven by the coherences $\rho_{\mathbf{a}, \mathbf{b}}^2$ with $\mathbf{a} \neq \mathbf{b}$ of the 2-RDM represented in permanents with respect the instantaneous NOs $|\phi_s^1\rangle$. More precisely, only such coherences in the irreducible component $\hat{\rho}_2^{\text{irr}}$ can induce non-trivial dynamics of the 1-RDM NPs.

Besides being of conceptual interest, this insight has also consequences for truncation approximations. Truncating the BBGKY hierarchy at the first order using the recipe outlined in Section IV B 3 means using the following closure approximation

$$\hat{\rho}_2^{\text{appr}} = \sum_{q,p=1}^m (1 + \delta_{qp}) \lambda_q^{(1)} \left(\frac{\lambda_p^{(1)}}{2} + \frac{1 - \lambda_q^{(1)}}{m+2} \right) |\mathbf{e}_q + \mathbf{e}_p\rangle \langle \mathbf{e}_q + \mathbf{e}_p| - \frac{1 - \text{tr}(\hat{\rho}_1^2)}{(m+2)(m+1)} \mathbb{1}_2^+, \quad (28)$$

where the number-states are given with respect to the instantaneous NOs $|\phi_s^1\rangle$. In this basis, $\hat{\rho}_2^{\text{appr}}$ turns out to be diagonal implying that the NPs $\lambda_r^{(1)}(t)$ are constant in time. Thus, when using the truncation scheme of Section IV B 3, the truncation order \bar{o} must be larger than one in order to account for dynamical quantum depletion (see also [88, 89, 91] for a similar discussion for the fermionic case).

Similarly, if the total system is in a multi-orbital mean-field state, i.e. a single permanent (cf. Eq. (E1) of Appendix E) or if one truncates the BBGKY hierarchy at order $\bar{o} = 1$ by means of the alternative cluster expansion outlined in Appendix E, the 2-RDM entering the right hand side of Eq. (27) is diagonal in the NO number-state basis, leading again to stationary NPs [99]. Consequently, for a system being initially prepared in a single permanent (as in the case of two independent BECs discussed in Section IV B 2), a Taylor expansion of $\lambda_r^{(1)}(t)$ about $t = 0$ lacks the linear term. This is a consequence of $|\Psi_t\rangle$ being continuous in time, which requires a continuous admixture of further number-states¹¹ (with respect

to the instantaneous NOs) for having a well-defined finite time-derivative of $\lambda_r^{(1)}$.

V. RDM REPRESENTABILITY AND PURIFICATION STRATEGIES

While the BBGKY EOM truncated by virtue of the cluster expansion discussed in Section IV B 3 conserve the trace and compatibility of the RDMs, other properties of RDMs are not ensured. As we shall investigate in detail in Section VI, the initial RDM lose e.g. their positive semi-definiteness in the course of the time evolution due to the applied truncation approximation, which has also been observed in [69, 72] when truncating the BBGKY hierarchy for fermionic problems at order $\bar{o} = 2$. In this Section, we first review important necessary representability conditions which $\hat{\rho}_o$ has to fulfill in order to represent an o -RDM of a bosonic N -particle system. Thereafter, we discuss purification strategies for preventing representability defects in the solution of the truncated BBGKY EOM.

A. Necessary representability conditions

Besides being compatible and of unit trace, which shall be assumed in the following, there are further important necessary representability conditions on the o -RDM. For reviewing them, we assume the total N -particle system to be in some pure state $|\Psi\rangle$ and follow the lines of [109–111]. Then one has $\langle \Psi | \hat{A}_o^\dagger \hat{A}_o | \Psi \rangle \geq 0$ for an arbitrary (not necessarily hermitian) polynomial \hat{A}_o of order o in the annihilation and creation operators $\hat{a}_r^{(\dagger)}$, e.g.

$$\begin{aligned} \hat{A}_2 = & \sum_{i,j=1}^m (c_{ij}^{(1)} \hat{a}_i \hat{a}_j + c_{ij}^{(2)} \hat{a}_i^\dagger \hat{a}_j^\dagger + c_{ij}^{(3)} \hat{a}_i \hat{a}_j^\dagger + c_{ij}^{(4)} \hat{a}_i^\dagger \hat{a}_j) \\ & + \sum_{i=1}^m (c_i^{(5)} \hat{a}_i + c_i^{(6)} \hat{a}_i^\dagger) + c^{(7)} \end{aligned} \quad (29)$$

with the $c^{(\kappa)}$'s being arbitrary complex numbers. Setting certain $c^{(\kappa)}$'s to zero while allowing the remaining ones to take arbitrary values, the inequality $\langle \Psi | \hat{A}_o^\dagger \hat{A}_o | \Psi \rangle \geq 0$ implies the positive semi-definiteness of various matrices such as the o -RDM $D_{(i_1, \dots, i_o), (j_1, \dots, j_o)}^o = \langle \Psi | \hat{a}_{j_1}^\dagger \dots \hat{a}_{j_o}^\dagger \hat{a}_{i_o} \dots \hat{a}_{i_1} | \Psi \rangle$ or the so-called o -hole RDM $Q_{(i_1, \dots, i_o), (j_1, \dots, j_o)}^o = \langle \Psi | \hat{a}_{j_1} \dots \hat{a}_{j_o} \hat{a}_{i_o}^\dagger \dots \hat{a}_{i_1}^\dagger | \Psi \rangle$. By normal ordering, all these matrices can be expressed in terms of the o -RDM and RDMs of lower order such that the

that the so-called time-dependent multi-orbital mean-field theory [98] has to rely on stationary occupations of the dynamically optimized orbitals.

¹¹ As a side remark, this can be seen as a deeper reason for the fact

required positive semi-definiteness of these matrices effectively induce necessary representability conditions for the RDMs. Fulfilling all these conditions implies that the Heisenberg uncertainty relation $\langle(\hat{A} - \langle\hat{A}\rangle)^2\rangle\langle(\hat{B} - \langle\hat{B}\rangle)^2\rangle \geq |\langle[\hat{A}, \hat{B}]\rangle|^2/4$, with the expectation values being evaluated with respect to $\hat{\rho}_o$, is fulfilled for any observables \hat{A}, \hat{B} involving at most $\lfloor o/2 \rfloor$ -body operators [110]. In contrast to this, violations of these conditions can imply an unphysical violation of the uncertainty relation between two such observables.

Since most observables of interest in the field of ultracold atoms involve at most two-body operators, we focus on representability conditions for the 1- and 2-RDM here. Whereas being positive semi-definite is necessary and sufficient for the representability of $\hat{\rho}_1$, the known necessary and sufficient representability conditions for the 2-RDM are not useful in practice [109] (see [111], which deals with a model system, for an exception). Therefore, we consider here only the important necessary D -, Q - and G -condition for representability [13, 109], which can be derived as outlined above. In the following, we assume $\hat{\rho}_1$ to be representable. Then, the D -condition, i.e. the positive semi-definiteness of $D_{(i_1, j_1), (i_2, j_2)}^2$, directly implies the positive semi-definiteness of the two-hole RDM $Q_{(i_1, j_1), (i_2, j_2)}^2$ (the Q -condition) [111]. In contrast to this, the positivity of the one-particle-one-hole RDM $G_{(i_1, j_1), (i_2, j_2)}^2 = \langle\Psi|\hat{a}_{i_1}^\dagger\hat{a}_{j_1}\hat{a}_{j_2}^\dagger\hat{a}_{i_2}|\Psi\rangle$ (the G -condition) is not inherited from the D -condition. This is because $G_{(i_1, j_1), (i_2, j_2)}^2$ is not related to the D_2 -matrix but its partial transposed via $G_{(i_1, j_1), (i_2, j_2)}^2 = D_{(i_2, j_1), (i_1, j_2)}^2 + \delta_{j_1 j_2} D_{i_2, i_1}^1$ [111]. Thereby, the G -condition constitutes an independent representability requirement on the 2-RDM, which can be crucial as highlighted by the numerical results of e.g. [111]. Besides the D -condition, we, however, do not employ the above G -condition but its more restrictive original variant [109], which demands the positive semi-definiteness of the following matrix

$$K_{(i_1, j_1), (i_2, j_2)}^2 = \frac{1}{\mathcal{N}_K} \left(G_{(i_1, j_1), (i_2, j_2)}^2 - D_{j_1, i_1}^1 D_{i_2, j_2}^1 \right). \quad (30)$$

In contrast to [109], however, we have included the normalization factor $\mathcal{N}_K = N(N+m-1) - \text{tr}(\hat{D}_1^2)$ in the definition in order to enforce¹² unit trace, $\sum_{i,j} K_{(i,j), (i,j)}^2 = 1$, such that the eigenvalues of $\hat{\rho}_2$ and $K_{(i_1, j_1), (i_2, j_2)}^2$ attain comparable values. This K -condition¹³ can be obtained by the above recipe by setting all $c^{(\kappa)}$ to zero except for $c_{ij}^{(3)}$ and $c^{(7)}$. Finally, we remark that violating the K -condition can have severe impact on the predictions for

density-density correlations being readily accessible in ultracold quantum gas experiments (see e.g. [112]). Namely in this case, the positive semi-definiteness of the density-fluctuation covariance matrix $C(x, y) = \langle\delta\hat{\rho}(x)\delta\hat{\rho}(y)\rangle$, with $\delta\hat{\rho}(x) = \hat{\psi}^\dagger(x)\hat{\psi}(x) - \langle\hat{\psi}^\dagger(x)\hat{\psi}(x)\rangle$ and $\hat{\psi}(x)$ denoting the field operator, is not guaranteed (see Eq. (7.14) of [109]).

B. Correction strategies

Since the truncated BBGKY EOM do not respect the above necessary representability constraints, we discuss here correction strategies. These strategies can be viewed as an attempt to approximately compensate that we neglect $\hat{I}_o(\hat{c}_{\sigma+1}^{\text{irr}})$ in the closure approximation (see Eq. (21)). First, we discuss how to correct the solution after propagating the truncated BBGKY EOM for a small time-step Δt . Thereafter, we summarize a strategy for correcting the truncated BBGKY EOM themselves.

1. Purification of the solution

Originally designed for correcting a 2-RDM with slight representability defects in the context of contracted Schrödinger equations, the iterative purification scheme by Mazziotti [113] has been employed for correcting the truncated BBGKY EOM for electronic problems in [72], which is known as dynamical purification. Since our approach relies partly on these concepts, we briefly review the main ideas of that dynamical purification scheme.

Assuming that $\hat{\rho}_2(t)$ is representable, propagating the truncated BBGKY EOM for a fixed, small time-step Δt results in $\hat{\rho}_2(t + \Delta t)$ which features a slight representability defect, i.e. slightly violates a necessary representability condition. In the following, we shall assume that its partial trace, $\hat{\rho}_1(t + \Delta t)$, is representable, i.e. positive semi-definite. Otherwise an appropriate purification scheme for $\hat{\rho}_1(t + \Delta t)$ has to be applied and the reducible part $[\hat{\rho}_2(t + \Delta t)]^{\text{red}}$ has to be updated accordingly [113].

Now the idea is to iteratively update the 2-RDM by adding a contraction-free correction term \hat{C}_2 , i.e. $\hat{\rho}_2(t + \Delta t) \rightarrow \hat{\rho}_2(t + \Delta t) + \hat{C}_2$, such that its partial trace remains invariant. The Mazziotti purification scheme relies on an ansatz for \hat{C}_2 . Namely for correcting a lack of positive semi-definiteness of $\hat{\rho}_2(t + \Delta t)$, one assumes $\hat{C}_2 = \sum_{i \in I} a_i [|\phi_i^2\rangle\langle\phi_i^2|]^{\text{irr}}$, where I denotes the set of indices of all NOs whose NPs $\lambda_i^{(2)}$ lie below a small negative threshold of e.g. $\epsilon = -10^{-10}$. The coefficients a_i are determined such that \hat{C}_2 raises all negative NPs of $\hat{\rho}_2(t + \Delta t)$ to zero in first order perturbation theory, i.e. $\lambda_i^{(2)} + \langle\phi_i^2|\hat{C}_2|\phi_i^2\rangle = 0$, which constitutes a system of linear equations for the a_i 's. The ansatz for \hat{C}_2 can simi-

¹² We note that this normalization factor is derived under the assumption of representability of the 2-RDM. Representability defects might lead to (slight) deviations from trace one.

¹³ Originally, this matrix was denoted as G in [109], but in order to distinguish it from the one-particle-one-hole matrix we decided to use the letter K in this work.

larly be extended¹⁴ to also improve negative eigenvalues of $G_{(i_1, j_1), (i_2, j_2)}^2$ [114]. The updated RDM $\hat{\rho}_2(t + \Delta t) + \hat{\mathcal{C}}_2$ may still violate a representability condition such that this update scheme has to be iterated.

While the dynamical purification based on the Mazziotti scheme has proven to be successful for the dynamics of electrons in atoms [72, 73], it is not minimal invasive by construction and may violate energy conservation. For this reason, we liberate the above dynamical-purification scheme from its underlying ansatz for the correction $\hat{\mathcal{C}}_2$, which is determined by solving an optimization problem in this work. First, we note that updating the 2-RDM to $\hat{\rho}_2(t + \Delta t) + \hat{\mathcal{C}}_2$ also implies an update of the K -operator $\hat{K}_2 = \sum_{i_1, i_2, j_1, j_2} K_{(i_1, j_1), (i_2, j_2)}^2 |\varphi_{i_1} \varphi_{j_1}\rangle \langle \varphi_{i_2} \varphi_{j_2}|$ to $\hat{K}_2 + \hat{\Delta}_2$ due to the relationship between \hat{K}_2 and \hat{D}_2 . We explicate the operator $\hat{\Delta}_2$ in Appendix H where also all the details for the following purification scheme are provided. Now, we determine the update $\hat{\mathcal{C}}_2$ by minimizing the p -norm

$$|\hat{\mathcal{C}}_2|_p \equiv \sum_{\mathbf{n}, \mathbf{m} | 2} |\mathcal{C}_{\mathbf{n}, \mathbf{m}}^2|^p \quad (31)$$

under the linear constraints of being (i) hermitian, (ii) contraction-free, $\text{tr}_1(\hat{\mathcal{C}}_2) = 0$, (iii) energy conserving, $\text{tr}(\hat{v}_{12}\hat{\mathcal{C}}_2) = 0$, (iv) symmetry respecting if existing, $[\hat{\Pi}_2, \hat{\mathcal{C}}_2] = 0$, (v) raising negative NPs below a threshold ϵ to zero in first order perturbation theory, $\lambda_i^{(2)} + \langle \phi_i^2 | \hat{\mathcal{C}}_2 | \phi_i^2 \rangle = 0$ for all i with $\lambda_i^{(2)} < \epsilon$ and (vi) raising negative eigenvalues ξ_i of \hat{K}_2 below a threshold ϵ to zero in first order perturbation theory, $\xi_i + \langle \Xi_i | \hat{\Delta}_2 | \Xi_i \rangle = 0$ for all i with $\xi_i < \epsilon$, where $|\Xi_i\rangle$ denotes the eigenvector of \hat{K}_2 corresponding to ξ_i . Having solved this optimization problem, we judge whether the updated 2-RDM fulfills the D - and K -condition and iterate the updating procedure if necessary.

Specifically, we have performed numerical experiments on the 1-norm as well as the 2-norm (also called Frobenius norm). Mathematically, the case $p = 1$ leads to the so-called basis pursuit problem [115, 116], which we solve by the linear-program solver SOPLEX of the SCIP optimization suite [117]. The case $p = 2$ results in a quadratic program, which we solve with Lagrange multipliers for the constraints. In our numerical simulations, however, we found that the 1-norm scheme has often a harder time to converge to a 2-RDM which respects the D - and the K -condition and results in a much more noisy time-evolution of e.g. the NPs $\lambda_i^{(2)}$, as compared to the Frobenius norm. This finding indicates that the correction operator $\hat{\mathcal{C}}_2$ is not a sparse matrix (as favored by the 1-norm). For this reason, we only apply the $p = 2$ approach in Section VI.

This minimal-invasive dynamical purification scheme can conceptually be extended for also purifying higher order RDMs, which, however, becomes computationally harder because of the resulting higher-dimensional minimization problems. For simplicity, we use the optimization approach for the 2-RDM only and make the Mazziotti ansatz for achieving $\hat{\rho}_o \geq 0$ at orders $o > 2$. For putting purifications on different orders together, we purify the lowest order where a purification defect has been observed first, update accordingly the reducible part of the next order RDM and continue with their purification (if necessary), etc.

Finally, let us remark that asking for a (small) correction $\hat{\mathcal{C}}_2$ which makes a given indefinite $\hat{\rho}_2(t + \Delta t)$ positive semi-definite constitutes a non-linear problem. Both the Mazziotti and our minimal invasive scheme replace this problem by a linear one (plus iteration) due to the requirement on the shift of eigenvalues in first order perturbation theory. Thereby, these two approaches are perturbative in some sense, which can hinder these iterative schemes to converge to a fixed point fulfilling the posed representability conditions as observed in Section VI. Therefore, we provide next a non-perturbative strategy aiming at correcting and stabilizing the truncated BBGKY EOM themselves.

2. Correction of the EOM

The central idea of this correction strategy is to allow slight representability defects in the RDM but modify its EOM in a minimal invasive way such that these defects are exponentially damped and the EOM thereby stabilized. As above, we first describe the correction strategy for the EOM of the 2-RDM with all technical details covered by Appendix I and then comment on an extension to the EOM of higher order RDM.

Let us abbreviate the EOM (6) for the o -RDM as follows $\partial_t \rho_{\mathbf{n}, \mathbf{m}}^o = \langle \mathbf{n} | \hat{R}_o | \mathbf{m} \rangle$ (note that the negative imaginary unit is absorbed in \hat{R}_o). Our aim now is to correct \hat{R}_2 by $\hat{R}_2 + \hat{\mathcal{C}}_2$ such that negative eigenvalues of $\hat{\rho}_2$ or \hat{K}_2 are exponentially damped to zero. First, we note that a correction of \hat{R}_2 also implies a modification of the EOM for \hat{K}_2 , which shall be denoted as $\partial_t K_{(i_1, j_1), (i_2, j_2)}^2 = \langle \varphi_{i_1} \varphi_{j_1} | \hat{T}_2 | \varphi_{i_2} \varphi_{j_2} \rangle$, namely to $\hat{T}_2 \rightarrow \hat{T}_2 + \hat{\Delta}_2$. This is due to the relationship between \hat{K}_2 and \hat{D}_1, \hat{D}_2 . In Appendix I, we explicate the respective expressions.

As for the RDM purification scheme discussed above, we determine the $\hat{\mathcal{C}}_2$ by minimizing the 2-norm (31) under certain linear constraints. (i) We demand $\hat{\mathcal{C}}_2$ to be hermitian because of $\hat{R}_2^\dagger = \hat{R}_2$. (ii) The correction term shall be contraction-free, $\text{tr}_1(\hat{\mathcal{C}}_2) = 0$, because the conservation of compatibility as ensured by our truncation approximation should not be affected by the EOM correction. Another way to motivate demand (ii) is to view $\hat{\mathcal{C}}_2$ as an effective approximation of the neglected term $-i \hat{I}_2(\hat{c}_3^{\text{irr}})$

¹⁴ In the case of fermions, where the Q -condition is independent of the D -condition, this ansatz can be extended to also correct slightly negative eigenvalues of the 2-hole RDM [113].

(when truncating at $\bar{o} = 2$). In Appendix J, we prove that the collision integral $I_o(\hat{A}_o)$ with a contraction-free argument \hat{A}_o is itself contraction-free. (iii) The energy conservation as ensured by the truncation approximation shall not be affected, which amounts to $\text{tr}(\hat{v}_{12}\hat{C}_2) = 0$ because of \hat{C}_2 being contraction-free. (iv) Symmetries if existent shall be respected by the correction, i.e. $[\hat{\Pi}_2, \hat{C}_2] = 0$. (v) In order to damp negative NPs $\lambda_r^{(2)}$, we make use of the NP EOM $\partial_t \lambda_r^{(2)} = -i\langle \phi_r^2 | \hat{I}_2(\hat{\chi}_3) | \phi_r^2 \rangle$ (see Section III C), where $\hat{\chi}_3$ stands for $\hat{\rho}_3^{\text{aPPF}}$ if $\bar{o} = 2$ and for $\hat{\rho}_3$ if $\bar{o} > 2$. Upon EOM correction, this equation is modified to $\partial_t \lambda_r^{(2)} = \langle \phi_r^2 | [\hat{C}_2 - i\hat{I}_2(\hat{\chi}_3)] | \phi_r^2 \rangle$, which we require to equal $-\eta\lambda_r^{(2)}$ for all negative NPs below a small threshold, $\lambda_r^{(2)} < \epsilon$. Thereby, all these negative NPs are damped with a damping rate η as $\lambda_r^{(2)}(t + \tau) = \lambda_r^{(2)}(t) \exp(-\eta\tau)$ for all t and $\tau \geq 0$ where $\lambda_r^{(2)}(t + \tau)$ is smaller than ϵ . At the same time, also the NPs above the threshold are forced to move such that the trace of the 2-RDM stays unity. Here, the damping constant η should be chosen to be much larger than any system frequency of physical relevance. (vi) Analogously, one can show that the modified EOM for the \hat{K}_2 eigenvalues reads $\partial_t \xi_r = \langle \Xi_r | [\hat{T}_2 + \hat{\Delta}_2] | \Xi_r \rangle$ which is again set to $-\eta\xi_r$ given that $\xi_r < \epsilon$.

As in the case of the RDM purification, one can in principle extend this minimal-invasive correction scheme of the EOM also to higher orders, incorporating various necessary representability conditions (see e.g. [110] for the cases $o = 3, 4$). In this work, however, we only make the Mazziotti ansatz $\hat{C}_o = \sum_{i|\lambda_i^{(o)} < \epsilon} a_i [|\phi_i^o\rangle\langle\phi_i^o|]^{\text{irr}}$ for orders $o > 2$ and determine the a_i coefficients such that (v) is fulfilled. Again, the corrections of the EOM on different orders can be combined in a bottom-up approach by successively updating the reducible part of the right-hand-side of the next-order EOM.

VI. APPLICATIONS

In the following, we apply the above methodological framework to two examples in order to analyze the accuracy and stability of this BBGKY approach in dependence on the truncation order. The scenarios involve tunneling dynamics in a double-well in Section VIA as well as interaction quenches in a harmonic trap in Section VIB, while details about the numerical integration of the truncated BBGKY EOM are given in Appendix K.

A. Tunneling dynamics in a Bose-Hubbard dimer

In this scenario, we assume that N bosonic atoms are loaded into an effectively one-dimensional double-well potential. Preparing the system in an initial state featuring a particle-number imbalance with a left and the

right well allows for studying the tunneling dynamics of such a many-body system, which has been subject of numerous studies covering both mean-field [118, 119] and many-body calculations taking correlations into account [76, 120–123]. Effects unraveled in such a realization of a bosonic Josephson junction cover macroscopic tunneling and self-trapping [118, 119, 124] as well a decay of tunneling oscillations due to the dephasing of populated many-body eigenstates of the post-quench Hamiltonian [76, 120–123].

For sufficiently deep wells, the microscopic many-body Hamiltonian of this system can be well approximated by a two-site Bose-Hubbard Hamiltonian within the lowest-band tight-binding approximation

$$\hat{H} = -J(\hat{a}_L^\dagger \hat{a}_R + \hat{a}_R^\dagger \hat{a}_L) + \frac{U}{2} [\hat{n}_L(\hat{n}_L - 1) + \hat{n}_R(\hat{n}_R - 1)] \quad (32)$$

where $\hat{a}_{L/R}$ annihilates a boson in the lowest-band Wannier state localized in the left/right well and $\hat{n}_i \equiv \hat{a}_i^\dagger \hat{a}_i$ denotes the corresponding occupation-number operator of the site $i \in \{L, R\}$. The first term in (32) describes tunneling between the two wells weighted with the hopping amplitude $J > 0$. The second term refers to on-site interaction of strength U and stems from the short-range van-der-Waals interaction between the atoms. For convenience, we take the hopping amplitude as our energy scale and state times in units of $1/J$.

The Bose-Hubbard dimer features an almost trivial computational complexity since the full many-body wavefunction depends only on $C_2^N = N + 1$ complex-valued coefficients such that the corresponding time-dependent Schrödinger equation can be numerically exactly solved for very large atom numbers. So there is no need for an alternative computational approach here. On the other hand, this system can serve as a good playground for analyzing the properties of the truncated BBGKY approach because (i) the corresponding numerically exact solution is available and (ii) we can easily represent RDMs of large order without using a dynamically optimized truncated single-particle basis. This allows for systematically investigating the accuracy of our results solely in dependence on the truncation order \bar{o} .

In the following, we consider the initial state $|\Psi_0\rangle = |N, 0\rangle$ with all atoms located in the left well and focus on the tunneling regime by setting the dimensionless interaction parameter $\Lambda = U(N - 1)/(2J)$ to 0.1, i.e. well below the critical value $\Lambda_{\text{crit}} = 2$ for self-trapping [118, 119]. In the weak interaction regime $\Lambda \ll 1$, beyond mean-field effects such as the aforementioned collapse of tunneling oscillation [120] and the universal formation of a two-fold fragmented condensate out of a single condensate [122] are expected to play a significant role after the time-scale $t_{\text{mf}} \approx \sqrt{2N + 1}/(J\Lambda)$, the so-called quantum break time [123].

Most of the following calculations deal with $N = 10$ atoms such that $t_{\text{mf}} \approx 46/J$. For comparison, we also increase N to 100 atoms while keeping Λ constant, which

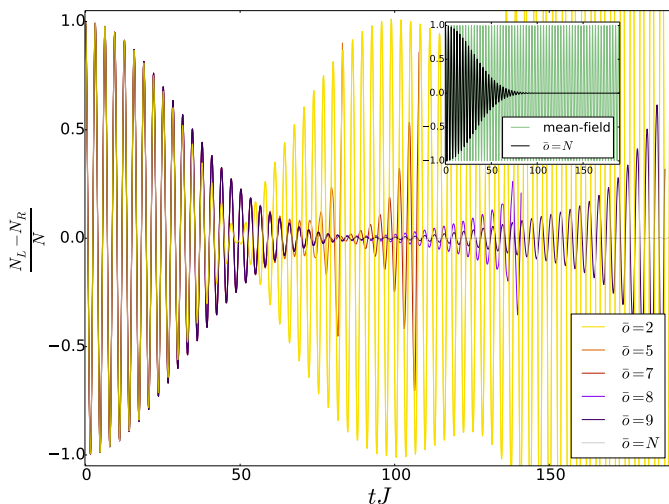


Figure 2. (color online) Time evolution of the particle-number imbalance $(N_L - N_R)/N$ with $N_i \equiv \langle \hat{n}_i \rangle$, $i \in \{L, R\}$ for various truncation orders \bar{o} . Inset: numerically exact solution of the many-body Schrödinger equation in comparison to the corresponding mean-field calculation. Parameters: $N = 10$ atoms located initially in the left well, dimensionless interaction parameter $\Lambda = 0.1$.

results in a longer quantum break time of $t_{\text{mf}} \approx 142/J$. We analyze the accuracy of the truncated BBGKY hierarchy approach in three steps. First, we inspect the particle-number imbalance, a highly-integrated quantity characterizing the tunneling dynamics, second turn to the eigenvalues of the lowest-order RDMs, which constitute a highly sensitive measure for correlations, and third compare the whole lowest order RDMs to the corresponding exact results. For a deeper interpretation of these findings, we thereafter analyze the exact results for the whole N -particle wavefunction as well as for the corresponding α -particle correlations. Finally, we investigate the performance of the correction strategies outlined in Section VB.

1. Particle-number imbalance

In order to study the tunneling dynamics, the imbalance of the particle numbers between the left and right well, $[\langle \hat{n}_L \rangle - \langle \hat{n}_R \rangle]/N$, is depicted in Figure 2 for $N = 10$ atoms. Focusing first on the inset, which shows the numerically exact results, we see the expected collapse of tunneling oscillations due to a dephasing of the populated post-quench Hamiltonian eigenstates. Indeed, this collapse happens on the time-scale $t_{\text{mf}} \approx 46/J$, while a corresponding Gross-Pitaevskii mean-field simulation (see inset of Figure 2) reveals undamped tunneling oscillations. After $t \sim 200/J$, a revival of the tunneling oscillations emerges in the numerically exact calculation (not shown).

Turning now to the truncated BBGKY approach, we

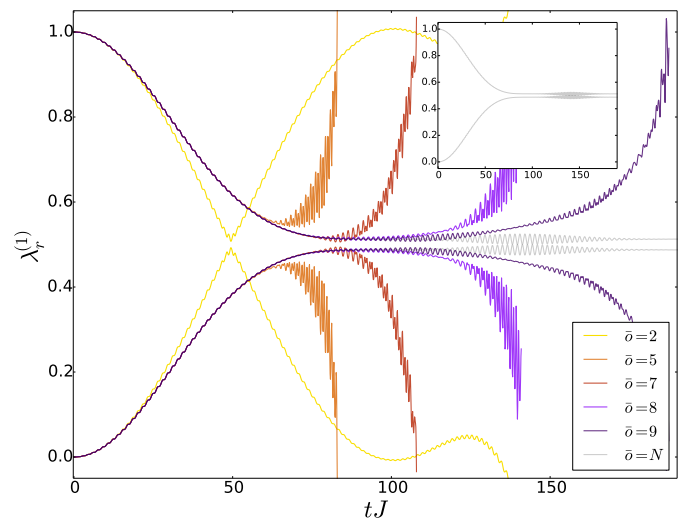


Figure 3. (color online) Natural populations of the 1-RDM for various truncation orders \bar{o} . Inset: numerically exact solution of the many-body Schrödinger equation. Parameters: same as in Figure 2.

see that all truncation orders $\bar{o} \geq 2$ give good results for the first ~ 8 tunneling oscillations. Thereafter, the $\bar{o} = 2$ curves depart from both the exact and the higher truncation-order results, and features a premature maximal suppression of tunneling oscillations at $t \sim 50/J$. In the subsequent premature revival of tunneling oscillations unphysical values $|\langle \hat{n}_L \rangle - \langle \hat{n}_R \rangle|/N > 1$ are reached at about $t = 100/J$, indicating a lack of 1-RDM representability.

These findings suggest that higher-order correlations than \hat{c}_2 play a significant role. Increasing the truncation order \bar{o} stepwise up to the maximally reasonable order $\bar{o} = N - 1 = 9$, we clearly see that the accuracy of our results improves systematically. The larger \bar{o} is, the more accurate is the collapse of the tunneling oscillations described. However, all non-trivial truncations $\bar{o} < N$ predict a premature revival of the tunneling oscillations, which goes hand and in hand with a maximal suppression of the tunneling-oscillation amplitude to small but noticeable values (while the exact results do not feature noticeable oscillations at the corresponding times). We note that for $2 < \bar{o} < 10$ the simulations suffer from drastic instabilities of the EOM, being discussed in the subsequent Section, such that we had to stop them after a certain time. This is why the corresponding curves in Figure 2 are not provided for the whole range of depicted times.

2. Natural populations

Next we analyze the NPs of the 1-RDM in Figure 3, which can diagnose beyond mean-field behavior. The numerically exact results (see corresponding inset) reveal

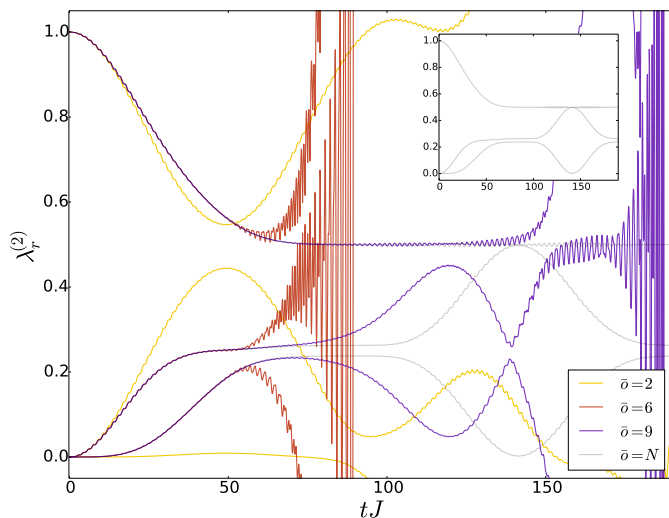


Figure 4. (color online) Natural populations of the 2-RDM for various truncation orders \bar{o} . Inset: numerically exact solution of the many-body Schrödinger equation. Parameters: same as in Figure 2.

dynamical quantum depletion leading to a two-fold fragmented condensate for $t \gtrsim 80/J$ with almost equal population of the corresponding NOs, $\lambda_1^{(1)} \approx 0.5 \approx \lambda_2^{(1)}$ (see also e.g. [122]). Strikingly fast oscillations in these NPs emerge and decay around $t \sim 140/J$, which we can connect to the periodical emergence and decay of a NOON state of the total system (see below).

The corresponding results of the truncated BBGKY approach feature a similar dependence on the truncation order \bar{o} as the particle-number imbalance does. While the $\bar{o} = 2$ prediction starts to deviate noticeably from the exact results already for $t \gtrsim 25/J$, we obtain trustworthy results for a longer time, the larger \bar{o} is chosen. In particular, the truncated BBGKY approach can accurately determine the achieved mean degree of fragmentation (see $\bar{o} = 8, 9$ results at $t \sim 100/J$). Even for the largest truncation order $\bar{o} = 9$, however, the truncated BBGKY simulations predict a premature and very fast revival of condensation (i.e. $\lambda_1^{(1)} \approx 1$), while this process starts only after $t \sim 200/J$ in the exact calculation and happens more slowly (not shown). Most importantly, this unphysical fast re-condensation overshoots the range of valid NPs such that the 1-RDM ceases to be positive semi-definite, indicating an exponential-like instability of the EOM.

While we have so far only studied the prediction of the truncated BBGKY approach for one-particle properties, we now inspect the NPs of the 2-RDM in Figure 4, also called natural geminal populations [22]. The exact dynamics (see the inset) features two important aspects, which we have also observed for the NPs of higher-order RDMs (not shown). (i) The dominant NP $\lambda_1^{(2)}$ first loses weight in favor of the other NPs. (ii) At about $t \sim 140/J$, all NPs are suppressed except for

$\lambda_1^{(2)} \approx 0.5 \approx \lambda_2^{(2)}$. Having observed the latter feature for the NPs of all orders $o \in \{1, \dots, 9\}$, we may conclude that in this stage of the dynamics a subsystem of o particles occupies approximately only two o -particle states with almost equal probabilities. As we will see below, this finding is caused by the periodical emergence and decay of a NOON state of the total system which is discussed below.

Turning now to the predictions of the truncated BBGKY approach, we see again a systematic improvement of accuracy with increasing truncation order \bar{o} . The maximal time for which the highest truncation order $\bar{o} = 9$ gives reliable results, however, has reduced from $t \sim 110/J$ for the 1-RDM NPs (see Figure 3) to $t \sim 70/J$ for the 2-RDM NPs (see Figure 4). Thereafter, the largest NP $\lambda_1^{(2)}$ is well described until $t \sim 130/J$, while the other two NPs already show strong deviations: it seems that the emergence of the feature (ii) discussed above happens premature, name at about $t \sim 120/J$. Furthermore, we also witness the exponential-like instabilities leading to 2-RDM NPs outside the interval $[0, 1]$.

In order to analyze how this unphysical behavior emerges, we depict the first time $t_{\text{neg}}(o)$ when the lowest o -RDM NP $\lambda_{o+1}^{(o)}$ is smaller than the threshold $\epsilon = -10^{-10}$ for various o and different truncation orders \bar{o} in Figure 5 a). For fixed truncation order \bar{o} , $t_{\text{neg}}(o)$ decreases with increasing order o . This means that the representability defect of $\hat{\rho}_o$ lacking positive semi-definiteness starts at the truncation order $o = \bar{o}$ and propagates then successively to lower orders due to coupling via the collision integral. For most orders o , we moreover find that $t_{\text{neg}}(o)$ increases with increasing truncation order \bar{o} , which fits to the above findings regarding enhanced accuracy for larger \bar{o} (exceptions occur at order $o = 1, 2$ in particular for $\bar{o} = 2$).

Increasing the number of atoms to $N = 100$ while keeping the dimensionless interaction parameter $\Lambda = 0.1$ constant, we again find a monotonous decrease of $t_{\text{neg}}(o)$ with increasing o for fixed truncation order \bar{o} (see Figure 5 b)). This confirms the above finding that the lack of positivity successively propagates from higher to lower orders. In contrast to the $N = 10$ case, we only find an enhancement of $t_{\text{neg}}(o)$ with increasing \bar{o} for orders $o \geq 6$. In particular, we see that the largest truncation order considered, $\bar{o} = 12$, features the smallest $t_{\text{neg}}(o = 2)$. It is quite possible that the an “enhancement” of non-linearity with increasing truncation order \bar{o} (note that the applied closure approximation, cf. Section IV B 3, is a polynomial of degree $(\bar{o} + 1)$ in $\hat{\rho}_1$ and of degree $[(\bar{o} + 1)/o]$ in the cluster \hat{c}_o) is the reason why the BBGKY EOM are more prone to these instabilities for larger \bar{o} .

Having compared so far only certain aspects of o -particle properties, we finally aim at comparing the prediction of the truncated BBGKY approach for the whole o -RDM to the exact results.

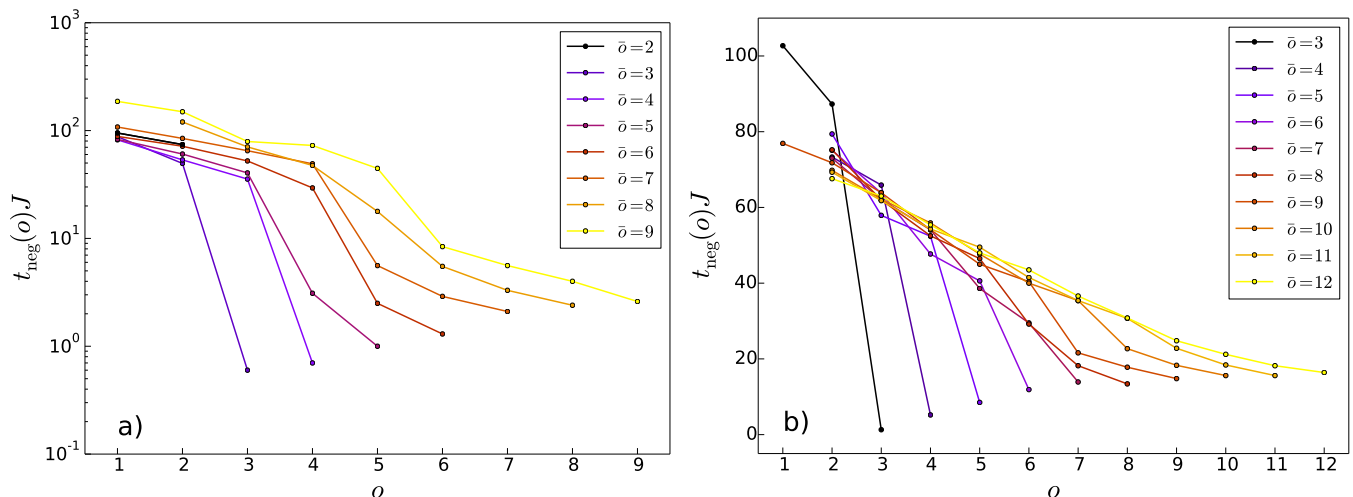


Figure 5. (color online) First time $t_{\text{neg}}(o)$ when the lowest o -RDM NP is smaller than $\epsilon = -10^{-10}$ in dependence on o for various truncation orders \bar{o} . a) Same parameters as in Figure 2. b) Same as a) but for the atom number N increased to 100 while keeping the interaction parameter $\Lambda = 0.1$ constant. The results for $\bar{o} = 2$ are not plotted in b) and read $t_{\text{neg}}(1) \approx 216/J$ as well as $t_{\text{neg}}(2) \approx 168/J$.

3. Reduced density operators

For this purpose, we take the trace distance $\mathcal{D}(\hat{\rho}_o^{\text{tr}}, \hat{\rho}_o^{\text{ex}}) \equiv \|\hat{\rho}_o^{\text{tr}} - \hat{\rho}_o^{\text{ex}}\|_1/2$ [125] as a measure for deviations between the truncated BBGKY prediction for the o -RDM denoted by $\hat{\rho}_o^{\text{tr}}$ and the numerically exact result $\hat{\rho}_o^{\text{ex}}$. Here, $\|\cdot\|_1$ refers to the trace-class norm (also called Schatten-1 norm) being defined as $\|\hat{A}\|_1 \equiv \text{tr}(\sqrt{\hat{A}^\dagger \hat{A}})$ for any trace-class operator \hat{A} . For hermitian operators \hat{A} , $\|\hat{A}\|_1$ equals the sum of absolute values of \hat{A} 's eigenvalues. One can easily prove the inequality $|\text{tr}(\hat{A}_o \hat{\rho}_o^{\text{tr}}) - \text{tr}(\hat{A}_o \hat{\rho}_o^{\text{ex}})| \leq 2\|\hat{A}_o\|_1 \mathcal{D}(\hat{\rho}_o^{\text{tr}}, \hat{\rho}_o^{\text{ex}})$ where \hat{A}_o denotes an arbitrary o -body observable. This means that $\mathcal{D}(\hat{\rho}_o^{\text{tr}}, \hat{\rho}_o^{\text{ex}})$ provides an upper bound for the deviations in the expectation value predictions for \hat{A}_o . Moreover, given that its arguments are density operators (i.e. hermitian, positive semi-definite and trace one), the trace-distance is bounded by $\mathcal{D}(\hat{\rho}_o^{\text{tr}}, \hat{\rho}_o^{\text{ex}}) \in [0, 1]$ and can be interpreted as the probability that these two quantum states can be distinguished by the outcome of a single measurement [125].

In Figure 6, we depict $\mathcal{D}(\hat{\rho}_o^{\text{tr}}, \hat{\rho}_o^{\text{ex}})$ for the orders $o = 1, \dots, 4$ and various truncation orders \bar{o} , where subfigures a) and b) refer to the $N = 10$ and $N = 100$ case with the same interaction parameter $\Lambda = 0.1$, respectively. For fixed truncation order \bar{o} , we clearly see that the accuracy of the truncated BBGKY prediction for the o -RDM decreases with increasing order o . Up to a certain time, which depends on the order o , we moreover find $\mathcal{D}(\hat{\rho}_o^{\text{tr}}, \hat{\rho}_o^{\text{ex}})$ to decrease with increasing truncation order \bar{o} .

The instabilities of the truncated BBGKY EOM manifest themselves in the trace distant exceeding its upper bound $\mathcal{D}(\hat{\rho}_o^{\text{tr}}, \hat{\rho}_o^{\text{ex}}) \leq 1$ for density operators, implying

that $\hat{\rho}_o^{\text{tr}}$ lacks to have trace one or to be positive semi-definite. Since the conservation of the initial RDM trace is ensured by the truncated BBGKY approach, violations of $\text{tr}(\hat{\rho}_o^{\text{tr}}) = 1$ can at most occur numerically if the system gets deep into the exponential-like instability (where we observe the truncated BBGKY EOM to become stiff such that the integrator has a hard time). Thus, exceeding the upper bound on the trace distance is connected to a lack of positive semi-definiteness and can be observed to happen earlier for increasing order o and fixed truncation order \bar{o} .

For the case of $N = 100$ atoms (see Figure 6 b)), we observe the additional particularity that in the vicinity of $t \sim 63/J$ the accuracy of the truncated BBGKY prediction for the o -RDM does not depend on the truncation order \bar{o} , which happens slightly earlier for larger o . Before this point, a systematic increase of accuracy is observed for increasing truncation order \bar{o} . Thereafter, lower truncation orders give (slightly) better results than higher ones. Furthermore, while in the $N = 10$ case one-body properties (such as e.g. the particle-number imbalance) can be described with reasonable accuracy up to $t \sim 2 t_{\text{mf}}$ (when the collapse of tunneling oscillations has already taken place), the instabilities hinders us to obtain accurate results for t larger than about $0.56 t_{\text{mf}}$ in the case of $N = 100$ (at this time, the tunneling oscillation amplitude is still significant).

4. Many-body state and o -particle correlations: exact results

In order to obtain physical insights into the above findings, we finally come back to the numerically exact results for $N = 10$ and measure the strength of o -particle correlations in terms of $\|\hat{c}_o\|_1$ in Figure 7 a). From the

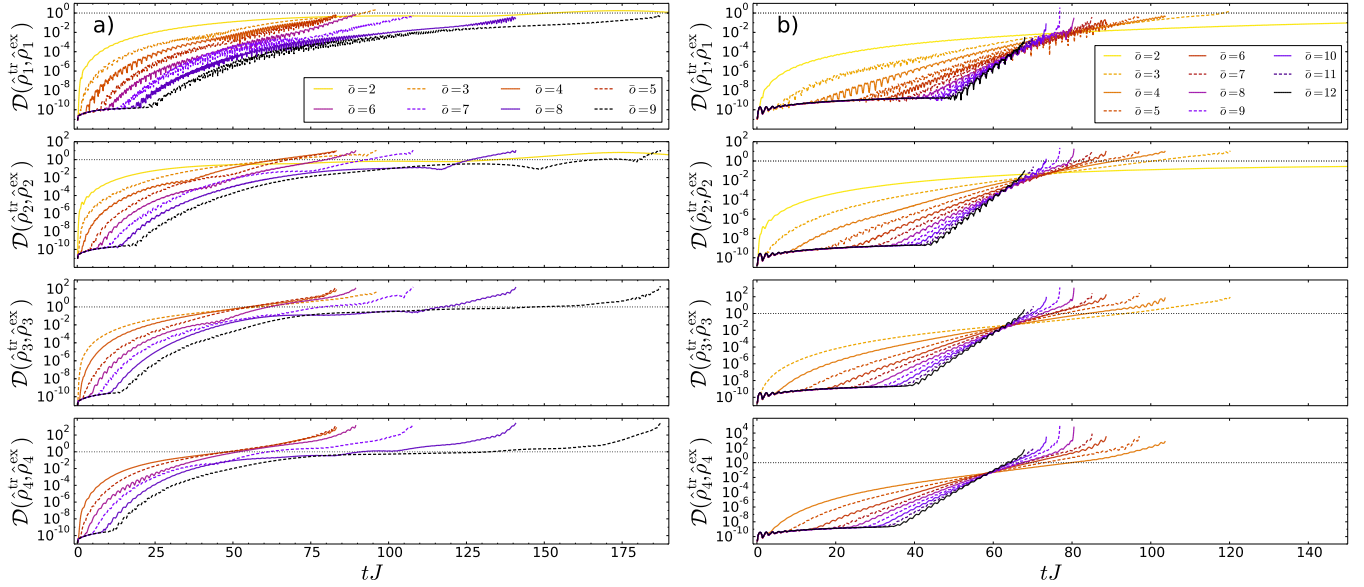


Figure 6. (color online) Time evolution of the trace distance $\mathcal{D}(\hat{\rho}_o^{\text{tr}}, \hat{\rho}_o^{\text{ex}})$ between the exact result and the truncated BBGKY prediction for the o -RDM ($o = 1, \dots, 4$) and various truncation orders \bar{o} . The dotted horizontal lines at unity ordinate value indicate the upper bound for the trace distance between two density operators (see main text). a) Same parameters as in Figure 2. b) Same as a) but for the atom number N increased to 100 while keeping the interaction parameter $\Lambda = 0.1$ constant.

inset, we infer that the correlations initially build up in a hierarchical manner. First, only two-particle correlations start to play a role, then three-particle correlations and so on. This hierarchy in $\|\hat{c}_o\|_1$ holds, however, only until $t \sim 8/J$, when the ordering of the $\|\hat{c}_o\|_1$'s with respect to the order o starts to become reversed. After a certain point, N -particle correlations become the most dominant ones. This holds in particular in the vicinity of $t \sim 140/J$, where we have observed fast oscillations in the NPs $\lambda_{1/2}^{(1)}$ and found for all orders $o = 1, \dots, 9$ that the RDMS feature approximately only two finite NPs $\lambda_1^{(o)} \approx 0.5 \approx \lambda_2^{(o)}$. At this stage of the dynamics, all clusters \hat{c}_o of odd order o are strongly suppressed.

For connecting the above findings regarding o -particle correlations to the full many-body state, we depict in the Subfigures 7 b) and c) the probability $|\langle N - n, n | \Psi_t \rangle|^2$ of finding n atoms in the right and $(N - n)$ atoms in the left well. For the early dynamics, we witness how the system becomes delocalized in the Fock space such that the tunneling oscillations become suppressed (Subfigure 7 b)). At later times, around $t \sim 140/J$, we, however, find the system to periodically oscillate between a NOON state $(|N, 0\rangle + e^{i\theta}|0, N\rangle)/\sqrt{2}$ (with some phase $\theta \in \mathbb{R}$) and some broad distribution being approximately symmetric with respect to its maximum at about $n = 5$ (Subfigure 7 c)). Due to this approximate symmetry of the distribution around $n = 5$, the particle-number imbalance approximately equals $|\langle \hat{n}_L \rangle - \langle \hat{n}_R \rangle|/N \approx 0.5$, i.e. tunneling oscillations are still suppressed. This approximate symmetry moreover leads to a doubling of the oscillation frequency compared to the initial tunneling-oscillation frequency, which is most probably linked to

the fast oscillations in $\lambda_{1/2}^{(1)}$. Finally, one can analytically show that the n -RDM of the above mentioned NOON state reads $\hat{\rho}_n = (|n, 0\rangle\langle n, 0| + |0, n\rangle\langle 0, n|)/2$, meaning that the state of an n -particle subsystem is an incoherent statistical mixture with all particles residing in the left (right) well with probability 0.5. Thereby, we can directly connect the fact that the RDMS of all orders feature approximately only two finite NPs of approximately equal value to the underlying many-body state. Coming back to the findings for $\|\hat{c}_o\|_1$ of Figure 7 a), we may conclude that a NOON state leads to strong high-order correlations \hat{c}_o such that truncating the BBGKY hierarchy by means of the applied cluster expansion cannot be expected to give accurate results.

In summary, we have seen following. (i) While the truncated BBGKY approach gives highly accurate results for short times with controllable accuracy via the truncation order \bar{o} , the BBGKY approach shows deviations at longer times. (ii) Exponential-like instabilities, induced by the non-linear truncation approximation, propagate from high to low orders and lead to unphysical results at a certain point. (iii) o -particle correlations arise very fast in this tunneling scenario and soon cease to be in decreasing order with respect to o . (iv) The system evolves into a NOON state being dominated by N -particle correlations.

There appear to be at least two plausible causes why the BBGKY approach fails at a certain point: First, the number of terms in the cluster expansion (23) drastically increases with the order o , which implies that clusters should decay fast for a controllable approximation. For example, at the largest truncation order considered

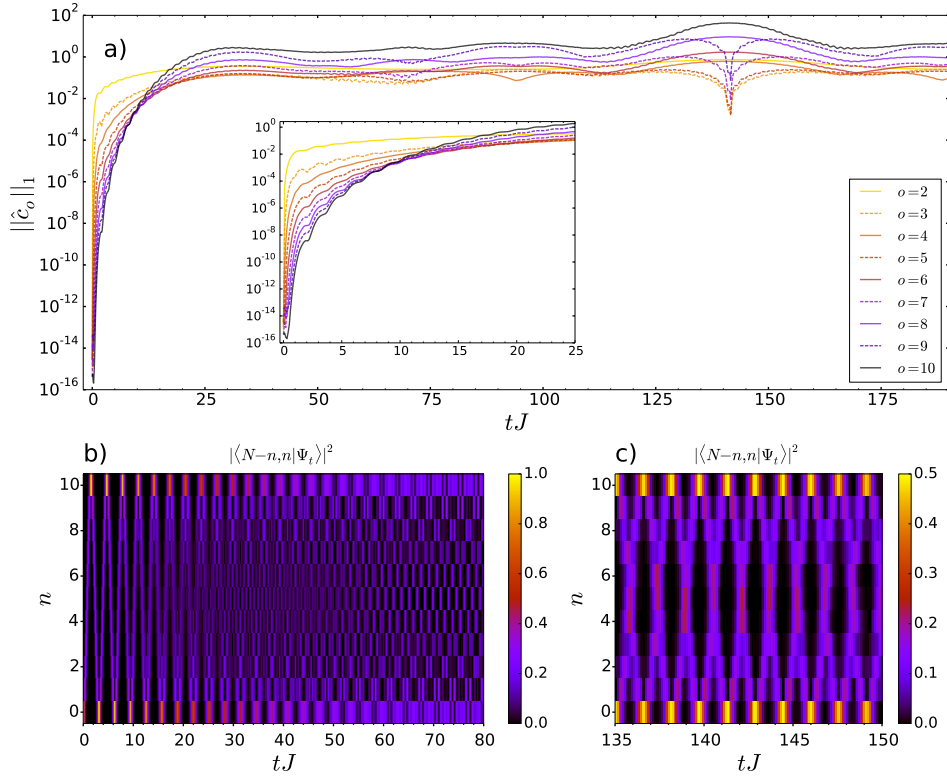


Figure 7. (color online) a) Time evolution of the cluster’s trace-class norm $\|\hat{c}_o\|_1$ for all orders o , obtained from the numerically exact solution of the time-dependent Schrödinger equation. Inset: zoom into early time dynamics. b) and c) Probability to find n atoms in the right and $(N - n)$ atoms in the left well, $|\langle N - n, n | \Psi_t \rangle|^2$, versus time for two characteristic stages of the dynamics. Parameters: same as in Figure 2.

above, $\bar{o} = 12$, the truncation approximation $\hat{\rho}_{13}^{\text{appr}}$ already involves 100 classes of terms. Our findings (iii) and (iv), however, might indicate that this system is not suitable for a truncation based on the o -particle correlations defined in Section IV B 3. Other truncation approximations might be more suitable.

Second, the exponential-like instabilities, being connected to a lack of representability, might be the main cause for the failure of the BBGKY EOM at longer times. This hypothesis is supported by the fast break-down of the BBGKY approach in the $N = 100$ case for the truncation order $\bar{o} = 12$. For this reason, we analyze next the performance of the correction strategies outlined in Section V B.

5. Performance of the correction algorithms

In the following, we first focus on the correction algorithms applied to the BBGKY hierarchy truncated at $\bar{o} = 2$. Thereafter, we comment on the performance of these algorithms if extended to larger truncation orders by means of a corresponding ansatz for the correction operator (see Section V B).

Figure 8 depicts the time evolution of the NPs $\lambda_i^{(2)}$ and the \hat{K}_2 eigenvalues ξ_i for the truncated BBGKY results

without correction, with the iterative minimal invasive purification of the 2-RDM and with the minimal invasive correction of the 2-RDM EOM in comparison to the exact results. Apparently, all cases deviate significantly from the exact results after $t \gtrsim 17/J$ so that we shall concentrate here solely on the stabilization performance of the correction algorithms.

Inspecting first the uncorrected results [Figures 8 (a.1), (a.2)], we observe that the K -condition (i.e. $\hat{K}_2 \geq 0$) diagnoses earlier a lack of representability compared to the D -condition (i.e. $\hat{\rho}_2 \geq 0$). For both operators, the falling of an eigenvalue below zero is accompanied by an avoided crossing which involves the next-larger eigenvalue (this is hardly visible in the case of the \hat{K}_2 eigenvalue where the avoided crossing happens at about $t \sim 71.5/J$). In fact, we have observed that level-repulsion “pushes” eigenvalues below zero in various other situations (see also Section VIB).

Now turning to the minimal invasive correction algorithms based on the 2-norm minimization of the correction operator \hat{C}_2 , we set the threshold ϵ below which an eigenvalue is regarded as negative to -10^{-10} . Let us first inspect the dimensionality of the optimization problem underlying both our purification algorithm of the 2-RDM and the correction algorithm of its EOM (see Appendix H for the details). The bosonic hermitian correction op-

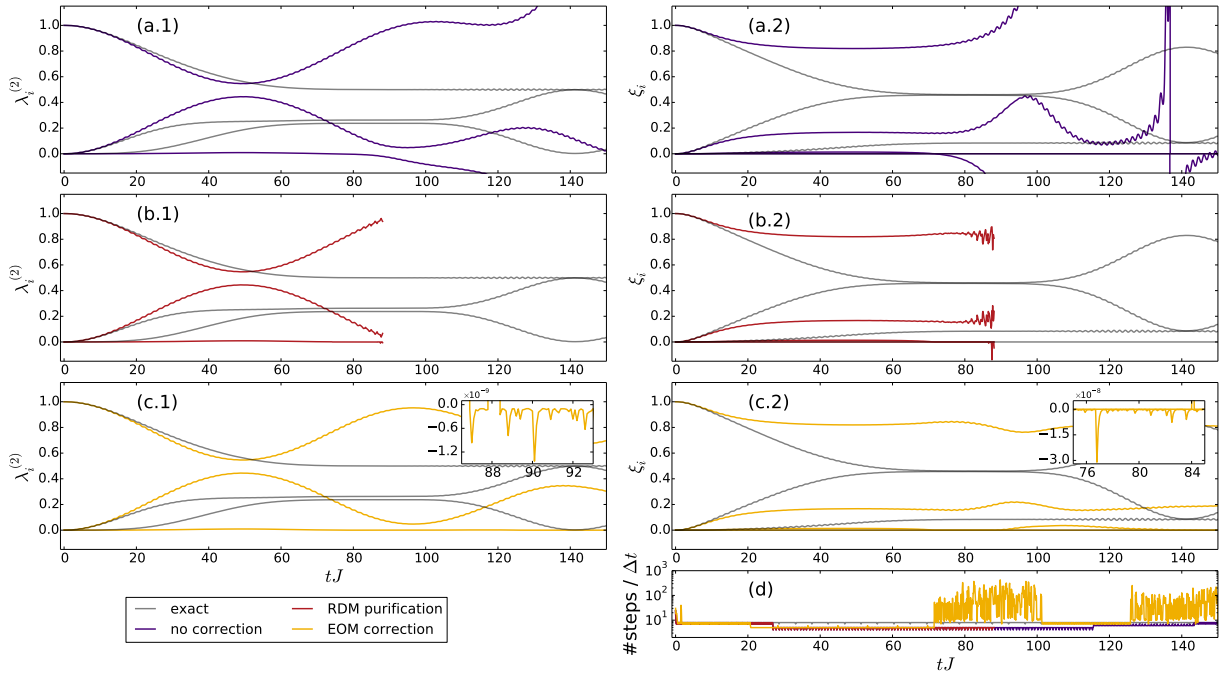


Figure 8. (color online) Comparison of the correction strategies outlined in Section VB (for the BBGKY hierarchy truncated at $\bar{o} = 2$). Left column: Time evolution of the NPs $\lambda_i^{(2)}$. Right column [except for (d)]: Time evolution of the \hat{K}_2 eigenvalues ξ_i . First row: Truncated BBGKY results without correction versus exact ones. Second row: Truncated BBGKY results with iterative minimal-invasive purification of the 2-RDM after each $\Delta t = 0.1/J$ (maximal number of iterations: 500). Third row: Truncated BBGKY results with minimal-invasive correction of the 2-RDM EOM (damping rate of negative eigenvalues: $\eta = 10J$). Insets of (c.1) and (c.2): close-ups showing the imposed exponential damping of negative eigenvalues. For both correction strategies, eigenvalues are regarded as negative if they are smaller than the threshold $\epsilon = -10^{-10}$. Subfigure (d): number of integrator steps [126] per write-out time-step Δt . Parameters: same as in Figure 2.

erator \hat{C}_2 can be parametrized by $m^2(m+1)^2/4 = 9$ real-valued parameters. Requiring \hat{C}_2 to be contraction-free and energy-conserving imposes $m^2 + 1 = 5$ constraints such that the system of linear equations corresponding to the constraints is underdetermined as long as the numbers of negative $\hat{\rho}_2$ eigenvalues d and negative \hat{K}_2 eigenvalues d' obey $d + d' < 4$.

Figure 8 (b.1) and (b.2) depict the results if the iterative minimal-invasive purification algorithm is applied after each $\Delta t = 0.1/J$. Clearly, we see that this correction algorithm induces strong noise in the \hat{K}_2 eigenvalues when the smallest eigenvalue ξ_i has reached significant negative values in the uncorrected BBGKY calculation [see subfigure (a.2)]. Actually, after $t = 86.5/J$, the iterative purification algorithm fails to converge after the maximal number of 500 steps. Thus, this iterative scheme fails to prevent that smallest eigenvalue is pushed to negative values due to level repulsion.

In a certain sense, we may view the iterative purification algorithm of the 2-RDM as being based on a fixed stepsize as well as perturbative. In each iteration step namely, we update $\hat{\rho}_2(t) \rightarrow \hat{\rho}_2(t) + \hat{C}_2$ with \hat{C}_2 shifting negative eigenvalues to zero in first-order perturbation theory. In the correction algorithm for the 2-RDM EOM, we effectively allow for variable update stepsizes by coupling

the correction scheme to the integration of the EOM, i.e. to the employed integrator ZVODE [126] featuring adaptive stepsizes. Moreover, by imposing constraints on the time-derivative of negative eigenvalues, we realize a non-perturbative correction scheme.

This can nicely be inferred from the insets of Figure 8 (c.1) and (c.2) showing a close-up of slightly negative eigenvalues. These are exponentially damped to zero, namely as e.g. $\xi_i(t + \tau) = \xi_i(t) \exp[-\eta\tau]$ for t and τ such that $\xi_i(t + \tau) < \epsilon$, with the chosen damping constant $\eta = 10J$. As a consequence, the truncated BBGKY EOM becomes stabilized and we have observed that the D - and K -representability condition are fulfilled to a good approximation for at least $t \leq 1000/J$ (times later than $t = 150/J$ not shown in Figure 8). When enforcing negative eigenvalues to be damped to zero, one might fear that eigenvalues accumulate in the range $[\epsilon, 0]$. This, however, is not the case as shown in the insets of Figure 8 (c.1) and (c.2) because no constraint on the time-derivative of an eigenvalue is enforced if its value exceeds the threshold ϵ such that the (corrected) EOM may lift this eigenvalue above zero. We finally remark that the number of integrator steps per Δt significantly increases in the vicinity of avoided crossings of $\hat{\rho}_2$ or \hat{K}_2 eigenvalues close to zero [see Figure 8 (d)]. This finding confirms the non-

perturbative, adaptive nature of the EOM correction algorithm and at the same time highlights the significance of controlling such avoided crossings for a successful stabilization of the truncated BBGKY EOM.

Without showing additional graphical illustrations, let us now briefly comment on the behavior of the correction algorithms for truncation orders $\bar{o} > 2$, using the Mazziotti ansatz [113] for the correction operators \hat{C}_o on orders $o > 2$ (see Section V B). Focusing first on the RDM purification, we have observed that $\hat{\rho}_{\bar{o}}$ can be kept positive semi-definite up to a few tens $1/J$ longer (compared to the uncorrected case) before this iterative correction algorithm fails to converge after 500 steps. Due to the losing of positive semi-definiteness in decreasing sequence with respect to the RDM order (see Figure 5), we found for $\bar{o} \geq 4$ that also $\hat{\rho}_{\bar{o}-1} \geq 0$ is valid for somewhat longer times compared to the uncorrected case. Unfortunately, however, this correction scheme fails to converge so early that it does not improve the timescale, on which the most important RDMs for making predictions for ultracold quantum gas experiments, namely $\hat{\rho}_1$ and $\hat{\rho}_2$, obey the considered representability conditions.

Extending the EOM correction scheme to higher truncation orders $\bar{o} > 2$ by means of the Mazziotti ansatz for the higher-order correction operators unfortunately proved to be quite unsuccessful. This failure manifests itself in an enormous increase of integrator steps per Δt , i.e. the EOM becoming stiff, in combination with the quadratic optimization problem for determining \hat{C}_2 having no solution, i.e. constraints contradicting one another. Unfortunately, we cannot tell whether the latter is a fundamental problem or whether it is only induced by the EOM to become stiff due to an inappropriate ansatz of \hat{C}_o for $o > 2$, potentially leading to integration errors.

To sum up, while we can successively stabilize the BBGKY EOM truncated at order $\bar{o} = 2$ by enforcing the D - and K -representability condition via a minimal invasive correction of the 2-RDM EOM, the issue of higher-order correlations becoming dominant after a certain time remains unsolved in this example. Since this tunneling scenario might well be unsuitable for a closure approximation based on neglecting certain few-particle correlations, we now turn to an example, where a BEC becomes only slightly depleted in the course of the quantum dynamics.

B. Interaction-quench induced breathing dynamics of harmonically trapped bosons

In this application, we are concerned with collective excitations of N ultracold bosons confined to a quasi one-dimensional harmonic trap. In harmonic oscillator units (HO units), the corresponding Hamiltonian reads

$$\hat{H} = \sum_{i=1}^N \frac{\hat{p}_i^2 + \hat{x}_i^2}{2} + g \sum_{1 \leq i < j \leq N} \delta(\hat{x}_i - \hat{x}_j) \quad (33)$$

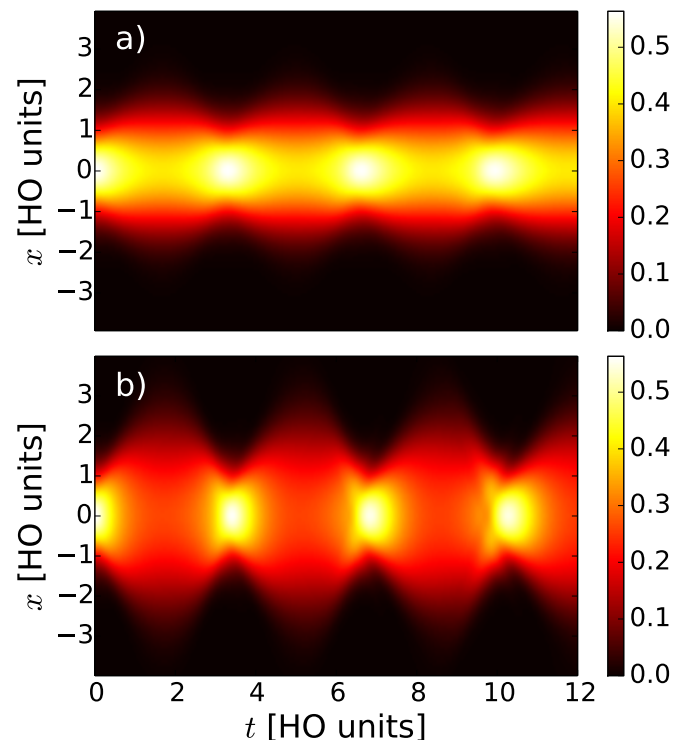


Figure 9. (color online) Time-evolution of the reduced one-body density $\rho_1(x; t) = \langle x | \hat{\rho}_1(t) | x \rangle$ for $N = 10$ [subfigure (a)] and $N = 30$ [subfigure (b)] bosons quenched from the non-interacting ground-state to a contact-interaction strength of $g = 0.2$. These results are obtained by MCTDHB simulations with $m = 4$ dynamically optimized SPFs.

where we model the short-range van-der-Waals interaction by the contact potential [27] of strength g . Initially, we assume all atoms to reside in the ground state of the single-particle Hamiltonian, i.e. a Gaussian orbital, which is the exact many-body ground state in the absence of interactions. Then, the interaction strength is instantaneously quenched to $g = 0.2$ such that the ideal BEC becomes slightly depleted and its density performs breathing oscillations, i.e. expands and contracts periodically. This so-called breathing mode has been investigated theoretically as well as experimentally in different settings (see e.g. [127–133] for single-component systems and e.g. [134] for mixtures), and measuring its frequency proves to be useful for characterizing the interaction regime [135].

Before we discuss the results of the truncated BBGKY approach, let us first inspect the results of MCTDHB simulations with $m = 4$ dynamically optimized SPFs, which we obtain by our implementation [81, 136, 137]. In fact, we find that the smallest natural population of the 1-RDM attains a maximal value of about $1.6 \cdot 10^{-3}$, which provides a good indicator in praxis that the contribution of this orbital is almost negligible in the calculation. One could improve the accuracy further by increasing the number of SPFs, of course. Yet since we aim at benchmarking the truncated BBGKY approach,

which can be viewed as an additional approximation to the MCTDHB approach, it is sufficient to take the MCTDHB simulations with $m = 4$ SPFs as reference results. For representing the SPFs, a harmonic discrete variable representation [75, 138] with $n = 256$ ($n = 320$) grid points is employed for case of $N = 10$ ($N = 30$) particles.

In Figure 9, we depict the time evolution of the reduced one-body density, i.e. the diagonal of the 1-RDM in position representation $\rho_1(x; t) = \langle x | \hat{\rho}_1(t) | x \rangle$, for $N = 10$ and $N = 30$ bosons. In both cases, we clearly see that the atomic density periodically expands and contracts. Since the interaction quench leads to a more than three times larger interaction energy per particle of the ensemble of $N = 30$ atoms compared to $N = 10$ (at $t = 0$), the density of the former expands much further into the outer parts of the trap. In contrast to this, the density of the $N = 10$ atom ensemble seems to stay Gaussian (with a time-dependent width) to a good approximation, indicating that we operate in the linear-response regime here. In both cases, the quench leads only to a slight quantum depletion of at most 3% (see below).

In the following, we first show that the truncated BBGKY approach leads to stable results in the $N = 10$ case, whose accuracy can be systematically improved by increasing \bar{o} . Thereafter, we turn to the $N = 30$ case where we again encounter instabilities of the EOM and thus apply correction algorithms. We stress that for both cases we operate with $m = 4$ dynamically optimized SPFs, solving the truncated BBGKY EOM coupled to the MCTDHB EOM for the SPFs, which is in contrast to the Bose-Hubbard tunneling scenario of Section VI A.

1. Breathing dynamics of $N = 10$ bosons

In Figure 10, we show the time-evolution of the 2-RDM NPs for various truncation orders. Focusing first on the MCTDHB results, we see that correlations (in the sense of deviations from a Gross-Pitaevskii mean-field state where on all orders o there is only one finite NP $\lambda_1^{(o)} = 1$ and all other NPs vanish) repeatedly emerge and decay. The deviations from the NP distribution of a Gross-Pitaevskii mean-field state is approximately most pronounced when the density is most spread-out and become almost negligible when the density has approximately recovered its initial width [see Figure 9 a)].

While the truncated BBGKY results for $\bar{o} = 2$ feature significant deviations from the MCTDHB results, the results drastically improve when going to $\bar{o} = 3$ and become practically indistinguishable from the MCTDHB results already at the truncation order $\bar{o} = 4$. Actually, convergence of the 1-RDM NPs $\lambda_i^{(1)}$ is reached even at $\bar{o} = 3$ (not shown). Coming back to $\bar{o} = 2$, we point out that the 2-RDM quickly becomes indefinite where small negative eigenvalues are in particular pushed further to larger negative values when the density contracts to its initial width and small but positive NPs approach

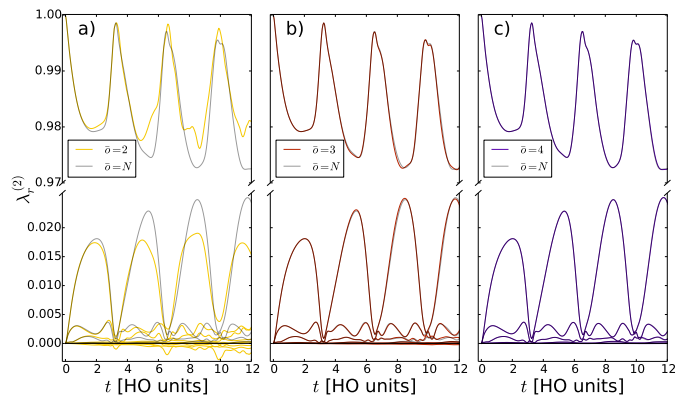


Figure 10. (color online) Natural populations of the 2-RDM for the truncation orders $\bar{o} = 2$ [a)], $\bar{o} = 3$ [b)] and $\bar{o} = 4$ [c)] in comparison to the MCTDHB results. Parameters: $N = 10$ atoms, post-quench interaction strength $g = 0.2$, $m = 4$ dynamically optimized SPFs.

zero. As in the case of the above tunneling scenario, we interpret this finding as “induced” by level repulsion. Upon increasing the truncation order, we see that the 2-RDM stays positive semi-definite on the considered time-interval, which is a nice example for how increasing the accuracy of the closure approximation also stabilizes the truncated BBGKY EOM.

For a systematic comparison, we next compare the trace-class distance $\mathcal{D}(\hat{\rho}_o^{\text{tr}}, \hat{\rho}_o^{\text{ex}})$ between the truncated BBGKY result for the o -RDM, $\hat{\rho}_o^{\text{tr}}$, and the corresponding MCTDHB result, $\hat{\rho}_o^{\text{ex}}$, in Figure 11 a). We remark that although the SPFs of the truncated BBGKY approach obey the same EOM (5) as the dynamically optimized SPFs of the MCTDHB method, we cannot expect these two sets of SPFs to coincide because the 1- and 2-RDM entering the SPF EOM differ in general, which has to be taken into account when calculating $\mathcal{D}(\hat{\rho}_o^{\text{tr}}, \hat{\rho}_o^{\text{ex}})$. In stark contrast to the tunneling scenario, we see that the accuracy of the truncated BBGKY results for the 1- and 2-RDM systematically improves upon increasing \bar{o} for all considered times.

Finally, we quantify the strength of few-particle correlations in terms of $\|\hat{c}_o\|_1$, as extracted from the $\bar{o} = 7$ calculation [see Figure 11 a)]. Here, we see that the correlations stay bounded on the considered time interval and are ordered in a clear hierarchy, i.e. $\|\hat{c}_{o+1}\|_1(t) < \|\hat{c}_o\|_1(t)$. Apparently, these are ideal working conditions for the truncated BBGKY approach.

2. Breathing dynamics of $N = 30$ bosons

Next, let us increase the quench-induced excitation energy per particle by more than a factor of three when going to $N = 30$ bosons and keeping the post-quench interaction strength $g = 0.2$ the same. Similarly to the tunneling scenario, we first inspect the natural populations, then compare lowest order RDMs and finally eval-

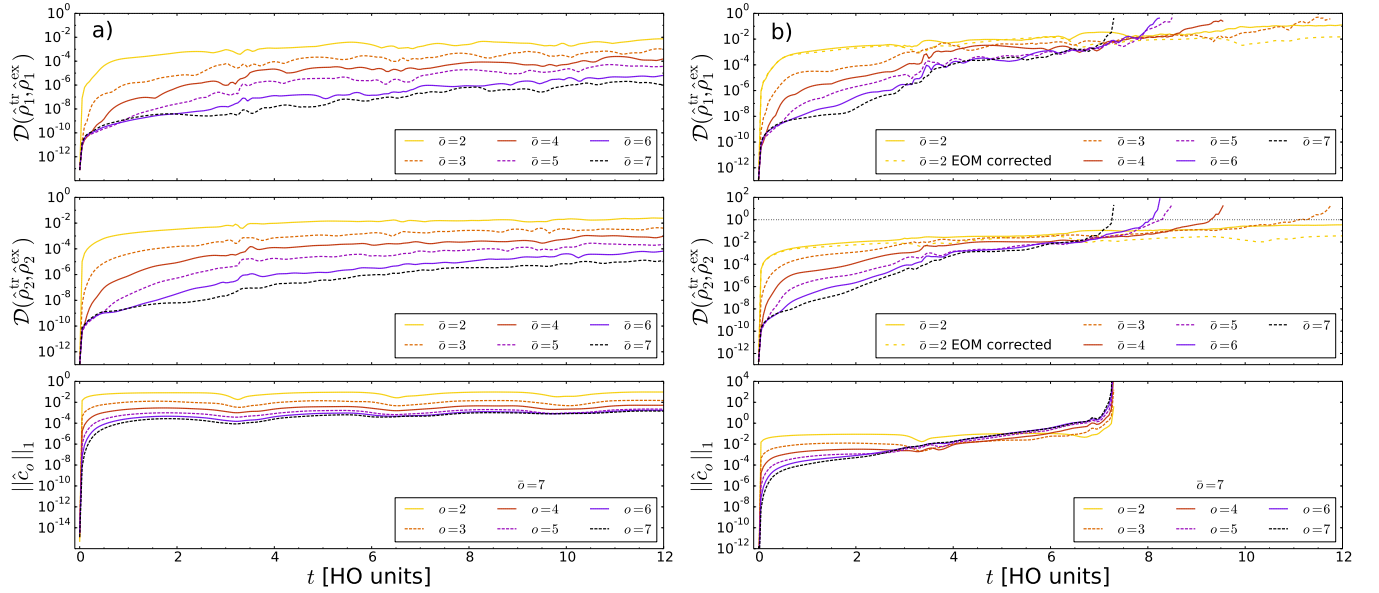


Figure 11. (color online) First and second row: Time evolution of the trace distance $\mathcal{D}(\hat{\rho}_o^{\text{tr}}, \hat{\rho}_o^{\text{ex}})$ between the MCTDHB and the truncated BBGKY prediction for the o -RDM ($o = 1, 2$) and various truncation orders \bar{o} . The dotted horizontal line at unity ordinate value indicate the upper bound for the trace distance between two density operators. Third row: Time-evolution of the cluster's trace-class norm $\|\hat{c}_o\|_1$ for $o = 1, \dots, 7$ obtained from the data of the $\bar{o} = 7$ simulations. Left column: $N = 10$ atoms. Right columns: $N = 30$. Otherwise, same parameters as in Figure 10.

uate the performance of the correction algorithms under discussion.

a. Natural populations In Figure 12, we show the NPs of the 1- and 2-RDM for various truncation orders \bar{o} in comparison to the MCTDHB results. Similarly to the $N = 10$ case, we see how the NP distributions as obtained from MCTDHB oscillates between the characteristics of the Gross-Pitaevskii mean-field state and a (slightly) correlated one, which is approximately synchronized to the strongest contraction and expansion of the density, respectively [see Figure 9 b)]. In contrast to the former case, however, we can converge the NPs to the MCTDHB results upon increasing the truncation order \bar{o} only for times $t \lesssim 5$ HO units. For all considered truncation orders, we witness an exponential-like instability in the 2-RDM NPs resulting in large negative eigenvalues while the 1-RDM stays positive semi-definite for the considered time-span. Fixing \bar{o} , we have observed also for this scenario that the lack of positive semi-definiteness of the o -RDMs happens in decreasing sequence with respect to the order o (not shown). Moreover, these instabilities in the 2-RDM NPs seem to be triggered by small positive NPs approaching zero from above, namely when the density approximately shrinks to its initial width, see e.g. Figure 12 (c.2). Finally, we have observed for the case $\bar{o} = 2$ that increasing the number of SPFs from $m = 4$ to $m = 8$ slightly enhances the time-scale on which the instability of the 2-RDM NPs takes place (not shown). This finding is reasonable since the projector $(\mathbb{1} - \hat{\mathbb{P}})$, occurring in the SPF EOM (5), projects onto a smaller subspace when increasing m such that the impact of the

non-linearity in the SPF EOM is effectively reduced.

b. Reduced density operators Comparing the BBGKY prediction for the complete 1- and 2-RDM with the corresponding MCTDHB results in terms of the trace-class distance in Figure 11 b), we see that deviations emerge much faster as compared to the $N = 10$ case. At longer times, we also observe that the accuracy of the BBGKY results does not monotonously increase anymore with increasing \bar{o} . Moreover, the above mentioned instabilities also partly manifest themselves in $\mathcal{D}(\hat{\rho}_2^{\text{tr}}, \hat{\rho}_2^{\text{ex}})$ attaining unphysical values above unity. Finally, we also depict $\|\hat{c}_o\|_1$ as a measure for correlations in Figure 11 b). While the correlations are hierarchically ordered in decreasing sequence with respect to the order o up to $t \sim 2.7$ HO units, this ordering becomes reversed later on. This finding, however, is not conclusive, i.e. might be unphysical and related to the observed instability, since the values of $\|\hat{c}_o\|_1$ have been extracted from the BBGKY data with $\bar{o} = 7$ (in contrast to the tunneling scenario where the numerically exact \hat{c}_o have been used).

At this point, we shall remark that we expect a much better agreement for the $N = 30$ case when quenching to much lower interaction strengths $g \ll 0.2$ and thereby reducing the overall excitation energy.

c. Performance of the correction algorithms Here, we again focus mainly on the performance of the correction algorithms applied to the $\bar{o} = 2$ BBGKY approach and comment later on larger truncation orders. In Figure

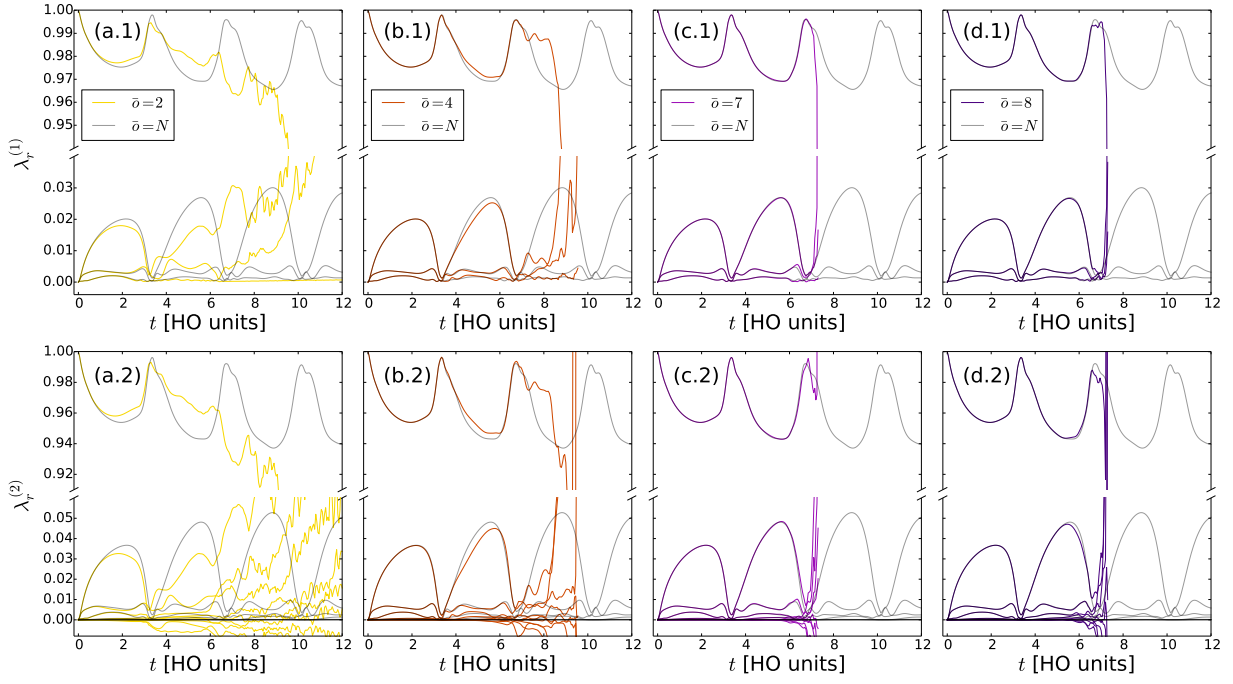


Figure 12. (color online) Top (bottom) row: Time-evolution of the 1-RDM (2-RDM) NPs for various truncation orders \bar{o} in comparison to the MCTDHB results. We note that the ordinates are broken into two parts for covering the whole range of relevant values. In some cases, this leads to discontinuous curves, see e.g. the $\bar{o} = 2$ curve in (a.2). Number of bosons: $N = 30$. Otherwise, same parameters as in Figure 10.

13, we depict the spectrum¹⁵ of \hat{K}_2 as well as a close-up to the 2-RDM spectrum in the vicinity of zero for the uncorrected BBGKY approach, the minimal invasive RDM purification algorithm and the minimal invasive EOM correction algorithm. In the minimization problem underlying both correction algorithms, we have to find the optimal \hat{C}_2 which depends on $m^2(m+1)^2/4 = 100$ real-valued parameters. Being contraction-free and energy conserving leads to $m^2 + 1 = 17$ constraints. Moreover, \hat{C}_2 has to obey the parity symmetry of our problem imposing $m^4/8 + m^3/4 = 48$ further constraints (see Appendix H). Thereby, our system of linear constraints remains underdetermined as long as the number d of negative $\hat{\rho}_2$ eigenvalues and number d' of negative \hat{K}_2 eigenvalues obey $d + d' < 35$.

In Figure 13, we see that the minimal-invasive RDM purification algorithm clearly suppresses significant negative eigenvalues until $t \sim 2.5$ HO units. Thereafter, noticeably negative eigenvalue emerge but stay bounded from below until $t \sim 6$ HO units when a drastic instability kicks in. Thus, this iterative algorithm soon fails to converge after the maximal number of 500 iteration

steps. In order to understand the deeper reason of this failure, we have analyzed the spectrum of the updated operators $\hat{\rho}_2(t) + \alpha \hat{C}_2$ and $\hat{K}_2(t) + \alpha \hat{\Delta}_2$ for $\alpha \in [0, 1]$ and the first few iteration steps at such an instant in time (not shown). Thereby, we have found that while the tangent on a negative eigenvalue (with respect to α) indeed crosses zero as imposed by our constraints, level repulsion with other (in most cases negative) eigenvalues often hinders this negative eigenvalue to significantly move towards zero. We cannot rigorously prove that this is indeed the only mechanism for the breakdown of this iterative purification algorithm, of course.

Yet at least, this finding gives a useful hint why our non-perturbative, adaptive approach, the minimal invasive correction scheme of the 2-RDM EOM, gives very stable results [see Figure 13 (c.1) and (c.2)]. Actually, we observe that the D - and K -conditions are fulfilled to a good approximation much longer, namely for at least $t \leq 36$ HO unit (not shown). From Figure 13 (d), we furthermore infer that the integrator variably adapts its step-size, but in contrast to the Bose-Hubbard tunneling scenario no systematic enhancement of integrator steps is observed when $\hat{\rho}_2$ or \hat{K}_2 eigenvalues avoid each other in the vicinity of zero. Apparently, the though stabilized result features noticeable deviations from the MCTDHB results for the respective eigenvalues. Yet, we find that the overall accuracy of the $\bar{o} = 2$ results for the 1- and 2-RDM as measured by the trace-class distance is systematically improved for most times by correcting the

¹⁵ We note that the \hat{K}_2 spectra at $t = 0$ in the tunneling and the interaction-quench scenario differ although the system is initially a fully condensed BEC in both cases (see Figures 8 and 13). This is due to the fact that the \hat{K}_2 spectrum is sensitive to the total number of SPFs m even if not all of them are occupied.

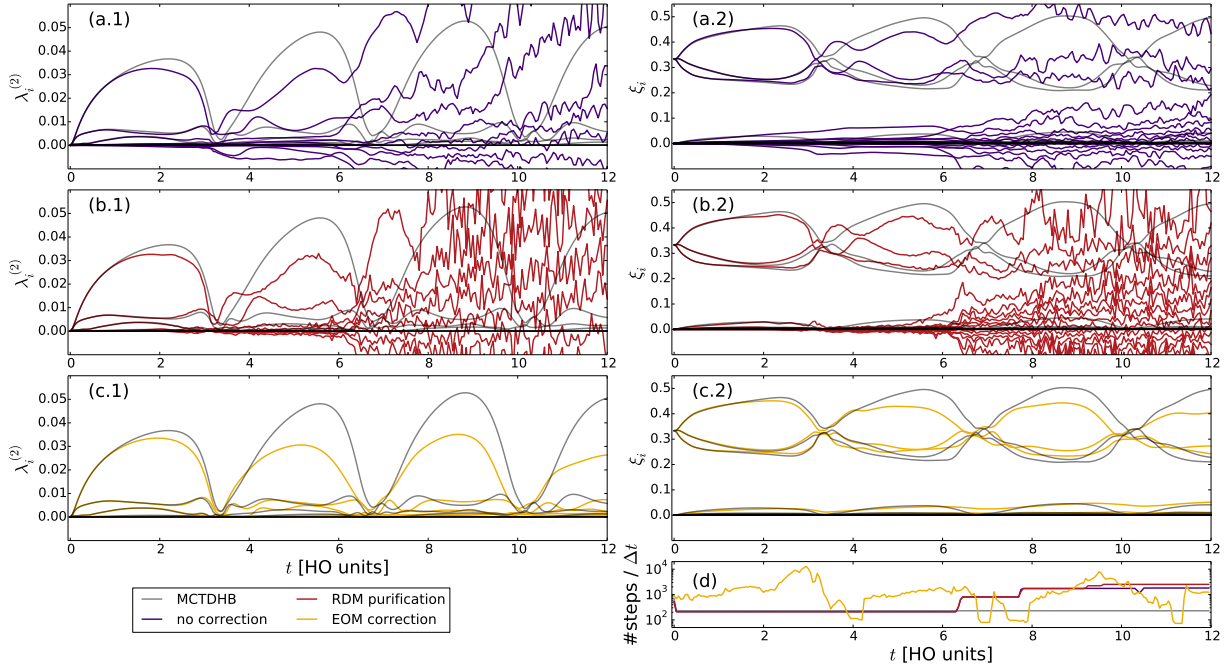


Figure 13. (color online) Comparison of the correction strategies outlined in Section VB (for the BBGKY hierarchy truncated at $\bar{o} = 2$), i.e. same as Figure 8 but for the interaction-quench scenario with $N = 30$ bosons. Parameters: threshold $\epsilon = -10^{-10}$, damping constant $\eta = 10$ HO units, write-out time-step $\Delta t = 0.05$ HO units, maximal number of iterations: 500. Otherwise, same parameters as in Figure 10.

2-RDM EOM, as one can infer from Figure 11 b).

In order to judge the accuracy of the EOM-corrected $\bar{o} = 2$ simulation more descriptively, we depict the deviations of its prediction for the reduced one-body density from the MCTDHB results in Figure 14. Note that this plot covers a longer time-span compared to the previous ones. As expected, we find that the deviations increase in time. Compared to the absolute values of the density, these deviations are, however, small and, most importantly, somewhat smaller than the deviations of corresponding Gross-Pitaevskii mean-field simulation from the $m = 4$ MCTDHB results (not shown). Finally, let us connect the errors in the one-body density to the errors measured by the trace-class distance $\mathcal{D}(\hat{\rho}_1^{\text{tr}}, \hat{\rho}_1^{\text{ex}})$ as depicted in Figure 11 b). For this purpose, we note that the density at position x can be expressed as the expectation value of the one-body observable $\hat{A}_1 = |x\rangle\langle x|$. Thereby, we can estimate $|\rho_1^{\text{tr}}(x; t) - \rho_1^{\text{ex}}(x; t)| \leq 2\|\hat{A}_1\|_1 \mathcal{D}(\hat{\rho}_1^{\text{tr}}(t), \hat{\rho}_1^{\text{ex}}(t)) = 2\mathcal{D}(\hat{\rho}_1^{\text{tr}}(t), \hat{\rho}_1^{\text{ex}}(t))$, which is consistent with the results depicted in Figure 14.

Going to higher truncation orders by making the Mazzotti ansatz for the corresponding higher-order correction operators \hat{C}_o unfortunately does not improve the BBGKY results, as already observed in the tunneling scenario. While the iterative RDM purification scheme fails to prevent the instabilities, we observe the same obstacle for the EOM correction algorithm as previously encountered, namely the optimization problem at order $o = 2$ lacking a solution (results not shown). Yet due to the

very promising results of the EOM correction algorithm when truncating the BBGKY hierarchy at order $\bar{o} = 2$, we believe that extending the EOM correction algorithm to higher orders without employing the Mazzotti ansatz for the correction operator is a highly promising direction to go.

VII. CONCLUSIONS

In this exploratory work, we have developed a novel methodological framework for simulating the quantum dynamics of finite ultracold bosonic systems. Instead of solving the time-dependent Schrödinger equation for the complete many-body system, our goal is to truncate the BBGKY hierarchy of equations of motion in order to obtain a closed theory for the dynamics of the low-order reduced density operators (RDMs). Here, we focus in particular on an efficient formulation of the underlying theory, which allows us to systematically study the impact of the truncation order on the accuracy and stability of the numerical results.

For this reason, we do not derive the BBGKY equations of motion from the exact von-Neumann equation by partial tracing but take the well-established variational Multi-Configuration Time-Dependent Hartree method for Bosons (MCTDHB) [74] for *ab-initio* wavefunction propagation as our starting-point. Thereby, we use time-dependent variationally optimized single-particle func-

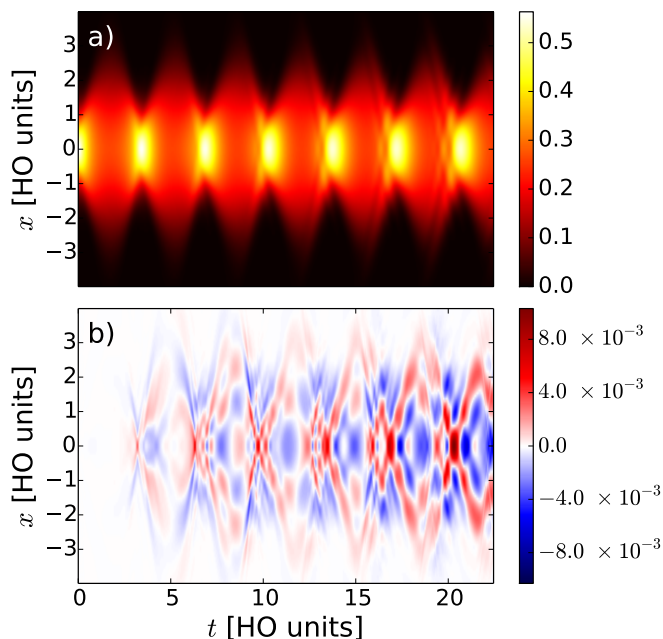


Figure 14. (color online) Subfigure a): Time-evolution of the reduced one-body density $\rho_1^{\text{ex}}(x; t)$ as obtained from MCTDHB on a longer time-scale. Subfigure b): Absolute deviation $\rho_1^{\text{tr}}(x; t) - \rho_1^{\text{ex}}(x; t)$ of the reduced one-body density $\rho_1^{\text{tr}}(x; t)$ as obtained from the BBGKY approach truncated at $\bar{o} = 2$ and stabilized by the minimal-invasive EOM correction algorithm with $\epsilon = -10^{-10}$ and $\eta = 10$ HO units. Number of bosons: $N = 30$. Otherwise, same parameters as in Figure 10.

tions (SPFs) as a our truncated single-particle basis, while being still able to recover the exact results if we formally let the number of SPFs tend to infinity. By expanding the RDMs with respect to bosonic number states using the dynamically optimized SPFs as the underlying basis states, we obtain a highly efficient representation of these high-dimensional objects, which also leads to an efficient and compact formulation of the corresponding BBGKY equations of motion (EOM) in the second quantization picture. These EOM are coupled to the SPF EOM of the MCTDHB theory.

By a careful analysis, we show that this coupled system of EOM features all properties, which are known for the BBGKY hierarchy as derived from the von-Neumann equation of the total system. Although being deduced from the zero-temperature MCTDHB theory, we find that the derived EOM for the RDM are also variationally optimal in a certain sense if the total many-body system is in a mixed initial state, which opens a promising route for including low-temperature effects in the simulation of ultracold atoms. Thus, truncating this BBGKY hierarchy of EOM can be viewed as on the one hand introducing an additional approximation to the MCTDHB approach for simulating larger particle numbers with more SPFs and on the other hand as an extension of the zero-temperature MCTDHB theory to finite temperatures.

We truncate the hierarchy of BBGKY EOM by using a reconstruction functional for the unknown RDM $\hat{\rho}_{\bar{o}+1}$ where \bar{o} denotes the truncation order. While the commonly employed cluster (cumulant) expansion for truncating the BBGKY hierarchy for fermionic systems is very well suited for taking correlations on top of a Hartree-Fock state into account [10], its corresponding bosonic variant has proven to be unfavorable for bosonic systems with a fixed number of particles since the correspondingly defined clusters diagnose that even an ideal Bose-Einstein condensate features few-particle correlations on all orders [50]. In this work, we cure this flaw by simply replacing the RDMs and symmetrization operators in this standard approach by the corresponding RDMs of unit trace and idempotent symmetrization operators, respectively. Since neglecting the complete cluster $\hat{c}_{\bar{o}+1}$ in the truncation approximation violates the compatibility to the lower order RDMs, we use the so-called unitarily invariant decomposition of bosonic operators [103–106] for restoring compatibility, as pursued in [72, 73] for electronic systems. Thereby, we obtain a closure approximation which conserves the compatibility of the RDMs as well as energy, respects symmetries such as parity or translational invariance if existent and is unitarily invariant, i.e. gauge invariant with respect to the choice of the constraint operator of the MCTDHB theory. In contrast to the cluster expansion for fermionic systems, however, the employed cluster-expansion lacks size-extensivity, i.e. testifies that two independent ideal Bose-Einstein condensates feature few-particle correlations stemming solely from the bosonic particle-exchange symmetry. Such correlations are physical, of course, but should not manifest themselves in the correlation *definition* on which a cluster expansion is build. Otherwise, truncating the expansion by neglecting clusters may imply neglecting correlations stemming from the bosonic symmetry. We show that this flaw can in principle be cured by minimal modifications of the cluster expansion, at the price, however, of losing the unitary invariance of the thereby defined correlations. For this reason, we do not apply these modifications to the truncation approximation in our numerical investigations.

Using appropriate super-operators and our bosonic number-state based framework, we derive two computational rules by means of which the clusters and thereby the closure approximation can be calculated highly efficiently for high orders in a recursive manner. This computational strategy allows us to go to truncation orders as high as $\bar{o} = 12$, meaning that up to 12-particle correlations are taken into account.

We have applied the above methodological framework to two scenarios, namely the tunneling dynamics in a double well and the interaction-quench induced breathing dynamics in a harmonic trap, in order to investigate the accuracy and stability of the numerical results in dependence on the truncation order. In both applications, we have found that the short-time dynamics can be highly accurately described by the truncated BBGKY approach,

where the accuracy of the results systematically improves with increasing truncation order \bar{o} . At longer times, the BBGKY gives also excellent results with controllable accuracy in the interaction-quench scenario for not too high excitation energies. However, severe deviations from the corresponding MCTDHB simulations occur at longer times in the tunneling scenario as well as for stronger interaction quenches. In these cases, the accuracy does not monotonously improve with increasing truncation order anymore and the truncated BBGKY EOM start to suffer from exponential instabilities, which lead to unphysical states. By inspecting the exact numerical results for the tunneling scenario, we find that few-particle correlations on all orders quickly play a significant role and eventually N -particle correlations dominate because the total system evolves into a NOON-state. This finding indicates that the long-time physics of this scenario prevents to use a truncation approximation which is based on neglecting $(\bar{o} + 1)$ -particle correlations.

Nevertheless, it is important to clearly separate the stability properties of the truncated BBGKY EOM from accuracy issues because (i) it is not desirable to have a highly accurate theory which is exponentially unstable under slight e.g. numerical perturbations and (ii) also a not highly accurate truncation approximation may give useful, sufficiently accurate results for low-dimensional observables such as the density if the EOM are sufficiently stable. Thus we have analyzed these instabilities for the two scenarios in depth. Thereby, we have found that the instability sets in at the truncation order \bar{o} and then propagates down to lower orders meaning that o -particle RDMs lack to be positive semi-definite in decreasing sequence with respect to the order o . The time until which the highest-order RDM, $\hat{\rho}_{\bar{o}}$, stays positive semi-definite only gradually increases with the truncation order \bar{o} , while the time when the lowest-order RDMs start lacking positivity decreases with increasing truncation order in some cases. This may be explained by the enhanced non-linearity of the closure approximation for higher truncation orders. Moreover, we have observed that the instabilities go often hand in hand with avoided crossings of RDM eigenvalues close to zero.

In order to stabilize the EOM, we have developed two novel minimal invasive and energy conserving correction algorithms: In our first attempt, we extend the dynamical purification algorithm [72, 73, 113]. Yet being based on a first-order perturbation theory argument, this algorithm cannot properly cope with the avoided crossings of the RDM eigenvalues in the vicinity of zero and thus fails to prevent the instabilities in our simulations. For this reason, we have developed a second, non-perturbative correction algorithm, which slightly alters the truncated BBGKY EOM such that negative RDM eigenvalues are exponentially damped to zero. We find that this approach indeed stabilizes the BBGKY EOM truncated at the second order and leads to reasonable long-time results for the interaction-quench scenario.

Besides these major methodological developments and

their numerical evaluation, we have also proposed an imaginary-time relaxation approach for calculating the lowest order ground-state RDMs of some reference Hamiltonian such that they can be used as the initial state for the BBGKY hierarchy. Moreover, we have analytically shown that certain coherences in the contraction-free component of the 2-RDM are responsible for dynamical quantum depletion and fragmentation of Bose gases.

Thereby, this exploratory work constitutes a major step forward to the treatment of correlated ultracold bosonic systems in terms of the truncated BBGKY hierarchy of EOM. In addition to the developed truncation approximation, we have presented numerous technical as well conceptual results, which are independent of the applied truncation approximation and as such also valuable for future works on closure approximations. In these regards, still open questions remain such as how to enforce size-extensivity in the cluster definition while keeping its unitary invariance. Although our numerical simulations reveal challenges for long-time propagations in far-off equilibrium situations, our thorough analysis gives valuable hints for future research, namely (i) extending the highly successful EOM correction algorithm of Section V B 2 to higher orders without using the Mazzionti ansatz and (ii) research on closure approximations for bosonic system with a fixed number of particles, going beyond the paradigm of the cluster expansion. Finding novel closure approximations by machine-learning techniques might be a promising first step.

ACKNOWLEDGMENTS

The authors thank Iva Březinová, Joachim Burgdörfer, Ignacio J. Cirac, Uwe Manthe, David A. Mazziotti, Hans-Dieter Meyer, Angel Rubio, Jan Stockhofe and Johannes M. Schurer for fruitful discussions. This work has been supported by the excellence cluster “The Hamburg Centre for Ultrafast Imaging - Structure, Dynamics and Control of Matter at the Atomic Scale” of the Deutsche Forschungsgemeinschaft.

Appendix A: Super-operators acting on bosonic operators

In this appendix, we define important super-operators acting on bosonic few-particle operators such as the o -RDM. These super-operators are represented in the second-quantization picture such that they can be applied efficiently to e.g. the RDMs being represented as outlined in Section II C. While only the basic concepts are discussed here, important technical details are covered by Appendix B. In the following, let \mathcal{B}_o denote the set of all hermitian bosonic o -body operators, meaning each $\hat{B}_o \in \mathcal{B}_o$ obeys $\hat{P}_\pi \hat{B}_o = \hat{B}_o \hat{P}_\pi = \hat{B}_o$ with the particle-permutation operator \hat{P}_π corresponding to an arbitrary

permutation $\pi \in S(o)$ of the first o integers.

1. Partial traces

Having \hat{B}_o expanded with respect to o -particle number states and using a mixed first and second quantization representation as outlined in Appendix B, the partial trace of \hat{B}_o over one particle can be expressed as¹⁶

$$\text{tr}_1(\hat{B}_o) \equiv \frac{1}{o} \sum_{r=1}^m \hat{a}_r \hat{B}_o \hat{a}_r^\dagger. \quad (\text{A1})$$

An explicit formula for the right hand side of (A1) as well as for the corresponding generalization to the partial trace over k particles, $\text{tr}_k(\hat{B}_o) \equiv \text{tr}_1 \circ \dots \circ \text{tr}_1(\hat{B}_o)$, for $k \leq o$ are provided in Appendix B.

2. Raising and joining operations

In our formal framework, we also need - loosely speaking - the inverse of the partial trace, meaning an operation which raises an operator $\hat{B}_o \in \mathcal{B}_o$ to an $(o+1)$ -body operator by adding a particle in an undefined state, i.e. the unit-operator. This raising operation is accomplished by¹⁷

$$\hat{R}_1(\hat{B}_o) \equiv \frac{1}{o+1} \sum_{r=1}^m \hat{a}_r^\dagger \hat{B}_o \hat{a}_r. \quad (\text{A2})$$

In Appendix F, we comment on the precise relationship between the raising and the partial-trace operation in terms of Eq. (F1).

For defining few-particle correlations in Section IV, we furthermore need a super-operator which joins two operators $\hat{A}_{o_1} \in \mathcal{B}_{o_1}$, $\hat{B}_{o_2} \in \mathcal{B}_{o_2}$ to a bosonic $(o_1 + o_2)$ -body operator

$$\hat{J}_{o_1}^{o_2}(\hat{A}_{o_1}, \hat{B}_{o_2}) \equiv \sum_{\mathbf{a}, \mathbf{b} | o_1} \sum_{\mathbf{c}, \mathbf{d} | o_2} A_{\mathbf{a}, \mathbf{b}}^{o_1} B_{\mathbf{c}, \mathbf{d}}^{o_2} \quad (\text{A3})$$

$$\left(\prod_{r=1}^m \binom{a_r + c_r}{c_r} \binom{b_r + d_r}{d_r} \right)^{\frac{1}{2}} |\mathbf{a} + \mathbf{c}\rangle \langle \mathbf{b} + \mathbf{d}|,$$

¹⁶ Although the number of particles, o , occurs on the right hand side of Eq. (A1), we do not incorporate it in the symbol tr_1 for the partial trace since one may replace the factor $1/o$ in Eq. (A1) by the inverse of the operator $(\hat{N} + 1)$ with the total particle-number operator $\hat{N} = \sum_{r=1}^m \hat{a}_r^\dagger \hat{a}_r$.

¹⁷ Similarly to Eq. (A1), the right hand side of (A2) does not explicitly depend on the number of particles since we may replace the right hand side by $\hat{N}^{-1} \sum_{r=1}^m \hat{a}_r^\dagger \hat{B}_o \hat{a}_r$ (see also footnote 16). This expression is well-defined because the inverse of the total particle-number operator acts only on states with at least one particle.

where $A_{\mathbf{a}, \mathbf{b}}^{o_1} \equiv \langle \mathbf{a} | \hat{A}_{o_1} | \mathbf{b} \rangle$ and $B_{\mathbf{c}, \mathbf{d}}^{o_2} \equiv \langle \mathbf{c} | \hat{B}_{o_2} | \mathbf{d} \rangle$. Expanding the argument \hat{B}_o in Eq. (A2) in number states and comparing the result with Eq. (A3), one can easily verify that raising \hat{B}_o effectively means joining with the one-body unit-operator of the subspace spanned by the instantaneous SPFs, i.e. $\hat{R}_1(\hat{B}_o) = \hat{J}_o^1(\hat{B}_o, \hat{\mathbb{P}})/(o+1)$ with $\hat{\mathbb{P}} \equiv \sum_{r=1}^m |\varphi_r\rangle \langle \varphi_r|$. Similarly, one can show that k -fold raising $\hat{R}_k(\hat{B}_o) \equiv \hat{R}_1 \circ \dots \circ \hat{R}_1(\hat{B}_o)$ effectively means joining with the corresponding bosonic k -body unit-operator, i.e. $\hat{R}_k(\hat{B}_o) = \hat{J}_o^k(\hat{B}_o, \hat{\mathbb{P}}_k^+)/\binom{o+k}{k}$ with $\hat{\mathbb{P}}_k^+ \equiv \sum_{\mathbf{n} | k} |\mathbf{n}\rangle \langle \mathbf{n}|$. Finally, we note that this bosonic joining operator plays the same role the wedge product for the cluster expansion for fermions (see e.g. [13]).

Appendix B: Mixed first and second quantization representation

While an efficient representation of RDMS requires working with bosonic number states, which is a second-quantization concept, operations such as partial traces are most conveniently performed if individual particles can be addressed by particle labels, i.e. in a first quantization framework. Here, we provide formulas for bridging between these two perspectives, which finally allows for evaluating all expressions in the second quantization picture. Our starting-point is the well-known relationship between an o -particle Hartree product $|\varphi_{j_1} \dots \varphi_{j_o}\rangle$, in which n_r particles reside in the SPF $|\varphi_r\rangle$, and the corresponding bosonic number state $|\mathbf{n}\rangle$ (normalized to unity) with $\mathbf{n} = (n_1, \dots, n_m)$ encoding the respective occupation numbers

$$|\mathbf{n}\rangle = \sqrt{\frac{o!}{\prod_i n_i!}} \hat{S}_o |\varphi_{j_1} \dots \varphi_{j_o}\rangle. \quad (\text{B1})$$

Here, \hat{S}_o refers to the idempotent o -particle symmetrization operator $\hat{S}_o = \sum_{\pi \in S(o)} \hat{P}_\pi / o!$ with the sum running over all particle permutations π and \hat{P}_π denoting the corresponding particle-exchange operator. After explicating the summation over all permutations of particle labels and renaming the summation index of the orbital in which the o th particle resides, we arrive at [81]

$$|\mathbf{n}\rangle = \sum_{r=1}^m \sqrt{\frac{n_r}{o}} |\mathbf{n} - \mathbf{e}_r\rangle^{(1, \dots, o-1)} \otimes |\varphi_r\rangle^{(o)} \quad (\text{B2})$$

$$= \sum_{r=1}^m \left(\frac{\hat{a}_r}{\sqrt{o}} |\mathbf{n}\rangle \right)^{(1, \dots, o-1)} \otimes |\varphi_r\rangle^{(o)},$$

where the super-indices of the ket-vectors indicate the particle-labels for the corresponding state and \mathbf{e}_r is an occupation number vector having vanishing elements except for the r th one being set to unity. In passing, we note that the state $\hat{a}_r |\mathbf{n}\rangle / \sqrt{o}$ coincides with the so-called single-hole function of $|\mathbf{n}\rangle$ with respect to the r th SPF as used in e.g. [75, 81]. The second identity in (B2) can

be used to prove and explicate the expression (A1) for the partial trace of $\hat{B}_o \in \mathcal{B}_o$ over one particle, given its representation $\sum_{\mathbf{n}, \mathbf{m}|o} B_{\mathbf{n}, \mathbf{m}}^o |\mathbf{n}\rangle\langle \mathbf{m}|$

$$\begin{aligned} \text{tr}_1(\hat{B}_o) &= \sum_{\mathbf{n}, \mathbf{m}|o} \sum_{r=1}^m B_{\mathbf{n}, \mathbf{m}}^o \langle \varphi_r | \mathbf{n} \rangle \langle \mathbf{m} | \varphi_r \rangle^{(o)} \quad (\text{B3}) \\ &= \frac{1}{o} \sum_{\mathbf{n}, \mathbf{m}|o} \sum_{r=1}^m B_{\mathbf{n}, \mathbf{m}}^o \hat{a}_r | \mathbf{n} \rangle \langle \mathbf{m} | \hat{a}_r^\dagger = \frac{1}{o} \sum_{r=1}^m \hat{a}_r \hat{B}_o \hat{a}_r^\dagger \\ &= \frac{1}{o} \sum_{\mathbf{a}, \mathbf{b}|o-1} \sum_{r=1}^m \sqrt{(a_r+1)(b_r+1)} B_{\mathbf{a}+\mathbf{e}_r, \mathbf{b}+\mathbf{e}_r}^o | \mathbf{a} \rangle \langle \mathbf{b} |. \end{aligned}$$

By successively applying the steps leading to (B2) to the respectively occurring number states and using the identity (B1) for the resulting Hartree products, we may decompose an o -particle number state into a sum over products of $(o-k)$ -particle and k -particle number states ($k < o$) associated with the “first” $o-k$ and the “last” k particles

$$|\mathbf{n}\rangle = \binom{o}{k}^{-\frac{1}{2}} \sum_{\mathbf{l}|k} \Theta(\mathbf{n}-\mathbf{l}) \left[\prod_{r=1}^m \binom{n_r}{l_r} \right]^{\frac{1}{2}} \quad (\text{B4})$$

$$|\mathbf{n}-\mathbf{l}\rangle^{(1, \dots, o-k)} \otimes |\mathbf{l}\rangle^{(o-k+1, \dots, o)},$$

where $\Theta(\mathbf{n}) \equiv \prod_{i=1}^m \Theta(n_i)$ with the Heavyside function Θ defined by $\Theta(x) = 1$ for $x \geq 0$ and zero otherwise. The relation (B4) is a central technical result, on which the recursive formulation of the cluster expansion is founded (see Section IV B 3 and Appendix G).

Furthermore, this identity allows for efficiently evaluating the partial trace $\text{tr}_k(\hat{B}_o)$ of a bosonic o -body operator \hat{B}_o over k particles ($k < o$). Expanding \hat{B}_o with respect to number states $|\mathbf{n}\rangle$, $|\mathbf{m}\rangle$ and inserting the decomposition (B4), one directly obtains the following expression

$$\begin{aligned} \text{tr}_k(\hat{B}_o) &\equiv \quad (\text{B5}) \\ &\equiv \sum_{i_1, \dots, i_k} \langle \varphi_{i_1} \dots \varphi_{i_k} | \hat{B}_o | \varphi_{i_1} \dots \varphi_{i_k} \rangle^{(o-k+1, \dots, o)} \\ &= \sum_{\mathbf{l}|k} \langle \mathbf{l} | \hat{B}_o | \mathbf{l} \rangle^{(o-k+1, \dots, o)} \\ &= \binom{o}{k}^{-1} \sum_{\mathbf{a}, \mathbf{b}|o-k} \sum_{\mathbf{l}|k} \left(\prod_{r=1}^m \binom{a_r + l_r}{l_r} \binom{b_r + l_r}{l_r} \right)^{\frac{1}{2}} \\ &\quad B_{\mathbf{a}+\mathbf{l}, \mathbf{b}+\mathbf{l}}^o | \mathbf{a} \rangle \langle \mathbf{b} |. \end{aligned}$$

We note that this expression is meaningful also for $k = o$, resulting in $\text{tr}_o(\hat{B}_o) = \text{tr}(\hat{B}_o) |0\rangle\langle 0|$ with $|0\rangle$ denoting the vacuum state. Besides, the above formula provides one way to derive the expression (3) for the o -RDM by setting o to the total number of atoms N , k to $N-o$ and \hat{B}_N to $|\Psi_t\rangle\langle \Psi_t|$ and using the expansion (1).

Appendix C: Finite temperatures

Let us now show that and in which sense the EOM (5) together with the possibly truncated RDM EOM (6) result in an optimal SPF dynamics also for mixed initial N -particle states, given that the N -particle dynamics is unitary. This line of argumentation strongly resembles the considerations on an alternative to the so-called ρ MCTDH type-2 method for simulating Lindblad master equations for distinguishable degrees of freedom in the limit of purely unitary dynamics, as discussed in [82]. Given the spectral representation of the initial state

$$\hat{\rho}_N(0) = \sum_{r=1}^{C_m^N} \lambda_r^{(N)}(0) |\phi_r^N(0)\rangle\langle \phi_r^N(0)|, \quad (\text{C1})$$

a unitary dynamics governed by the Hamiltonian \hat{H} leaves the probabilities $\lambda_r^{(N)}(t)$ invariant. Instead of solving the von-Neumann equation for $\hat{\rho}_N$, one may purify the density operator to

$$|\Phi_t\rangle = \sum_{r=1}^{C_m^N} \sqrt{\lambda_r^{(N)}} |\phi_r^N(t)\rangle \otimes |u_r\rangle, \quad (\text{C2})$$

where $\{|u_r\rangle\}$ denotes some fixed time-independent orthonormal basis of a C_m^N -dimensional auxiliary Hilbert space. This pure state is propagated according to $i\partial_t |\Phi_t\rangle = \hat{H} \otimes \mathbb{1} |\Phi_t\rangle$ and one exactly recovers the solution of the von-Neumann equation by taking the partial trace over the auxiliary space, i.e. $\hat{\rho}_N(t) = \text{tr}_{\text{aux}}(|\Phi_t\rangle\langle \Phi_t|)$. Now one can expand each $|\phi_r^N(t)\rangle$ in the MCTDHB manner $\sum_{\mathbf{n}|N} A_{\mathbf{n}}^r |\mathbf{n}\rangle$, where all states share the same set of SPFs, and minimize the action functional with the Lagrangian $\langle \Phi_t | (i\partial_t - \hat{H} \otimes \mathbb{1}) | \Phi_t \rangle$ under orthonormality constraints on both the SPFs and the N -particle states $|\phi_r^N(t)\rangle$. Thereby, one finds that the coefficients $A_{\mathbf{n}}^r$ for fixed r obey Eq. (4). Differentiating $\rho_{\mathbf{n}, \mathbf{m}}^N = \sum_r \lambda_r^{(N)} (A_{\mathbf{n}}^r)^* A_{\mathbf{m}}^r$ with respect to time, we directly obtain the RDM EOM (6) at order $o = N$. Varying the action with respect to the SPFs exactly results in the SPF EOM (5) where the elements of the 1- and 2-RDM entering the equations are the convex sum over the corresponding matrices (3) for the state $|\phi_r^N\rangle$ weighted with the probability $\lambda_r^{(N)}$. The latter means that the 1- and 2-RDM in the EOM for the SPFs are exactly the $(N-1)$ - and $(N-2)$ -fold partial trace of $\hat{\rho}_N$, respectively.

Thereby, it is shown that the EOM (5), (6) applied to a mixed, e.g. thermal initial N -particle state also result in a well-defined variationally optimal dynamics, where the dynamical adaption of the SPFs is a compromise between an optimal representation of the various eigenvectors $|\phi_r^N(t)\rangle$ of $\hat{\rho}_N(t)$. Here, eigenstates of higher probability $\lambda_r^{(N)}$ have a stronger impact on the SPF dynamics than weakly occupied eigenstates.

Appendix D: Propagation in negative imaginary time

The purpose of this appendix is to show how one can derive EOM for the RDMs in imaginary time which contract an initial guess to the ground-state RDMs. While the case of the N -RDM, i.e. the state of the full system, has already been addressed in Section IIIB2, we illustrate the derivation by exemplarily inspecting the case of the 1-RDM.

Fixing the constraint operator to $g_{ij} = 0$ here, we may write the MCTDHB EOM in imaginary time in the following compact form

$$\begin{aligned} \partial_\tau |\Psi_\tau\rangle &= (E_\tau - \hat{H}_0) |\Psi_\tau\rangle \\ &+ \sum_{i=m+1}^{\infty} \sum_{j=1}^m \langle \varphi_i | (\partial_\tau |\varphi_j\rangle) \hat{a}_i^\dagger \hat{a}_j |\Psi_\tau\rangle. \end{aligned} \quad (\text{D1})$$

Here, \hat{H}_0 is defined via Eq. (7) with the constraint-operator g_{ij} set to zero and with the Hamiltonian \hat{H} being replaced by the reference Hamiltonian \hat{H}_0 , whose ground-state RDMs shall be calculated. The term proportional to the energy expectation value $E_\tau \equiv \langle \Psi_\tau | \hat{H}_0 | \Psi_\tau \rangle = \langle \Psi_\tau | \hat{H}_0 | \Psi_\tau \rangle$ ensures that the norm of $|\Psi_\tau\rangle$ does not contract to zero but stays unity. In Eq. (D1), we have furthermore expanded the SPF notation: $|\phi_r\rangle$ still refers to the dynamically adapted MCTDHB SPFs for $r = 1, \dots, m$. For larger r , $|\phi_r\rangle$ refers to an unoccupied, i.e. virtual orbital outside of the space spanned by the instantaneous SPFs. For the sake of concreteness, we assume the single-particle Hilbert space to be infinite dimensional, while in a numerical implementation r would be bounded from above by the number of time-independent single-particle states used to represent the MCTDHB SPFs. Accordingly, we extend the notation of creation and annihilation operators also to the space of virtual orbitals. Finally, $\partial_\tau |\varphi_j\rangle$ coincides with the negative of the right hand side of Eq. (5) with \hat{g} set to zero.

Now we can derive the corresponding EOM for the 1-RDM where we use the representation (2) for simplicity. When differentiating $D_{i,j}^1 = \langle \Psi_\tau | \hat{a}_j^\dagger \hat{a}_i | \Psi_\tau \rangle$ for $i, j = 1, \dots, m$ with respect to τ , we can make use for the fact $\partial_\tau \hat{a}_i^{(\dagger)} = \sum_{r=m+1}^{\infty} \langle \partial_\tau \varphi_i | \varphi_r \rangle^{(*)} \hat{a}_r^{(\dagger)}$ for $i = 1, \dots, m$, which is a consequence of $\hat{g} = 0$. Thereby, one obtains

$$\partial_\tau \langle \Psi_\tau | \hat{a}_j^\dagger \hat{a}_i | \Psi_\tau \rangle = \langle \Psi_\tau | \{ E_\tau - \hat{H}_0, \hat{a}_j^\dagger \hat{a}_i \} | \Psi_\tau \rangle. \quad (\text{D2})$$

Inserting \hat{H}_0 into the right hand side and normal ordering under consideration of the permutation symmetry of both

the occurring RDMs and v_{ijqp} results in

$$\begin{aligned} \partial_\tau D_{i,j}^1 &= 2E_\tau D_{i,j}^1 - 2 \left(\sum_{r=1}^m (h_{rj} D_{i,r}^1 + h_{ir} D_{r,j}^1) \right) \\ &+ \sum_{q,p=1}^m h_{qp} D_{(ip),(jq)}^2 \\ &+ \sum_{q,p,r=1}^m (v_{irqp} D_{(qp),(jr)}^2 + v_{qpjr} D_{(ir),(qp)}^2) \\ &+ \sum_{q,p,r,s=1}^m v_{qprs} D_{(irs),(jqp)}^3 \end{aligned} \quad (\text{D3})$$

with

$$E_\tau = \sum_{q,p=1}^m h_{qp} D_{p,q}^1 + \frac{1}{2} \sum_{q,p,r,s=1}^m v_{qprs} D_{(rs),(qp)}^2. \quad (\text{D4})$$

Therefore, as in the case of a contracted Schrödinger equation [12, 13, 56, 58], the dynamics of the 1-RDM couples to both the 2- and the 3-RDM. The EOM (D3) can be easily translated to the more compact representation of RDMs (3), of course. This derivation can be applied also for the EOM of higher-order RDMs, with the result that $\partial_\tau D^o$ couples to both the $(o+1)$ - and the $(o+2)$ -RDM as well as to the 1- and 2-RDM by virtue of Eq. (D4). The latter coupling, however, can be transformed away by expressing E_τ solely as a functional of D^o , which is always possible for $o \geq 2$ when using a truncation approximation which conserves the compatibility of the RDMs. As a starting-point for the truncation of the resulting hierarchy of EOM, one can try the various closure approximations derived for contracted Schrödinger equations [12, 13, 56, 58].

Appendix E: An alternative cluster expansion for bosons

In this part of the appendix, we outline how to construct an alternative cluster expansion which is termwise compatible and has multi-orbital mean-field states as (approximately) correlation-free reference states. The latter is a desirable property that implies (approximate) size-extensivity in the sense specified in Section IVB2. First, we discuss how to appropriately modify the terms $\otimes_{\kappa=1}^o \hat{\rho}_1^{(\kappa)} \hat{S}_o$ of the expansion (19). Then we exemplarily describe the modification of terms such as $[\hat{c}_2^{(1,2)} \hat{\rho}_1^{(3)} + \dots] \hat{S}_3$ and finally a crucial mathematical subtlety is discussed.

For constructing this alternative cluster expansion, we first inspect the structure of the o -RDM given that the total system is in a multi-orbital mean-field state $|\Psi_{\text{MMF}}\rangle = |\mathbf{k}\rangle$. Tracing out $(N-o)$ atoms by means of (B5), we obtain

$$\hat{\rho}_o^{\text{MMF}} = \binom{N}{o}^{-1} \sum_{\mathbf{n}|o} \Theta(\mathbf{k} - \mathbf{n}) \left[\prod_{r=1}^m \binom{k_r}{n_r} \right] |\mathbf{n}\rangle \langle \mathbf{n}|, \quad (\text{E1})$$

which at first order boils down to $\hat{\rho}_1^{\text{MMF}} = \sum_r \frac{k_r}{N} |\hat{r}\rangle\langle\hat{r}|$. The latter means that the NOs $|\phi_r^1\rangle$ coincide with the single-particle states underlying the permanent $|\mathbf{k}\rangle$ and that the NPs read $\lambda_r^{(1)} \equiv k_r/N$. Now let us inspect why the cluster expansion (19) diagnoses few-particle correlations for $|\Psi_{\text{MMF}}\rangle$. This means inspecting why the first term in the expansion (19) at order o deviates from the analytical result (E1). Using the spectral decomposition of $\hat{\rho}_1^{\text{MMF}}$ and the relationship between symmetrized Hartree products and permanents (B1), such a symmetrized product of 1-RDMs can be calculated as

$$\begin{aligned} \bigotimes_{\kappa=1}^o \hat{\rho}_1^{(\kappa)} \hat{S}_o &= \hat{S}_o \bigotimes_{\kappa=1}^o \hat{\rho}_1^{(\kappa)} \hat{S}_o \\ &= \sum_{i_1, \dots, i_o=1}^m \left[\prod_{\kappa=1}^o \lambda_{i_\kappa}^{(1)} \right] \hat{S}_o |\phi_{i_1}^1 \dots \phi_{i_o}^1\rangle \langle \phi_{i_1}^1 \dots \phi_{i_o}^1| \hat{S}_o \\ &= \sum_{\mathbf{n}|_o} \left[\prod_{r=1}^m (\lambda_r^{(1)})^{n_r} \right] |\mathbf{n}\rangle\langle\mathbf{n}|, \end{aligned} \quad (\text{E2})$$

where we have abbreviated $\hat{\rho}_1 \equiv \hat{\rho}_1^{\text{MMF}}$. Straightforward calculations show that (E2) is neither termwise compatible in the sense $\text{tr}_1(\bigotimes_{\kappa=1}^{o+1} \hat{\rho}_1^{(\kappa)} \hat{S}_{o+1}) \neq \bigotimes_{\kappa=1}^o \hat{\rho}_1^{(\kappa)} \hat{S}_o$ nor does it serve as a good approximation for (E1). These flaws can actually be linked to the fact that the norm of a symmetrized Hartree product $\hat{S}_o |\phi_{i_1}^1 \dots \phi_{i_o}^1\rangle$, as it occurs in the second identity of (E2), depends on the corresponding occupation numbers (see Eq. (B1)). The latter, however, can be compensated by introducing a modified symmetrization operator

$$\hat{S}_o \equiv \left(\frac{o!}{\bigotimes_{r=1}^m \hat{n}_r!} \right)^{\frac{1}{2}} \hat{S}_o \quad (\text{E3})$$

where $\bigotimes_{r=1}^m \hat{n}_r!$ is defined as $\sum_{\mathbf{n}} (\prod_r n_r!) |\mathbf{n}\rangle\langle\mathbf{n}|$ with the NOs $|\phi_r^1\rangle$ as the underlying single-particle basis. Thereby, we ensure $\hat{S}_o |\phi_{i_1}^1 \dots \phi_{i_o}^1\rangle = |\mathbf{n}\rangle$. Now we are equipped to replace the 1-RDM product terms (E2) of the cluster expansion (19) by the following expression

$$\hat{S}_o \bigotimes_{\kappa=1}^o \hat{\rho}_1^{(\kappa)} \hat{S}_o = o! \sum_{\mathbf{n}|_o} \left[\prod_{r=1}^m \frac{(\lambda_r^{(1)})^{n_r}}{n_r!} \right] |\mathbf{n}\rangle\langle\mathbf{n}|. \quad (\text{E4})$$

It is easy to see that the partial trace of (E4) equals (E4) with o replaced by $(o-1)$ implying that this class of terms in the alternative cluster expansion is termwise compatible indeed. Inserting $\lambda_r^{(1)} \equiv k_r/N$ into (E4), we see that (E4) coincides with (E1) up to $1/N$ corrections if $o \ll k_r$ for all finite k_r , i.e. in the case of a multi-orbital mean-field state with only macroscopically occupied orbitals. Thus, size-extensivity is approximately ensured. In passing, we note that the relationship between anti-symmetrized Hartree products and fermionic number states does not involve a state-dependent normalization factor, which might be the reasons why the anti-symmetrization of the cluster expansion (18) leads to size-extensivity.

We further illustrate how to construct a termwise compatible cluster expansion by inspecting how the terms $[\hat{c}_\sigma^{(1, \dots, \sigma)} \hat{\rho}_1^{(\sigma+1)} + \dots] \hat{S}_{\sigma+1}$ have to be modified. Let us abbreviate the modified version of this term by $\hat{G}_{1, \sigma}^{1,1}$ (in analogy to the notation (22)) and assume that termwise compatibility has already been ensured up to order σ implying $\text{tr}_1(\hat{c}_\sigma) = 0$. For the term $\hat{G}_{1, \sigma}^{1,1}$, we then make the ansatz

$$\hat{G}_{1, \sigma}^{1,1} = \sum_{\mathbf{n}, \mathbf{m}|\sigma+1} |\mathbf{n}\rangle\langle\mathbf{m}| \sum_{\substack{r=1 \\ n_r, m_r > 0}}^m c_{\mathbf{n}-\mathbf{e}_r, \mathbf{m}-\mathbf{e}_r}^\sigma \lambda_r^{(1)} f_{\mathbf{n}, \mathbf{m}, r}, \quad (\text{E5})$$

where again the NOs $|\phi_r^1\rangle$ serve as the underlying single-particle basis. Motivated by the factorial factors of Eq. (E4) compared to (E2), we have introduced a real-valued occupation-number factor $f_{\mathbf{n}, \mathbf{m}, r}$ to be determined by the termwise compatibility requirement $\text{tr}_1(\hat{G}_{1, \sigma}^{1,1}) = \hat{c}_\sigma$. When evaluating the left hand side of this requirement, one realizes that one can only benefit from $\text{tr}_1(\hat{c}_\sigma) = 0$ if f depends only on n_r and m_r , i.e. $f_{\mathbf{n}, \mathbf{m}, r} = g(n_r, m_r)$. Then the requirement $\text{tr}_1(\hat{G}_{1, \sigma}^{1,1}) = \hat{c}_\sigma$ becomes equivalent to g solving

$$\sqrt{(l+1)(k+1)} g(l+1, k+1) - \sqrt{lk} g(l, k) = \sigma + 1, \quad (\text{E6})$$

for all $l, k = 0, \dots, \sigma$. This set of linear equations possess the unique solution $g(l, k) = (\sigma + 1)[\delta_{lk} + (1 - \delta_{lk}) \sqrt{\min\{l/k, k/l\}}]$. By making a similar ansatz involving occupation-number factors, other classes of terms in the cluster expansion (19) can be modified to obey termwise compatibility.

Although termwise compatibility and (approximate) size-extensivity are desirable properties which the cluster expansion (19) lacks, we do not employ this alternative approach for truncating the BBGKY hierarchy because the thereby defined clusters fail to be unitarily invariant in the case of NP degeneracies. Suppose that there are only two SPFs ($m = 2$) and that the NPs are degenerate, i.e. $\lambda_1^{(1)} = \lambda_2^{(1)} = 0.5$. Then one can analytically show that the alternative definition for the two-particle cluster $\hat{c}_2 = \hat{\rho}_2 - \hat{S}_2 \hat{\rho}_1^{(1)} \hat{\rho}_1^{(2)} \hat{S}_2$ does depend on the concrete choice for the degenerate NOs. This ambiguity stems from the fact that the operator $\bigotimes_{r=1}^m \hat{n}_r!$ is not form-invariant under unitary transformations of the NOs. Due to this finding, we do not develop this alternative cluster expansion further but use the unitarily invariant decomposition, being described in the following section, for making the symmetrized cluster expansion (19) compatible.

Appendix F: Unitarily invariant decomposition of bosonic operators

According to the UID [103–106], any given hermitian bosonic o -body operator $\hat{B}_o \in \mathcal{B}_o$ can be uniquely decomposed into $\hat{B}_o = \bigoplus_{k=0}^o \hat{B}_{o;k}$ with respect to all irreducible

representations of the unitary group $U(m)$ (the unitary transformations within the SPF space) on \mathcal{B}_o . This decomposition has the property that the l -fold partial trace of \hat{B}_o is fully determined by the first $(o-l+1)$ addends: $\text{tr}_l(\hat{B}_o) = \text{tr}_l(\oplus_{k=0}^{o-l} \hat{B}_{o;k})$. Explicit formulas for the components can be obtained by making use of the fact that for each¹⁸ $l = 0, \dots, o-1$ there is a unique $\hat{T}_l \in \mathcal{B}_l$ such that $\oplus_{k=0}^l \hat{B}_{o;k} = \hat{R}_{o-l}(\hat{T}_l)$ and determining the \hat{T}_l 's recursively by employing the relation between the raising operation (A2) and the partial trace (A1) [106, 139]

$$\text{tr}_1(\hat{R}_1(\hat{B}_o)) = \frac{2o+m}{(o+1)^2} \hat{B}_o + \left(\frac{o}{o+1}\right)^2 \hat{R}_1(\text{tr}_1(\hat{B}_o)). \quad (\text{F1})$$

We, however, are not interested in the individual terms of the complete UID but only in separating the contraction-free component $\hat{B}_o^{\text{irr}} \equiv \hat{B}_{o;o}$ from the rest, i.e. in the decomposition¹⁹ $\hat{B}_o = \hat{B}_o^{\text{red}} \oplus \hat{B}_o^{\text{irr}}$. Using the results of [106] for $\hat{B}_{o;k}$ and a computer algebra program [140] for summing over k , we find

$$\hat{B}_o^{\text{red}} = - \sum_{k=0}^{o-1} (-1)^{o+k} \frac{\binom{o}{k}^2}{\binom{2o+m-2}{o-k}} \hat{R}_{o-k}(\text{tr}_{o-k}(\hat{B}_o)) \quad (\text{F2})$$

and $\hat{B}_o^{\text{irr}} = \hat{B}_o - \hat{B}_o^{\text{red}}$. Eq. (F2) implies that the reducible component \hat{B}_o^{red} depends linearly on all partial partial

traces of \hat{B}_o . We stress here that all considerations regarding the UID rely on having a finite-dimensional single-particle Hilbert space, i.e. on m being finite [103–106]. For the actual evaluation of (F2), we use the relationship between the k -fold raising operation and the joining operation as stated in Sect. A 2 together with Eq. (A3).

Appendix G: Proof of the recursive formulation of the bosonic cluster expansion

The proofs of the recursion relations (24), (25) rely on (i) the property $\hat{S}_o|\mathbf{n}\rangle = |\mathbf{n}\rangle$ for any o -particle number state $|\mathbf{n}\rangle$ and (ii) the number-state decomposition (B4). To prove (24), we first inspect the matrix element of \hat{F}_σ^n with respect to any two $(n\sigma)$ -particle number states

$$\begin{aligned} \langle \mathbf{a} | \hat{F}_\sigma^n | \mathbf{b} \rangle &\stackrel{(i)}{=} \langle \mathbf{a} | [\hat{c}_\sigma^{(1, \dots, \sigma)} \dots \hat{c}_\sigma^{([n-1]\sigma+1, \dots, n\sigma)} + \text{dist. perm.}] | \mathbf{b} \rangle \\ &= \frac{(n\sigma)!}{n!(\sigma!)^n} \langle \mathbf{a} | \hat{c}_\sigma^{(1, \dots, \sigma)} \dots \hat{c}_\sigma^{([n-1]\sigma+1, \dots, n\sigma)} | \mathbf{b} \rangle \end{aligned} \quad (\text{G1})$$

where we have also used the invariance of number states under particle permutations in the last identity. The resulting prefactor denotes the number of distinct sequences of n pairwise distinct σ -tuple if the order of the sequence does not matter. Next we apply (B4) to both $|\mathbf{a}\rangle$ and $|\mathbf{b}\rangle$

$$\begin{aligned} \langle \mathbf{a} | \hat{F}_\sigma^n | \mathbf{b} \rangle &= \frac{(n\sigma)!}{n!(\sigma!)^n} \binom{n\sigma}{\sigma}^{-1} \sum_{\mathbf{r}, \mathbf{s} | \sigma} \Theta(\mathbf{a} - \mathbf{r}) \Theta(\mathbf{b} - \mathbf{s}) \left[\prod_{i=1}^m \binom{a_i}{r_i} \binom{b_i}{s_i} \right]^{\frac{1}{2}} \times \\ &\times \langle \mathbf{a} - \mathbf{r} | \hat{c}_\sigma^{(1, \dots, \sigma)} \dots \hat{c}_\sigma^{([n-2]\sigma+1, \dots, [n-1]\sigma)} | \mathbf{b} - \mathbf{s} \rangle \langle \mathbf{r} | \hat{c}_\sigma | \mathbf{s} \rangle. \end{aligned} \quad (\text{G2})$$

By re-using the result (G1), we may express the second last factor of (G2) as

$$\begin{aligned} \langle \mathbf{a} - \mathbf{r} | \hat{c}_\sigma^{(1, \dots, \sigma)} \dots \hat{c}_\sigma^{([n-2]\sigma+1, \dots, [n-1]\sigma)} | \mathbf{b} - \mathbf{s} \rangle &= \\ \frac{(n-1)!(\sigma!)^{n-1}}{[(n-1)\sigma]!} \langle \mathbf{a} - \mathbf{r} | \hat{F}_\sigma^{n-1} | \mathbf{b} - \mathbf{s} \rangle. \end{aligned} \quad (\text{G3})$$

Inserting (G2), (G3) into the expansion $\hat{F}_\sigma^n =$

$\sum_{\mathbf{a}, \mathbf{b} | n\sigma} \langle \mathbf{a} | \hat{F}_\sigma^n | \mathbf{b} \rangle |\mathbf{a}\rangle \langle \mathbf{b}|$ and substituting the sum over \mathbf{a} (\mathbf{b}) by a sum over $\mathbf{a}' \equiv \mathbf{a} - \mathbf{r}$ ($\mathbf{b}' \equiv \mathbf{b} - \mathbf{s}$) we finally find $\hat{F}_\sigma^n = \hat{J}_{(n-1)\sigma}^\sigma(\hat{F}_\sigma^{n-1}, \hat{c}_\sigma)/n$.

In order to prove the second relation (25), we abbreviate $o' = \sum_{r=1}^{K-1} n_r \sigma_r$ as well as $o = o' + n_K \sigma_K$ and decompose the distinguishable permutations over particle labels in (22) as follows

¹⁸ We note that the space of hermitian bosonic 0-body operators is given by $\mathcal{B}_0 = \{\alpha |0\rangle\langle 0|, \alpha \in \mathbb{R}\}$.

¹⁹ We note that the superscripts “red” and “irr” do not refer to (irr)reducible representations of the unitary group $U(m)$ but encode whether or not the component contains genuine o -particle correlations (see Section IV B 3).

$$\begin{aligned}
\langle \mathbf{a} | \hat{F}_{\sigma_1, \dots, \sigma_K}^{n_1, \dots, n_K} | \mathbf{b} \rangle &= \langle \mathbf{a} | \left[\hat{c}_{\sigma_1}^{(1, \dots, \sigma_1)} \dots \hat{c}_{\sigma_{K-1}}^{(o' - \sigma_{K-1} + 1, \dots, o')} + \text{dist. perm.} \right] \times \\
&\quad \times \left[\hat{c}_{\sigma_K}^{(o' + 1, \dots, o' + \sigma_K)} \dots \hat{c}_{\sigma_K}^{(o - \sigma_K + 1, \dots, o)} + \text{dist. perm.} \right] | \mathbf{b} \rangle \\
&\stackrel{(i)}{=} \langle \mathbf{a} | \left[\hat{c}_{\sigma_1}^{(1, \dots, \sigma_1)} \dots \hat{c}_{\sigma_{K-1}}^{(o' - \sigma_{K-1} + 1, \dots, o')} + \text{dist. perm.} \right] \hat{S}_{o'}^{(1, \dots, o')} \times \\
&\quad \times \left[\hat{c}_{\sigma_K}^{(o' + 1, \dots, o' + \sigma_K)} \dots \hat{c}_{\sigma_K}^{(o - \sigma_K + 1, \dots, o)} + \text{dist. perm.} \right] \hat{S}_{n_K \sigma_K}^{(o' + 1, \dots, o)} + \text{dist. perm.} \Big] | \mathbf{b} \rangle \\
&= \langle \mathbf{a} | \left[\left[\hat{F}_{\sigma_1, \dots, \sigma_{K-1}}^{n_1, \dots, n_{K-1}} \right]^{(1, \dots, o')} \left[\hat{F}_{\sigma_K}^{n_K} \right]^{(o' + 1, \dots, o)} + \text{dist. perm.} \right] | \mathbf{b} \rangle \\
&= \langle \mathbf{a} | \left[\hat{F}_{\sigma_1, \dots, \sigma_{K-1}}^{n_1, \dots, n_{K-1}} \right]^{(1, \dots, o')} \left[\hat{F}_{\sigma_K}^{n_K} \right]^{(o' + 1, \dots, o)} | \mathbf{b} \rangle \binom{o}{o'}
\end{aligned} \tag{G4}$$

where we have again employed the bosonic symmetry of the number states for the last identity. Using (B4), the binomial factor in (G4) is canceled and eventually the same number-state substitutions as before lead to $\hat{F}_{\sigma_1, \dots, \sigma_K}^{n_1, \dots, n_K} = \hat{J}_{o - n_K \sigma_K}^{n_K \sigma_K} (\hat{F}_{\sigma_1, \dots, \sigma_{K-1}}^{n_1, \dots, n_{K-1}}, \hat{F}_{\sigma_K}^{n_K})$.

Appendix H: Minimal invasive purification of the RDM

In this appendix, we show how one can translate the minimal-invasive purification scheme as outlined in Section VB 1 into a linear (quadratic) program when using the 1-norm (2-norm). The hermiticity of the correction operator \hat{C}_2 is incorporated in the following formalism by decomposing $C_{\mathbf{n}, \mathbf{m}}^2 = C_{\mathbf{n}, \mathbf{m}}^{2, \Re} + i C_{\mathbf{n}, \mathbf{m}}^{2, \Im}$ with $C_{\mathbf{n}, \mathbf{m}}^{2, \Re}$ ($C_{\mathbf{n}, \mathbf{m}}^{2, \Im}$) denoting a real-valued symmetric (anti-symmetric) matrix and mapping the upper triangles of these matrices to real-valued vectors \mathbf{c}^{\Re} and \mathbf{c}^{\Im} , respectively, which are stacked to the vector $\mathbf{c} = (\mathbf{c}^{\Re}, \mathbf{c}^{\Im})^T$ containing $[C_m^2]^2$ elements where $C_m^2 = m(m+1)/2$ denotes the number of distinct bosonic two-body configurations. Having determined \mathbf{c} as a solution of an optimization problem, we use it in order to reconstruct the hermitian matrix $C_{\mathbf{n}, \mathbf{m}}^2$.

The aim of this appendix is to formulate our correction scheme as the problem of minimizing²⁰ $|\mathbf{c}|_p \equiv \sum_r |c_r|^p$ under the linear constraints $\mathbf{A} \mathbf{c} = \mathbf{b}$. In the following, we construct the matrix \mathbf{A} and the vector \mathbf{b} of this under-determined system of linear equations. Here, the overall strategy is to formulate the i -th constraint as follows $\sum_{\mathbf{n}, \mathbf{m}} O_{\mathbf{m}, \mathbf{n}}^i C_{\mathbf{n}, \mathbf{m}}^2 = b_i$. Mapping the number states \mathbf{n} , \mathbf{m} to integer-valued indices I, J , we may decompose the

latter equation as

$$\begin{aligned}
b_i &= \sum_{I \leq J} \tilde{A}_{I, J}^{i, \Re} C_{I, J}^{2, \Re} + i \sum_{I < J} \tilde{A}_{I, J}^{i, \Im} C_{I, J}^{2, \Im} \\
&\equiv [\mathbf{a}^{i, \Re}]^T \cdot \mathbf{c}^{\Re} + [\mathbf{a}^{i, \Im}]^T \cdot \mathbf{c}^{\Im} = [\mathbf{a}^i]^T \cdot \mathbf{c},
\end{aligned} \tag{H1}$$

where $\tilde{A}_{I, J}^{i, \Re} = [O_{I, J}^i + O_{J, I}^i] / (1 + \delta_{I, J})$ and $\tilde{A}_{I, J}^{i, \Im} = O_{J, I}^i - O_{I, J}^i$. In the second identity of (H1), we have mapped the upper triangles of the matrices $\tilde{A}_{I, J}^{i, \Re}$ and $i \tilde{A}_{I, J}^{i, \Im}$ to the vectors $\mathbf{a}^{i, \Re}$ and $\mathbf{a}^{i, \Im}$, respectively, which turn out to be real-valued for hermitian $O_{I, J}^i$. In this case, these vectors are stacked to $\mathbf{a}^i = (\mathbf{a}^{i, \Re}, \mathbf{a}^{i, \Im})^T$, which constitutes the i -th row of the matrix \mathbf{A} .

(i) Let us translate the constraints of \hat{C}_2 being contraction-free. Due to hermiticity of $\langle \phi_i | \text{tr}_1(\hat{C}_2) | \phi_j \rangle$, we obtain m^2 independent constraints. Using the expression (A1) for the partial trace, we have

$$\sum_{l=1}^m \sqrt{(1 + \delta_{il})(1 + \delta_{jl})} C_{\mathbf{e}_i + \mathbf{e}_l, \mathbf{e}_j + \mathbf{e}_l}^2 = 0, \tag{H2}$$

which can be expressed as (H1) with $b_r = 0$ (r shall label the constraint corresponding to $i \leq j$) and

$$O_{\mathbf{m}, \mathbf{n}}^r = \sum_{l=1}^m \sqrt{(1 + \delta_{il})(1 + \delta_{jl})} \delta_{\mathbf{n}, \mathbf{e}_i + \mathbf{e}_l} \delta_{\mathbf{m}, \mathbf{e}_j + \mathbf{e}_l} \tag{H3}$$

where we introduced the Kronecker delta for number states as $\delta_{\mathbf{a}, \mathbf{b}} = \prod_{k=1}^m \delta_{a_k, b_k}$. Now, we have to distinguish two cases. If $i = j$, $O_{\mathbf{m}, \mathbf{n}}^r$ is a real-valued symmetric matrix such that $\tilde{A}_{I, J}^{r, \Im} = 0$. Thereby, we obtain m constraints affecting only the symmetric component $C_{\mathbf{n}, \mathbf{m}}^{2, \Re}$. For $i < j$, however, $O_{\mathbf{m}, \mathbf{n}}^r$ turns out to be a real-valued asymmetric matrix, resulting in non-vanishing real-valued matrices $\tilde{A}_{I, J}^{r, \Re}$ and $\tilde{A}_{I, J}^{r, \Im}$. Thus, we obtain for each $i < j$ two independent constraints affecting either the symmetric component $C_{\mathbf{n}, \mathbf{m}}^{2, \Re}$ or the antisymmetric component $C_{\mathbf{n}, \mathbf{m}}^{2, \Im}$ only. The corresponding rows of

²⁰ We note that this cost functional differs slightly from (31) because pairs of off-diagonal elements $C_{\mathbf{n}, \mathbf{m}}^2$, $C_{\mathbf{m}, \mathbf{n}}^2$ enter $|\mathbf{c}|_p$ only by a single representative off-diagonal element. We, however, do not expect that differences between (31) and $|\mathbf{c}|_p$ have a severe impact on the purification scheme.

\mathbf{A} are given by $\mathbf{a}^i = (\mathbf{a}^{i,\Re}, \mathbf{a}^{i,\Im})^T$ with $\mathbf{a}^{i,\Re}$ covering the upper triangle of $\tilde{A}_{I,J}^{r,\Re}$ as well as $\mathbf{a}^{i,\Im}$ set to zero and $\mathbf{a}^{i,\Re}$ set to zero as well as $\mathbf{a}^{i,\Im}$ covering the upper triangle of $\tilde{A}_{I,J}^{r,\Im}$, respectively. Thereby, we obtain further $m(m-1)$ constraints, which amounts to m^2 constraints related to the partial trace of $\hat{\mathcal{C}}_2$ in total.

(ii) Energy conservation can be easily formulated as a linear constraint. By means of the relation $\langle \hat{H} \rangle_t = N \text{tr}(\hat{k}_2 \hat{\rho}_2)$ with the auxiliary 2-particle Hamiltonian $\hat{k}_2 = [\hat{h}_1 + \hat{h}_2 + (N-1)\hat{v}_{12}]/2$ [15], we have to require $\text{tr}(\hat{k}_2 \hat{\mathcal{C}}_2) = 0$. The latter boils down to $\text{tr}(\hat{v}_{12} \hat{\mathcal{C}}_2) = 0$ as $\hat{\mathcal{C}}_2$ shall be contraction-free. Apparently, we have $b_r = 0$ for this constraint. Using the cyclic invariance of the trace and $\hat{\mathcal{C}}_2$ being bosonic, we obtain $\text{tr}(\hat{S}_2 \hat{v}_{12} \hat{S}_2 \hat{\mathcal{C}}_2) = 0$, which allows for identifying $O_{\mathbf{m},\mathbf{n}}^r$ with the matrix elements of $\hat{S}_2 \hat{v}_{12} \hat{S}_2$ in the number-state basis, namely as

$$O_{\mathbf{e}_i+\mathbf{e}_j, \mathbf{e}_q+\mathbf{e}_p}^r = \frac{v_{ijqp} + v_{jiqp}}{\sqrt{(1+\delta_{ij})(1+\delta_{qp})}}. \quad (\text{H4})$$

(iii) In the case of a symmetry such as invariance under parity or translation operations, we proceed as follows. We remind that the SPFs stay invariant under the corresponding symmetry operation, $\hat{\pi}_1|\phi_j\rangle = \exp(i\theta_j)|\phi_j\rangle$ with some real phase θ_j (see Section IV A). Correspondingly, an o -particle number-state transforms as $\hat{\Pi}_o|\mathbf{n}\rangle = \exp[i\theta(\mathbf{n})]|\mathbf{n}\rangle$ with $\theta(\mathbf{n}) = \sum_{j=1}^m n_j \theta_j$. Now we introduce the following equivalence relation between number states $\mathbf{n} \sim \mathbf{m}$ if $\theta(\mathbf{n}) \bmod 2\pi = \theta(\mathbf{m}) \bmod 2\pi$. Then the correction respects the symmetry if $\mathcal{C}_{\mathbf{n},\mathbf{m}}^2 = 0$ for all $\mathbf{n} \sim \mathbf{m}$. In order to construct the corresponding rows in \mathbf{A} , we loop over all pairs of inequivalent number states $\mathbf{f} \approx \mathbf{g}$ whose corresponding integer labels I (for \mathbf{f}) and J (for \mathbf{g}) obey $I < J$ in order to avoid redundant constraints. For each such \mathbf{f}, \mathbf{g} , we set $b_r = 0$ and $O_{\mathbf{m},\mathbf{n}}^r = \delta_{\mathbf{m},\mathbf{g}} \delta_{\mathbf{n},\mathbf{f}}$. The latter constitutes a real-valued asymmetric matrix such that for each $\mathbf{f} \approx \mathbf{g}$ two independent constraints arise, affecting either $\mathcal{C}_{\mathbf{n},\mathbf{m}}^{2,\Re}$ or $\mathcal{C}_{\mathbf{n},\mathbf{m}}^{2,\Im}$ only (see constraints (i)).

(iv) The constraint that each negative NP below a certain threshold $\lambda_r^{(2)} < \epsilon$ is raised to zero in first order perturbation theory with respect to $\hat{\mathcal{C}}_2$ can be expressed as $\text{tr}(|\phi_r^2\rangle\langle\phi_r^2|\hat{\mathcal{C}}_2) = -\lambda_r^{(2)}$. From this, we may directly read-off $b_r = -\lambda_r^{(2)}$ as well as $O_{\mathbf{m},\mathbf{n}}^r = [\phi_{r,\mathbf{n}}^2]^* \phi_{r,\mathbf{m}}^2$ where $\phi_{r,\mathbf{m}}^2 = \langle \mathbf{m} | \phi_r^2 \rangle$.

(v) In order to formulate the constraints related to negative \hat{K}_2 eigenvalues, we first need to clarify the relation between \hat{K}_2 and $\hat{\rho}_1, \hat{\rho}_2$. Explicating (30), we find

$$K_{(i_1,j_1),(i_2,j_2)}^2 \mathcal{N}_K = N(N-1) f_{i_2 j_1} f_{i_1 j_2} \rho_{\mathbf{e}_{i_2}+\mathbf{e}_{j_1}, \mathbf{e}_{i_1}+\mathbf{e}_{j_2}}^2 + \delta_{j_1, j_2} N \rho_{i_2 i_1}^1 - N^2 \rho_{j_1, i_1}^1 \rho_{i_2, j_2}^1, \quad (\text{H5})$$

where we have again used the abbreviation $f_{ij} = \sqrt{(1+\delta_{i,j})}/2$. Updating $\hat{\rho}_2$ by the contraction-free operator $\hat{\mathcal{C}}_2$ apparently leaves $\hat{\rho}_1$ and thus also $\mathcal{N}_K = N(N+m-1) - N^2 \text{tr}([\hat{\rho}_1]^2)$ invariant. Thereby, the

update of $\hat{\rho}_2$ implies the update $\hat{K}_2 + \hat{\Delta}_2$ with

$$\Delta_{(i_1,j_1),(i_2,j_2)}^2 = \frac{N(N-1)}{\mathcal{N}_K} f_{i_2 j_1} f_{i_1 j_2} \mathcal{C}_{\mathbf{e}_{i_2}+\mathbf{e}_{j_1}, \mathbf{e}_{i_1}+\mathbf{e}_{j_2}}^2. \quad (\text{H6})$$

Now the constraint that a negative \hat{K}_2 eigenvalue ξ_r below the threshold ϵ shall be raised to zero in first-order perturbation theory with respect to $\hat{\Delta}_2$, i.e. $\text{tr}(|\Xi_r\rangle\langle\Xi_r|\hat{\Delta}_2) = -\xi_r$, can be rephrased in terms of the correction $\hat{\mathcal{C}}_2$. The result is setting $b_r = -\xi_r$ and

$$O_{\mathbf{e}_q+\mathbf{e}_p, \mathbf{e}_i+\mathbf{e}_j}^r \equiv \frac{N(N-1)}{4\mathcal{N}_K f_{ij} f_{qp}} \left(M_{(i,p),(q,j)}^r + M_{(j,p),(q,i)}^r + M_{(i,q),(p,j)}^r + M_{(j,q),(p,i)}^r \right) \quad (\text{H7})$$

where $M_{(i,p),(q,j)}^r \equiv \langle \varphi_i \varphi_p | \Xi_r \rangle \langle \Xi_r | \varphi_q \varphi_j \rangle$.

We remark that the inhomogeneity \mathbf{b} of the system of linear equations features only extremely small or vanishing numerical values. For increasing the numerical stability when solving the optimization problem, we replace \mathbf{b} by \mathbf{b}/\mathcal{N}_b with $\mathcal{N}_b = (\sum_i |\lambda_i^{(2)}| < \epsilon |\lambda_i^{(2)}| + \sum_i |\xi_i| < \epsilon |\xi_i|)/(d+d')$ where d (d') denotes the number of $\hat{\rho}_2$ (\hat{K}_2) eigenvalues below the threshold. Thereafter, the solution \mathbf{c} is rescaled as $\mathbf{c}\mathcal{N}_b$.

Finally, let us investigate how underdetermined the correction operator $\hat{\mathcal{C}}_2$ is, which can be parametrized by $[\mathcal{C}_m^2]^2 = m^2(m+1)^2/4$ independent real numbers. If no symmetry has to be incorporated, there are $m^2 + d + d' + 1$ independent constraints (note that the energy-conservation constraint has to be imposed also in cases where the total Hamiltonian is explicitly time-dependent, otherwise $\frac{d}{dt}\langle \hat{H} \rangle = \langle \partial_t \hat{H} \rangle$ would be violated). If there is parity symmetric and half of the initial SPFs are of even and half of them are of odd parity (m shall be even), then $m^4/8 + m^3/4$ additional constraints have to be taken into account.

Appendix I: Minimal invasive correction of the EOM

The technical implementation of the minimal-invasive correction scheme for the 2-RDM EOM is very much alike the steps discussed in Appendix H. Therefore, we only work out differences here.

The constraints on the correction $\hat{\mathcal{C}}_2$ to be (i) contraction-free, (ii) energy conserving and (iii) respecting symmetries if existent can be exactly implemented as discussed in Appendix H. For enforcing negative NPs $\lambda_r^{(2)}$ below the threshold ϵ to be exponentially damped to zero, we may use the same $O_{\mathbf{m},\mathbf{n}}^r$ as described in Appendix H (vi), where one has to replace, however, $b_r = -\lambda_r^{(2)}$ by $b_r = -\eta \lambda_r^{(2)} + i \langle \phi_r^2 | \hat{I}_2(\hat{\chi}_3) | \phi_r^2 \rangle$ with $\hat{\chi}_3 = \hat{\rho}_3^{\text{appr}}$ for $\bar{o} = 2$ and $\hat{\chi}_3 = \hat{\rho}_3$ for $\bar{o} > 2$.

For the requirement that also negative \hat{K}_2 eigenvalues are damped to zero, we first have to express the EOM

for \hat{K}_2 in terms of $\hat{\rho}_1$, $\hat{\rho}_2$, \hat{R}_1 and \hat{R}_2 by differentiating (H5) with respect to time

$$\begin{aligned} \partial_t K_{(i_1, j_1), (i_2, j_2)}^2 &\equiv \langle \varphi_{i_1} \varphi_{j_1} | \hat{T}_2 | \varphi_{i_2} \varphi_{j_2} \rangle = \frac{1}{\mathcal{N}_K} \left(2N^2 \text{tr}(\hat{R}_1 \hat{\rho}_1) K_{(i_1, j_1), (i_2, j_2)}^2 + N(N-1) f_{i_2 j_1} f_{i_1 j_2} R_{\mathbf{e}_{i_2} + \mathbf{e}_{j_1}, \mathbf{e}_{i_1} + \mathbf{e}_{j_2}}^2 \right. \\ &\quad \left. + \delta_{j_1, j_2} N R_{i_2, i_1}^1 - N^2 R_{j_1, i_1}^1 \rho_{i_2, j_2}^1 - N^2 R_{i_2, j_2}^1 \rho_{j_1, i_1}^1 \right). \end{aligned} \quad (\text{I1})$$

Since \hat{C}_2 is enforced to be contraction-free, \hat{R}_1 is left invariant under the correction of \hat{R}_2 . Thus, we induce the correction $\hat{T}_2 \rightarrow \hat{T}_2 + \hat{\Delta}_2$ with $\hat{\Delta}_2$ given by (H6). Thereby, we may use the same $O_{\mathbf{m}, \mathbf{n}}^r$ as in Appendix H (v) but need to substitute $b_r = -\xi_r$ by $b_r = -\eta \xi_r - \langle \Xi_r | \hat{T}_2 | \Xi_r \rangle$.

Appendix J: Unitarily invariant decomposition of the collision integral

While we have so far applied the UID only to the RDM, the purpose of this appendix is to gain insights into the

unitarily invariant components of the collision integral. Let $\hat{A}_{o+1} \in \mathcal{B}_{o+1}$. By means of (A1), we may evaluate the partial trace of the collision integral

$$\begin{aligned} \text{tr}_1(\hat{I}_o(\hat{A}_{o+1})) &= \frac{N-o}{o(o+1)} \sum_{r, i, j, q, p=1} v_{qjpi} \hat{a}_r [\hat{a}_q^\dagger \hat{a}_p, \hat{a}_i \hat{A}_{o+1} \hat{a}_j^\dagger] \hat{a}_r^\dagger = \frac{N-o}{o(o+1)} \sum_{r, i, j, q, p=1} v_{qjpi} [\hat{a}_q^\dagger \hat{a}_p, \hat{a}_i \hat{a}_r \hat{A}_{o+1} \hat{a}_r^\dagger \hat{a}_j^\dagger] \\ &= \hat{I}_o(\text{tr}_1(\hat{A}_{o+1})). \end{aligned} \quad (\text{J1})$$

From this identity, we may conclude that the reducible component of the collision integral depends solely on the reducible component of its argument, $[\hat{I}_o(\hat{A}_{o+1})]^{\text{red}} = [\hat{I}_o(\hat{A}_{o+1}^{\text{red}})]^{\text{red}}$. The irreducible component of the collision integral $[\hat{I}_o(\hat{A}_{o+1})]^{\text{irr}}$, however, depends on both reducible and the irreducible component of \hat{A}_{o+1} in general, which we have confirmed by an explicit calculation for the cases $o = 1, 2$. Thus, the collision integral with a contraction-free argument is itself contraction-free.

Appendix K: Numerical integration of the truncated BBGKY EOM

In both scenarios of Section VI, we employ the variable-coefficient ordinary differential equation solver ZVODE

[126] for integrating the EOM (5), (6). The conservation of hermiticity of the RDMs is numerically ensured by only propagating the lower triangle of the matrix-valued EOM (6), which at the same time reduces the number of variables to be integrated. Since the applied truncation approximation conserves the compatibility of the RDMs, we propagate only the BBGKY EOM (6) at the truncation order \bar{o} and obtain the RDMs of lower order by partial tracing. Moreover, we operate in the single-particle Hamiltonian gauge, $g_{ij} = h_{ij}$ (see Section III C).

- [1] P. Hohenberg and W. Kohn. Inhomogeneous electron gas. *Phys. Rev.*, 136:B864, 1964.
 [2] W. Kohn and L. J. Sham. Self-Consistent Equations Including Exchange and Correlation Effects. *Phys. Rev.*, 140:A1133, 1965.

- [3] M. Uhlmann R. Schützhold and U. R. Fischer. Effect of fluctuations on the superfluid-supersolid phase transition on the lattice. *Phys. Rev. A*, 78:033604, 2008.
 [4] P. Navez and R. Schützhold. Emergence of coherence in the Mott-insulator superfluid quench of the Bose-

- Hubbard model. *Phys. Rev. A*, 82:063603, 2010.
- [5] K. V. Krutitsky, P. Navez, F. Queisser, and R. Schützhold. Propagation of quantum correlations after a quench in the Mott-insulator regime of the Bose-Hubbard model. *EPJ Quantum Technology*, 1:12, 2014.
- [6] P. Navez, F. Queisser, and R. Schützhold. Quasi-particle approach for lattice Hamiltonians with large coordination numbers. *J. Phys. A*, 47:225004, 2014.
- [7] F. Queisser, K. V. Krutitsky, P. Navez, and R. Schützhold. Equilibration and prethermalization in the Bose-Hubbard and Fermi-Hubbard models. *Phys. Rev. A*, 89:033616, 2014.
- [8] A. L. Fetter and J. D. Walecka. *Quantum Theory of Many-Particle Systems*. McGraw-Hill, 1971.
- [9] K. Balzer and M. Bonitz. *Nonequilibrium Green's Function Approach to Inhomogeneous Systems*. Lecture Notes in Physics. Springer, 2013.
- [10] M. Bonitz. *Quantum Kinetic Theory*, volume 33 of *Teubner-Texte zur Physik*. B. G. Teubner, 1998.
- [11] A. J. Coleman. Reduced Density Matrices - Then and Now. *Int. J. Quant. Chem.*, 85:196, 2001.
- [12] A. John Coleman et. al. *Many-Electron Densities and Reduced Density Matrices*. Springer, 2000.
- [13] David A. Mazziotti, editor. *Reduced-Density-Matrix Mechanics: with Application to Many-Electron Atoms and Molecules*, volume 134i of *Advances in Chemical Physics*. Wiley, 2007.
- [14] K. J. H. Giesbertz and M. Ruggenthaler. One-body reduced density-matrix functional theory in finite basis sets at elevated temperatures. *Preprint. arXiv:1710.08805*, 2017.
- [15] F. Bopp. Ableitung der Bindungsenergie von N-Teilchen-Systemen aus 2-Teilchen-Dichtematrizen. *Z. Physik*, 156:348, 1959.
- [16] A. Polkovnikov, K. Sengupta, A. Silva, and M. Vengalattore. Colloquium: Nonequilibrium dynamics of closed interacting quantum systems. *Rev. Mod. Phys.*, 83:863, 2011.
- [17] P.-O. Löwdin. Quantum Theory of Many-Particle Systems. I. Physical Interpretations by Means of Density Matrices, Natural Spin-Orbitals, and Convergence Problems in the Method of Configurational Interaction. *Phys. Rev.*, 97:1474, 1955.
- [18] O. Penrose and L. Onsager. Bose-Einstein Condensation and Liquid Helium. *Phys. Rev.*, 104:576, 1956.
- [19] C. N. Yang. Concept of Off-Diagonal Long-Range Order and the Quantum Phases of Liquid He and of Superconductors. *Rev. Mod. Phys.*, 34:694, 1962.
- [20] R. J. Glauber. The Quantum Theory of Optical Coherence. *Phys. Rev.*, 130:2529, 1963.
- [21] A. J. Coleman and V. I. Yukalov. Order indices for boson density matrices. *Il Nuovo Cimento*, 107:535, 1992.
- [22] K. Sakmann, A. I. Streltsov, O. E. Alon, and L. S. Cederbaum. Reduced density matrices and coherence of trapped interacting bosons. *Phys. Rev. A*, 78:023615, 2008.
- [23] S. Krönke and P. Schmelcher. Two-body correlations and natural-orbital tomography in ultracold bosonic systems of definite parity. *Phys. Rev. A*, 92:023631, 2015.
- [24] P. Nozières and D. S. James. Particle vs. pair condensation in attractive bose liquids. *J. Physique*, 43:1133, 1982.
- [25] M. Ueda E. J. Mueller, T.-L. Ho and G. Baym. Fragmentation of bose-einstein condensates. *Phys. Rev. A*, 74:033612, 2006.
- [26] M.-K. Kang and U. R. Fischer. Revealing Single-Trap Condensate Fragmentation by Measuring Density-Density Correlations after Time of Flight. *Phys. Rev. Lett.*, 113:140404, 2014.
- [27] C. J. Pethick and H. Smith. *Bose-Einstein Condensates in Dilute Gases*. Cambridge University Press, 2nd edition, 2008.
- [28] I. Bloch, J. Dalibard, and W. Zwerger. Many-body physics with ultracold gases. *Rev. Mod. Phys.*, 80:885, 2008.
- [29] M. Lewenstein, A. Sanpera, and V. Ahufinger. *Ultracold Atoms in Optical Lattices: Simulating quantum many-body systems*. Oxford University Press, 2012.
- [30] N. N. Bogoliubov. *The Dynamical Theory in Statistical Physics*. Hindustan Pub. Corp., Delhi, 1965.
- [31] M. Born and H. S. Green. A general kinetic theory of liquids. iv. quantum mechanics of fluids. *Proc. R. Soc. London, Ser. A*, 191:168, 1947.
- [32] J. Kirkwood. The Statistical Mechanical Theory of Transport Processes I. General Theory. *J. Chem. Phys.*, 14:180, 1946.
- [33] J. Yvon. Une méthode d'étude des corrélations dans les fluides quantiques en équilibre. *Nucl. Phys.*, 4:1, 1957.
- [34] M. Gessner and A. Buchleitner. On the reduced dynamics of a subset of interacting bosonic particles. *Ann. Phys.*, 390:192, 2018.
- [35] L. Cohen and C. Lee. Exact reduced density matrices for a model problem. *J. Math. Phys.*, 26:3105, 1985.
- [36] N. Helbig, I. V. Tokatly, and A. Rubio. Physical meaning of the natural orbitals: Analysis of exactly solvable models. *Phys. Rev. A*, 81:022504, 2010.
- [37] C. Schilling. Natural orbitals and occupation numbers for harmonium: Fermions versus bosons. *Phys. Rev. A*, 88:042105, 2013.
- [38] K. J. H. Giesbertz and R. van Leeuwen. Natural occupation numbers: When do they vanish? *J. Chem. Phys.*, 139:104109, 2013.
- [39] O. Osenda, F. M. Pont, A. Okopińska, and P. Serra. Exact finite reduced density matrix and von neumann entropy for the calogero model. *J. Phys. A*, 48:485301, 2015.
- [40] S. Klaiman, A. I. Streltsov, and O. E. Alon. Solvable model of a trapped mixture of bose-einstein condensates. *Chem. Phys.*, 482:362, 2017.
- [41] O. E. Alon. Solvable Model of a Generic Trapped Mixture of Interacting Bosons: Reduced Density Matrices and Proof of Bose-Einstein Condensation. *J. Phys. A: Math. Theor.*, 50:295002, 2017.
- [42] J. Rapp, M. Brics, and D. Bauer. Equations of motion for natural orbitals of strongly driven two-electron systems. *Phys. Rev. A*, 90:012518, 2014.
- [43] D. B. Boercker and J. W. Dufty. Degenerate quantum gases in the binary collision approximation. *Ann. Phys.*, 119:43, 1979.
- [44] R. F. Snider, W. J. Mullin, and F. Laloë. Analysis of certain binary collision approximation closures of the bbgky hierarchy. *Physica A*, 218:155, 1995.
- [45] W. Shun-Jin and W. Cassing. Explicit treatment of n-body correlations within a density-matrix formalism. *Ann. Phys.*, 159:328, 1985.

- [46] W. Cassing and A. Pfitzner. Self-consistent truncation of the BBGKY hierarchy on the two-body level. *Z. Physik A - Hadrons and Nuclei*, 342:161, 1992.
- [47] J. M. Häuser, W. Cassing, and A. Peter. Two-body correlations in pionic systems. *Nucl. Phys. A*, 585:727, 1995.
- [48] M. Kira and S. W. Koch. Cluster-expansion representation in quantum optics. *Phys. Rev. A*, 78:022102, 2008.
- [49] M. Kira and S. W. Koch. *Semiconductor Quantum Optics*. Cambridge University Press, 2011.
- [50] M. Kira. Excitation picture of an interacting Bose gas. *Ann. Phys. (N. Y.)*, 351:200, 2014.
- [51] M. Kira. Coherent quantum depletion of an interacting atom condensate. *Nat. Commun.*, 6, 2015.
- [52] M. Kira. Hyperbolic Bloch equations: atom-cluster kinetics of an interacting Bose gas. *Ann. Phys. (N. Y.)*, 356:185, 2015.
- [53] A. Foerster H. A. M. Leymann and J. Wiersig. Expectation value based equation-of-motion approach for open quantum systems: A general formalism. *Phys. Rev. B*, 89:085308, 2014.
- [54] H. A. M. Leymann A. Foerster and J. Wiersig. Computer-aided cluster expansion: An efficient algebraic approach for open quantum many-particle systems. *Comput. Phys. Commun.*, 212:210, 2017.
- [55] C. Valdemoro. Approximating the second-order reduced density matrix in terms of the first-order one. *Phys. Rev. A*, 45:4462, 1992.
- [56] F. Colmenero and C. Valdemoro. Approximating q -order reduced density matrices in terms of lower-order ones. ii. applications. *Phys. Rev. A*, 47:979, 1993.
- [57] K. Yasuda and H. Nakatsuji. Direct determination of the quantum-mechanical density matrix using the density equation. II. *Phys. Rev. A*, 56:2648, 1997.
- [58] D. A. Mazziotti. Contracted schrödinger equation: Determining quantum energies and two-particle density matrices without wave functions. *Phys. Rev. A*, 57:4219, 1998.
- [59] A. Vardi and J. R. Anglin. Bose-Einstein Condensates beyond Mean Field Theory: Quantum Backreaction as Decoherence. *Phys. Rev. Lett.*, 86:568, 2001.
- [60] J. R. Anglin and A. Vardi. Dynamics of a two-mode Bose-Einstein condensate beyond mean-field theory. *Phys. Rev. A*, 64:013605, 2001.
- [61] I. Tikhonenkov, J. R. Anglin, and A. Vardi. Quantum dynamics of Bose-Hubbard Hamiltonians beyond the Hartree-Fock-Bogoliubov approximation: The Bogoliubov back-reaction approximation. *Phys. Rev. A*, 75:013613, 2007.
- [62] F. Trimborn, D. Witthaut, H. Hennig, G. Kordas, T. Geisel, and S. Wimberger. Decay of a Bose-Einstein condensate in a dissipative lattice - the mean-field approximation and beyond. *Eur. Phys. J. D*, 63:63, 2011.
- [63] D. Witthaut, F. Trimborn, H. Hennig, G. Kordas, T. Geisel, and S. Wimberger. Beyond mean-field dynamics in open Bose-Hubbard chains. *Phys. Rev. A*, 83:063608, 2011.
- [64] G. Kordas, D. Witthaut, P. Buonsante, A. Vezzani, R. Burioni, A. I. Karanikas, and S. Wimberger. The Dissipative Bose-Hubbard Model. *Eur. Phys. J. Spec. Top.*, 224:2127, 2015.
- [65] T. Köhler and K. Burnett. Microscopic quantum dynamics approach to the dilute condensed Bose gas. *Phys. Rev. A*, 65:033601, 2002.
- [66] T. Köhler, T. Gasenzer, and K. Burnett. Microscopic theory of atom-molecule oscillations in a Bose-Einstein condensate. *Phys. Rev. A*, 67:013601, 2003.
- [67] P. Elliott and N. T. Maitra. Density-matrix propagation driven by semiclassical correlation. *Int. J. Quant. Chem.*, 116:772, 2016.
- [68] D. B. Jeffcoat and E. A. DePrince. N-representability-driven reconstruction of the two-electron reduced-density matrix for a real-time time-dependent electronic structure method. *J. Chem. Phys.*, 141:214104, 2014.
- [69] A. Akbari, M. J. Hashemi, A. Rubio, R. M. Nieminen, and R. van Leeuwen. Challenges in truncating the hierarchy of time-dependent reduced density matrices equations. *Phys. Rev. B*, 85:235121, 2012.
- [70] M. Tohyama and P. Schuck. Truncation scheme of time-dependent density-matrix approach. *Eur. Phys. J. A*, 50:77, 2014.
- [71] M. Tohyama and P. Schuck. Truncation scheme of time-dependent density-matrix approach ii. *Eur. Phys. J. A*, 53:186, 2017.
- [72] F. Lackner, I. Březinová, T. Sato, K. L. Ishikawa, and J. Burgdörfer. Propagating two-particle reduced density matrices without wave functions. *Phys. Rev. A*, 91:023412, 2015.
- [73] F. Lackner, I. Březinová, T. Sato, K. L. Ishikawa, and J. Burgdörfer. High-harmonic spectra from time-dependent two-particle reduced-density-matrix theory. *Phys. Rev. A*, 95:033414, 2017.
- [74] O. E. Alon, A. I. Streltsov, and L. S. Cederbaum. Multiconfigurational time-dependent Hartree method for bosons: Many-body dynamics of bosonic systems. *Phys. Rev. A*, 77:033613, 2008.
- [75] M. H. Beck, A. Jäckle, G. A. Worth, and H. D. Meyer. The multiconfiguration time-dependent hartree (mctdh) method: a highly efficient algorithm for propagating wavepackets. *Physics Reports*, 324:1, 2000.
- [76] K. Sakmann, A. I. Streltsov, O. E. Alon, and L. S. Cederbaum. Exact Quantum Dynamics of a Bosonic Josephson Junction. *Phys. Rev. Lett.*, 103:220601, 2009.
- [77] A. U. J. Lode, K. Sakmann, O. E. Alon, L. S. Cederbaum, and A. I. Streltsov. Numerically exact quantum dynamics of bosons with time-dependent interactions of harmonic type. *Phys. Rev. A*, 86:063606, 2012.
- [78] S. Krönke and P. Schmelcher. Many-body processes in black and gray matter-wave solitons. *Phys. Rev. A*, 91:053614, 2015.
- [79] U. Manthe. The multi-configurational time-dependent Hartree approach revisited. *J. Chem. Phys.*, 142:244109, 2015.
- [80] H.-D. Meyer and H. Wang. On regularizing the MCTDH equations of motion. *J. Chem. Phys.*, 148:124105, 2018.
- [81] L. Cao, S. Krönke, O. Vendrell, and P. Schmelcher. The multi-layer multi-configuration time-dependent Hartree method for bosons: Theory, implementation, and applications. *J. Chem. Phys.*, 139:134103, 2013.
- [82] A. Raab and H.-D. Meyer. Multiconfigurational expansions of density operators: equations of motion and their properties. *Theor. Chem. Acc.*, 104:358, 2000.
- [83] H.-D. Meyer and G. A. Worth. Quantum molecular dynamics: propagating wavepackets and density operators using the multiconfiguration time-dependent Hartree method. *Theor. Chem. Acc.*, 109:251, 2003.
- [84] David A. Mazziotti. Anti-Hermitian Contracted Schrödinger Equation: Direct Determination of the

- Two-Electron Reduced Density Matrices of Many-Electron Molecules. *Phys. Rev. Lett.*, 97:143002, 2006.
- [85] A. P. J. Jansen. A multiconfiguration time-dependent Hartree approximation based on natural single-particle states. *J. Chem. Phys.*, 99:4055, 1993.
- [86] U. Manthe. Comment on “A multiconfiguration time-dependent Hartree approximation based on natural single-particle states” [*J. Chem. Phys.* **99**, 4055 (1993)]. *J. Chem. Phys.*, 101:2652, 1994.
- [87] O. Pernal, K. and Gritsenko and E. J. Baerends. Time-dependent density-matrix-functional theory. *Phys. Rev. A*, 75:012506, 2007.
- [88] H. Appel. *Time-Dependent Quantum Many-Body Systems: Linear Response, Electronic Transport, and Reduced Density Matrices*. PhD thesis, Free University Berlin, 2007.
- [89] H. Appel and E. K. U. Gross. Time-dependent natural orbitals and occupation numbers. *Europhys. Lett.*, 92:23001, 2010.
- [90] K. J. H. Giesbertz. *Time-Dependent One-Body Reduced Density Matrix Functional Theory; Adiabatic Approximations and Beyond*. PhD thesis, Free University Amsterdam, 2010.
- [91] M. Brics and D. Bauer. Time-dependent renormalized natural orbital theory applied to the two-electron spin-singlet case: Ground state, linear response, and autoionization. *Phys. Rev. A*, 88:052514, 2013.
- [92] M. Brics, J. Rapp, and D. Bauer. Single-photon double ionization: renormalized-natural-orbital theory versus multi-configurational Hartree-Fock. *J. Phys. B*, 50:144003, 2017.
- [93] J. von Neumann and E. P. Wigner. Über merkwürdige diskrete Eigenwerte. über das Verhalten von Eigenwerten bei adiabatischen Prozessen. *Z. Phys.*, 30:467, 1929.
- [94] Private communication with H. D. Meyer and U. Manthe.
- [95] M. Bonitz, M. Scharnke, and N. Schlünzen. Time-reversal invariance of quantum kinetic equations II: Density operator formalism. *Contrib. Plasma Phys.*, page 1.
- [96] Y. Castin. *Coherent atomic matter waves*, chapter Course 1. Bose-Einstein Condensates in Atomic Gases: Simple Theoretical Results, pages 1–136. Springer, 2001.
- [97] L.S. Cederbaum and A.I. Streltsov. Best mean-field for condensates. *Phys. Lett. A*, 318:564, 2003.
- [98] Ofir E. Alon, Alexej I. Streltsov, and Lorenz S. Cederbaum. Time-dependent multi-orbital mean-field for fragmented bose-einstein condensates. *Phys. Lett. A*, 362:453, 2007.
- [99] S. Krönke. *Correlated Quantum Dynamics of Ultracold Bosons and Bosonic Mixtures: the Multi-Layer Multi-Configuration Time-Dependent Hartree Method for Bosons*. PhD thesis, University of Hamburg, 2015.
- [100] J. M. Schurer, A. Negretti, and P. Schmelcher. Capture dynamics of ultracold atoms in the presence of an impurity ion. *New J. Phys.*, 17:083024, 2015.
- [101] W. Kutzelnigg and D. Mukherjee. Cumulant expansion of the reduced density matrices. *J. Chem. Phys.*, 110:2800, 1999.
- [102] J. M. Herbert. *Reconstructive approaches to one- and two-electron density matrix theory*. PhD thesis, University of Wisconsin-Madison, 2003.
- [103] A. J. Coleman. *Reduced Density Operators with Applications to Physical and Chemical Systems II*, volume 40 of *Queen’s Papers in Pure and Applied Mathematics*, page 2. Queen’s University: Kingston, Ontario, 1974.
- [104] A. J. Coleman and I. Absar. Reduced hamiltonian orbitals. III. Unitarily invariant decomposition of hermitian operators. *Int. J. Quant. Chem.*, 18:1279, 1980.
- [105] T. Au-Chin and G. Hong. Characteristic operators and unitarily invariant decomposition of hermitian operators. *Int. J. Quant. Chem.*, 23:217, 1983.
- [106] C.-C. Sun, X.-Q. Li, and A.-C. Tang. On the unitarily invariant decomposition of Hermitian operators. *Int. J. Quant. Chem.*, 25:1045, 1984.
- [107] A. I. Streltsov, O. E. Alon, and L. S. Cederbaum. General mapping for bosonic and fermionic operators in Fock space. *Phys. Rev. A*, 81:022124, 2010.
- [108] H.-P. Breuer and F. Petruccione. *The Theory of Open Quantum Systems*. Oxford University Press, 2002.
- [109] C. Garrod and J. K. Percus. Reduction of the N-Particle Variational Problem. *J. Math. Phys.*, 5:1756, 1964.
- [110] D. A. Mazziotti and R. M. Erdahl. Uncertainty relations and reduced density matrices: Mapping many-body quantum mechanics onto four particles. *Phys. Rev. A*, 63:042113, 2001.
- [111] G. Gidofalvi and D. A. Mazziotti. Boson correlation energies via variational minimization with the two-particle reduced density matrix: Exact N -representability conditions for harmonic interactions. *Phys. Rev. A*, 69:042511, 2004.
- [112] C.-L. Hung, X. Zhang, L.C. Ha, S.-K. Tung, N. Gemelke, and C. Chin. Extracting density-density correlations from in situ images of atomic quantum gases. *New J. Phys.*, 13:075019, 2011.
- [113] D. A. Mazziotti. Purification of correlated reduced density matrices. *Phys. Rev. E*, 65:026704, 2002.
- [114] Fabian Lackner. Dynamics of correlated many body systems: propagating reduced two-particle density matrices without wave functions. Diploma thesis, Technischen Universität Wien, 2014.
- [115] S. Chen, D. Donoho, and M. Saunders. Atomic Decomposition by Basis Pursuit. *SIAM Rev.*, 43:129, 2001.
- [116] D. A. Lorenz, M. E. Pfetsch, and A. M. Tillmann. Solving Basis Pursuit: Heuristic Optimality Check and Solver Comparison. *ACM Trans. Math. Softw.*, 41:8:1, 2015.
- [117] S. J. Maher, T. Fischer, T. Gally, G. Gamrath, A. Gleixner, R. L. Gottwald, G. Hendel, T. Koch, M. E. Lübbecke, M. Miltenberger, B. Müller, M. E. Pfetsch, C. Puchert, D. Rehfeldt, S. Schenker, R. Schwarz, F. Serrano, Y. Shinano, D. Weninger, J. T. Witt, and J. Witzig. The scip optimization suite 4.0. Technical Report 17-12, ZIB, Takustr.7, 14195 Berlin, 2017.
- [118] S. Raghavan, A. Smerzi, S. Fantoni, and S. R. Shenoy. Coherent oscillations between two weakly coupled Bose-Einstein condensates: Josephson effects, π oscillations, and macroscopic quantum self-trapping. *Phys. Rev. A*, 59:620, 1999.
- [119] A. Smerzi, S. Fantoni, S. Giovanazzi, and S. R. Shenoy. Quantum Coherent Atomic Tunneling between Two Trapped Bose-Einstein Condensates. *Phys. Rev. Lett.*, 79:4950, 1997.
- [120] G. J. Milburn, J. Corney, E. M. Wright, and D. F. Walls. Quantum dynamics of an atomic Bose-Einstein condensate in a double-well potential. *Phys. Rev. A*, 55:4318,

- 1997.
- [121] K. Sakmann, A. I. Streltsov, O. E. Alon, and L. S. Cederbaum. Quantum dynamics of attractive versus repulsive bosonic Josephson junctions: Bose-Hubbard and full-Hamiltonian results. *Phys. Rev. A*, 82:013620, 2010.
- [122] K. Sakmann, A. I. Streltsov, O. E. Alon, and L. S. Cederbaum. Universality of fragmentation in the schrödinger dynamics of bosonic josephson junctions. *Phys. Rev. A*, 89:023602, 2014.
- [123] B. Gertjerenken and C. Weiss. Beyond-mean-field behavior of large Bose-Einstein condensates in double-well potentials. *Phys. Rev. A*, 88:033608, 2013.
- [124] M. Albiez, R. Gati, J. Fölling, S. Hunsmann, M. Cristiani, and M. K. Oberthaler. Direct Observation of Tunneling and Nonlinear Self-Trapping in a Single Bosonic Josephson Junction. *Phys. Rev. Lett.*, 95:010402, 2005.
- [125] M. A. Nielsen and I. L. Chuang. *Quantum Computation and Quantum Information*. Cambridge University Press, 2000.
- [126] A. C. Hindmarsh. *ODEPACK, a Systematized Collection of ODE Solvers*, page 55. Scientific Computing. North-Holland, Amsterdam, 1983.
- [127] C. Menotti and S. Stringari. Collective oscillations of a one-dimensional trapped bose-einstein gas. *Phys. Rev. A*, 66:043610, 2002.
- [128] H. Moritz, T. Stöferle, M. Köhl, and T. Esslinger. Exciting collective oscillations in a trapped 1d gas. *Phys. Rev. Lett.*, 91:250402, 2003.
- [129] S. Bauch, K. Balzer, C. Henning, and M. Bonitz. Quantum breathing mode of trapped bosons and fermions at arbitrary coupling. *Phys. Rev. B*, 80:054515, 2009.
- [130] J. W. Abraham and M. Bonitz. Quantum breathing mode of trapped particles: From nanoplasmas to ultracold gases. *Contrib. Plasma Phys.*, 54:27, 2014.
- [131] R. Schmitz, S. Krönke, L. Cao, and P. Schmelcher. Quantum breathing dynamics of ultracold bosons in one-dimensional harmonic traps: Unraveling the pathway from few-to many-body systems. *Phys. Rev. A*, 88:043601, 2013.
- [132] W. Tschischik, R. Moessner, and M. Haque. Breathing mode in the bose-hubbard chain with a harmonic trapping potential. *Phys. Rev. A*, 88:063636, 2013.
- [133] B. Fang, G. Carleo, A. Johnson, and I. Bouchoule. Quench-induced breathing mode of one-dimensional bose gases. *Phys. Rev. Lett.*, 113:035301, 2014.
- [134] M. Pyzh, S. Krönke, C. Weitenberg, and P. Schmelcher. Spectral properties and breathing dynamics of a few-body Bose-Bose mixture in a 1d harmonic trap. *New J. Phys.*, 20:015006, 2018.
- [135] E. Haller, M. Gustavsson, M. J. Mark, J. G. Danzl, R. Hart, G. Pupillo, and Hanns-Christoph H.-C. Nägerl. Realization of an excited, strongly correlated quantum gas phase. *Science*, 325:1224, 2009.
- [136] S. Krönke, L. Cao, O. Vendrell, and P. Schmelcher. Non-equilibrium quantum dynamics of ultra-cold atomic mixtures: the multi-layer multi-configuration time-dependent hartree method for bosons. *New J. Phys.*, 15:063018, 2013.
- [137] L. Cao, V. Bolsinger, S. I. Mistakidis, G. M. Koutentakis, S. Krönke, J. M. Schurer, and P. Schmelcher. A unified ab initio approach to the correlated quantum dynamics of ultracold fermionic and bosonic mixtures. *J. Chem. Phys.*, 147:044106, 2017.
- [138] J.C. Light and T. Carrington. Discrete-variable representations and their utilization. *Adv. Chem. Phys.*, 114:263, 2000.
- [139] H. Kummer. n -Representability Problem for Reduced Density Matrices. *J. Math. Phys.*, 8:2063, 1967.
- [140] Wolfram Research, Inc. *Mathematica*. Version 10.0, Champaign, Illinois (2014).